NAVAL POSTGRADUATE SCHOOL

MONTEREY, CALIFORNIA

THESIS

**AN INNOVATIVE APPROACH FOR THE
DEVELOPMENT OF FUTURE MARINE CORPS
AMPHIBIOUS CAPABILITY**

by

Jeffrey D. Parker, Jr.

June 2015

Thesis Co-Advisor:	Susan M. Sanchez
	Paul T. Beery
Second Reader	Eugene P. Paulo

Approved for public release; distribution is unlimited

THIS PAGE INTENTIONALLY LEFT BLANK

REPORT DOCUMENTATION PAGE		*Form Approved OMB No. 0704–0188*

Public reporting burden for this collection of information is estimated to average 1 hour per response, including the time for reviewing instruction, searching existing data sources, gathering and maintaining the data needed, and completing and reviewing the collection of information. Send comments regarding this burden estimate or any other aspect of this collection of information, including suggestions for reducing this burden, to Washington headquarters Services, Directorate for Information Operations and Reports, 1215 Jefferson Davis Highway, Suite 1204, Arlington, VA 22202-4302, and to the Office of Management and Budget, Paperwork Reduction Project (0704-0188) Washington, DC 20503.

1. AGENCY USE ONLY *(Leave blank)*	2. REPORT DATE June 2015	3. REPORT TYPE AND DATES COVERED Master's Thesis
4. TITLE AND SUBTITLE AN INNOVATIVE APPROACH FOR THE DEVELOPMENT OF FUTURE MARINE CORPS AMPHIBIOUS CAPABILITY		**5. FUNDING NUMBERS**
6. AUTHOR(S) Jeffrey D. Parker, Jr.		
7. PERFORMING ORGANIZATION NAME(S) AND ADDRESS(ES) Naval Postgraduate School Monterey, CA 93943-5000		**8. PERFORMING ORGANIZATION REPORT NUMBER**
9. SPONSORING /MONITORING AGENCY NAME(S) AND ADDRESS(ES) N/A		**10. SPONSORING/MONITORING AGENCY REPORT NUMBER**

11. SUPPLEMENTARY NOTES The views expressed in this thesis are those of the author and do not reflect the official policy or position of the Department of Defense or the U.S. Government. IRB Protocol number ____N/A____.

12a. DISTRIBUTION / AVAILABILITY STATEMENT Approved for public release; distribution is unlimited	**12b. DISTRIBUTION CODE** A

13. ABSTRACT (maximum 200 words)

The United States Marine Corps will bring toughness, vision, and refined tactics, techniques, and procedures (TTPs) from a 13-year desert fight into the next major combat operation or small contingency. This Marine Corps proclivity for action is reflected in driven Marines, doctrine and the personnel carriers or vehicles used by Marines to execute maneuver warfare from the sea. The first responder for the next contingency will likely be the Marine Expeditionary Unit (MEU), which is the smallest seabased configuration of a Marine Air Ground Task Force. The MEU provides rapid crisis response from U.S. Navy ships and is likely to be the principal component of the future force at sea. This research informs the top procurement priorities for the United States Navy by evaluating the MEU's expeditionary amphibious assault capability and the use of ship-to-shore connectors. In hundreds of thousands of simulated assaults, it identifies TTPs and mission profiles that achieve increased operational effectiveness, while employing less operational energy. The major results quantify the benefits of debarking amphibious forces at closer distances, show that a self-deployer presents a significant advantage to the landing force, and reveal the diminishing returns of high water speed.

14. SUBJECT TERMS agent-based, dashboard, design of experiment, amphibious combat vehicle, MANA , robust solution, simulation, amphibious assault, data farming, ship-to-shore connectors	**15. NUMBER OF PAGES** 181
	16. PRICE CODE

17. SECURITY CLASSIFICATION OF REPORT Unclassified	**18. SECURITY CLASSIFICATION OF THIS PAGE** Unclassified	**19. SECURITY CLASSIFICATION OF ABSTRACT** Unclassified	**20. LIMITATION OF ABSTRACT** UU

NSN 7540–01-280-5500

Standard Form 298 (Rev. 2–89)
Prescribed by ANSI Std. 239–18

THIS PAGE INTENTIONALLY LEFT BLANK

AN INNOVATIVE APPROACH FOR THE DEVELOPMENT OF FUTURE MARINE CORPS AMPHIBIOUS CAPABILITY

Jeffrey D. Parker, Jr.
Captain, United States Marine Corps
B.S., United States Naval Academy, 2006

Submitted in partial fulfillment of the
requirements for the degree of

MASTER OF SCIENCE IN OPERATIONS RESEARCH

from the

NAVAL POSTGRADUATE SCHOOL
June 2015

Author: Jeffrey D. Parker, Jr.

Approved by: Susan M. Sanchez
                    Thesis Advisor

                    Paul T. Beery
                    Co-Advisor

                    Eugene P. Paulo
                    Second Reader

                    Robert F. Dell
                    Chair, Department of Operations Research

THIS PAGE INTENTIONALLY LEFT BLANK

ABSTRACT

The United States Marine Corps will bring toughness, vision, and refined tactics, techniques, and procedures (TTPs) from a 13-year desert fight into the next major combat operation or small contingency. This Marine Corps proclivity for action is reflected in driven Marines, doctrine and the personnel carriers or vehicles used by Marines to execute maneuver warfare from the sea. The first responder for the next contingency will likely be the Marine Expeditionary Unit (MEU), which is the smallest seabased configuration of a Marine Air Ground Task Force. The MEU provides rapid crisis response from U.S. Navy ships and is likely to be the principal component of the future force at sea. This research informs the top procurement priorities for the United States Navy by evaluating the MEU's expeditionary amphibious assault capability and the use of ship-to-shore connectors. In hundreds of thousands of simulated assaults, it identifies TTPs and mission profiles that achieve increased operational effectiveness, while employing less operational energy. The major results quantify the benefits of debarking amphibious forces at closer distances, show that a self-deployer presents a significant advantage to the landing force, and reveal the diminishing returns of high water speed.

THIS PAGE INTENTIONALLY LEFT BLANK

TABLE OF CONTENTS

THIS PAGE INTENTIONALLY LEFT BLANK

LIST OF FIGURES

xiv

LIST OF TABLES

THIS PAGE INTENTIONALLY LEFT BLANK

LIST OF ACRONYMS AND ABBREVIATIONS

A2/AD	anti-access/area-denial
AAV	Amphibious Assault Vehicle
ACE	Aviation Combat Element
ACV	Amphibious Combat Vehicle
ADA	air defense artillery
ANOVA	analysis of variance
AoA	Analysis of Alternatives
AoR	Area of Responsibility
APC	armored personnel carrier
APOD	air point of debarkation
ARG	Amphibious Ready Group
ATF	Amphibious Task Force
BLT	battalion landing team
BN	battalion
C2	command and control
CAAT	combined anti-armor team
CAS	close air support
CASEVAC	casualty evacuation
CATF	Commander Amphibious Task Force
CERTEX	certification exercise
CI	confidence interval
CJTF	Combined joint Task Force
CLF	Commander, Landing Force (CLF)
CMC	Commandant of the Marine Corps
COMPTUEX	Composite Training Unit Exercise
CONOP	concept of operation
CR	crisis response
CSV	comma-separated values

DC	displacement craft
DES	discrete-event simulation
DOD	Department of Defense
DOE	design of experiments
E2O	Expeditionary Energy Office
EF-21	Expeditionary Force 21
EFSS	Expeditionary Fire Support System
EFV	Expeditionary Fighting Vehicle
ESG	Expeditionary Strike Group
EW 12	Expeditionary Warrior 2012
FARP	forward arming and refuel points
FCS	Future Combat Systems
FER	force exchange ratio
FLOT	forward line of troops
FOC	full operational capability
FPR	final project review
FSM	Free Savanna Movement
FT	fire team
GB	gigabyte
GCE	Ground Combat Element
GUI	graphical user interface
HA/DR	Humanitarian Aid and Disaster Relief
HMMWV	High Mobility Multipurpose Wheeled Vehicle
hr	hour
ICD	initial capabilities document
IED	improvised explosive device
IEEE	Institute of Electrical and Electronics Engineers
Inf	Infantry
IOC	initial operating capability
IQR	interquartile range

JFEO	joint forcible entry operation
JHSV	Joint High Speed Vessel
JP-5	jet propellant 5
km/hr	kilometers per hour
kts	knots
LAVGrp	light armored vehicle group
lbs	pounds
LCAC	landing craft air cushion
LCU	landing craft unit
LF	landing force
LHA	amphibious assault ship (general purpose)
LHD	amphibious assault ship (multipurpose)
LPD	amphibious transport dock
LSD	dock landing ship
m	meters
MAGTF	Marine Air Ground Task Force
MANA	Map Aware Non-Uniform Automata
Max	maximum
MCDP	Marine Corps Doctrinal Publication
MCO	major combat operation
MEB	Marine Expeditionary Brigade
MEDEVAC	Medical Evacuation
MET	Mission Essential Task
MEU	Marine Expeditionary Unit
Min	minimum
MLP	Maritime Landing Platform
mm	millimeter
MOE	measure of effectiveness
MOP	measures of performance
MPC	Marine Personnel Carrier

mph	miles per hour
MRAP	Mine-Resistant Ambush Protected
nm	nautical miles
No.	number
NOB	nearly orthogonal-and-balanced
NOLH	nearly orthogonal Latin hypercubes
NPS	Naval Postgraduate School
OE2	Operational Energy/Operational Effectiveness
OEF	Operation ENDURING FREEDOM
OIF	Operation IRAQI FREEDOM
OMFTS	operational maneuver from the sea
Ops	operations
OR	operations research
OTH	over the horizon
QRF	quick reaction force
RAM	random-access memory
RGB	red, green, and blue
ROMO	range of military operations
RWS	remote weapon station
SAR	search and rescue
SAS	Suite of Analytics Software
SBME	sea-based maneuver echelon
SE	systems engineering
SEED	Simulation Experiments & Efficient Designs
Simio	SImulation Modeling framework based on Intelligent Objects
SLEP	service life extension program
SOC	special operations capable
SOM	scheme of maneuver
SPMAGTF-CR	Special Purpose MAGTF-Crisis Response
SPOD	sea point of debarkation

SSC	ship-to-shore connector
STOM	Ship-to-Objective Maneuver
STOM-V/S	Ship-to-Objective Maneuver-vertically/surface
T/M/S	Type/Model/Series
TOS	time on station
TOW	tube-launched, optically tracked, wire-guided
TRL	technology readiness level
UAMBL	Unit of Action Maneuver Battle Lab
UHAC	Ultra Heavy-lift Amphibious Connector
U.N.	United Nations
USMC	United States Marine Corps
USS	United States Ship
VBA	visual basic for applications
VBSS	visit, board, search, and seizure
VMM	Marine Medium Tiltrotor Squadron
WAF	West African Federation
WBS	work breakdown structure
XML	EXtensible Markup Language

THIS PAGE INTENTIONALLY LEFT BLANK

EXECUTIVE SUMMARY

In the wake of cost overruns the Expeditionary Fighting Vehicle in 2011 was terminated, and the U.S. Marine Corp transitioned to a tough amphibian, the Amphibious Combat Vehicle (ACV). This vehicle, in its current increment, will leverage ship-to-shore connectors (SSCs) to meet the challenges presented from objective maneuver from the sea (OMFTS). Marines perform amphibious operations with forces that are scalable and tailorable, meaning that these operations may elevate from a benign landing (e.g., New Orleans during Katrina) to a joint forcible entry operation (e.g., Omaha Beach) on distant shore. Incidentally, amphibious operations are highly complex, which raises many questions:

- Does the U.S. Marine corps require a self-deploying capability similar to the legacy Amphibious Assault Vehicle (AAV), which conducts ship to objective maneuver (STOM)?

- What are the right measures of performance (MOP) for an amphibious operation, namely a system of connectors delivering many systems of amphibious combat vehicles?

- What ranges from the shore and speeds present challenges to an amphibious operation given modern technology?

- What are the impacts and drivers of operational energy and how can the U.S. Marine Corps maintain mission effectiveness?

- Are there solutions that afford the same operational effectiveness, yet reduce operational energy from the seabase being distributed?

This research uses a two-stage simulation to model an end-to-end amphibious assault, which addresses these questions. The sponsor for this research was the Expeditionary Energy Office (E2O), USMC. Initial progress reviews revealed that the Marine Corps has many spreadsheet-based and specific tools; however, the stakeholder needed a broad analysis of expeditionary operations. The top acquisitions priority for the Marine Corps pertains to Title 10 amphibious requirements. Thus, a broad analysis for an amphibious operation is conducted. A discrete event simulation in a Simulation Modeling framework based on Intelligent Objects (Simio) models aircraft launch constraints from

the seabase. Meanwhile, an agent-based adversarial model in Map Aware Non-Uniform Automata (MANA) models the amphibious assault.

Once the model structure was established, the author used a model-test-model approach that refined terrain, adversary capabilities, and landing force scheme of maneuver (SOM) to gain operational insights. Many hundreds of thousands of simulated amphibious assaults were conducted with a broad range of parameters in efficient, space-filling experiments, involving 77 mixed (i.e., discrete and continuous) factors with 512 design points for four different scenarios. Run times for a single experiment took approximately 10 minutes, so the excursions were completed using a high-performance computing cluster. In the end, advanced metamodels were selected from linear, non-linear, regression, and partition tree analyses.

The ACV, AAV upgrade, and next SSC all present major Department of Defense programmatic decisions. This research informs these decisions leveraging a traceable scenario throughout to better assist decision makers in providing the warfighter the right capabilities. The major findings follow.

- STOM-vertically (STOM-V) presents a future challenge for the Marine Corp—not in the distance that can be covered, but in the force protection provided to Marines once on the ground.

- The adversary will be highly influenced by the ends, ways, and means of an attacking force during amphibious assault.

- The ACV swim and on-land speed do not need to be as fast as current top capabilities.

- An ACV with an autonomous ship-to-shore increment (i.e., self-deployer) presents a significant advantage to the landing force.

- Distances offshore can range as far as 12 nm without interference to the amphibious assault.

- Different types of urban terrain may degrade the defending forces ability to target the landing force.

This thesis provides an innovative approach for developing meta-models of operational effectiveness. These meta-models are part of a prototype "dashboard" for

E2O that links operational effectiveness and operational energy to facilitate trade-space explorations.

In summary, the force that responds to the next crisis or contingency will be the force that is closest to it—the Marine Expeditionary Units (MEUs) embarked on ships. This research is leaning forward by making a first attempt at modeling an end-to-end amphibious assault. In hundreds of thousands of simulated amphibious assaults, we observe the trade-space formed by the many complex parameters considered when employing concept complementary platforms of surface and vertical ship-to-objective-maneuver. In the end, we realize quantifiable values that maximize mission effectiveness and better inform the top procurement priorities for the United States Naval forces.

THIS PAGE INTENTIONALLY LEFT BLANK

ACKNOWLEDGMENTS

THIS PAGE INTENTIONALLY LEFT BLANK

I.   INTRODUCTION

The farther backward you can look, the farther forward you can see

—Winston Churchill
Prime Minister of the United Kingdom,
October 1951–April 1955

A.   PURPOSE

The purpose of this research is to further analyze complex, amphibious operations in anti-access/area-denial (A2/AD) situations, based on a traceable scenario, in order to provide a tool for decision makers to explore operational effectiveness and operational energy in amphibious operations. The United States Marine Corps (USMC) has been using amphibious vehicles for launching assaults from the sea since 1776, but modern-day circumstances are driving the need for an agent-based tool—primarily, the advent of expensive technology in the amphibious vehicle capability and the variety of equipment that can be based at sea against an adaptive adversary. The Marine Corps can explore new technology based at sea in a cost-effective environment that allows stakeholders to visualize billions of dollars of equipment prior to it being procured. This thesis uses campaign analysis techniques, agent-based simulation, and discrete event simulation in a broad analysis of conceptual ship-to-shore connectors and developing Marine amphibious combat vehicle technology during a seabased amphibious assault.

The principal arm for scalable Marine amphibious operations is the Marine Expeditionary Unit (MEU). In order to provide rapid crisis response from U.S. Navy ships, the MEU must be highly trained to this end, the over 2,200 Marines and hundreds of aircraft in a MEU regularly conduct a minimum of six months of work-ups, followed by certification-at-sea periods, and deployments around the globe. The principal benefit of this thesis is incorporating the findings of this research and applying them to persistent, regularly scheduled operations. Findings that, once applied to all seven of the currently active MEUs, may very well influence operational energy consumption for the United States. This effect would be multiplied annually by the three operational and four in reserves, rotation cycle of the MEU. Even MEUs that are not deployed operationally,

those conducting work-ups to replace them, conduct hundreds of theater security cooperation and training operations. Furthermore, the agent-based model employed in this analysis is unlike any other—for it models that which has been too complex to model until now—amphibious assault.

B.   BACKGROUND

The amphibious combat community is highly capable, and the aim of this research is to help inform the vision of the future amphibious assault force. To better serve the leadership of Marines fighting in future wars and to aid in making better data-driven decisions, this model tackles what has been avoided for too long due to complexity—modeling the amphibious assault. Marines need a tool that attacks the complex, ship-to-shore amphibious transition with the same level of intensity that they will be expected to produce when they launch an amphibious assault. Additional motivation for this thesis stems from combined research between the Operations Research (OR) and Systems Engineering (SE) Departments at the Naval Postgraduate School (NPS). Professors from both departments at NPS have dedicated much of their research to providing a dashboard for the United States Marine Corps that uses ensembles of models, commonly referred to as metamodels, to show operational energy and operational effectiveness. The author is incorporating work from a year-long SE capstone, *Operational Energy/Operational Effectiveness Investigation for Scalable Marine Expeditionary Brigade Forces in Contingency Response Scenarios* (Team Expeditionary & Cohort 311-132, 2014) to further investigate the feasibility of using amphibious assault operations with future programs and technology, such as concept ship-to-shore connectors (SSCs), amphibious combat vehicles (ACVs) and other Marine Personnel Carriers (MPCs). Sponsoring this research is the Marine Corp's Expeditionary Energy Office (E2O). In 2009, then Commandant of the Marine Corps (CMC), James T. Conway, formed E2O to "analyze, develop, and direct the Marine Corps' energy strategy in order to optimize expeditionary capabilities across all warfighting functions" (Marine Corps Expeditionary Energy Office [E2O], 2012). The modeling implemented in this thesis is currently being used by a second systems engineering research team in support of their master's research, and lays the groundwork for further studies as well.

C. OBJECTIVES

This research is guided by the following research questions, whereby the measures of effectiveness (MOEs) are mission time, friendly casualties, and Red casualties:

- What are the ACV measures of performance (MOPs) that positively contribute to the MOEs?

- What are the SSC MOPs that positively contribute to the MOEs?

While we do not know exactly what enemies future Marine amphibious combat systems will face, it would be unwise to assume away the threat and that future adversary as being anything less than formidable, adaptive, and located deep inside a complex coastal defense. While the U.S. has invested in ships, other states have taken advantage of more affordable coastal defense missile systems. The natural defense created by the terrain of sea, surf, and sand gives an edge to the enemy. This is further complicated by asymmetric threats, A2/AD capabilities, and modern warfare technologies, making it difficult for decision makers to select the right capabilities amid uncertainty. In order for Marine leadership to continue to function and successfully conduct amphibious assault operations, new technology must be robust to a variety of missions and scenarios. This research delivers results, facts, and a *tool* for the future rapid, data-driven decision making—appropriate for Marines to adopt and use to destroy the enemy.

D. SCOPE

The primary focus of this thesis is to quantify the benefits of distributing assets among platforms found in seabase operations during an amphibious assault. In support of that focus, this thesis develops a visualization tool of the amphibious assault operation. This thesis uses agent based simulation software, Map Aware Non-uniform Automata (MANA, version 5.0 [V]), and discrete event simulation software, SImulation Modeling framework based on Intelligent Objects (Simio, version 7.0), to develop scenarios and simulations. The MANA and Simio scenarios and simulations used work well with numerous vertical and surface Marine platforms. The Simio simulation is particularly useful to realize the benefit to operating Marine aircraft distributed across air capable

ships. Meanwhile, the MANA scenario uses a large number of agents and decision factors to model everything from an M1A1 tank, to an SSC, to a Marine infantry fire team (FT).

The following five chapters develop an innovative approach for the expansion of future Marine Corps amphibious capability using simulation modeling. Amphibious operations require logistics. As a result, others have developed several limited tools implementing visual basic for applications (VBA) and discrete-event simulations (DES) to calculate massing force ashore absent the enemy. These tools may include stochastic elements, but are incapable of providing insight when an adaptive adversary is present. In contrast, the research in this thesis is unique, combining both discrete and agent-based simulations to explore a range of specifications and impacts on operational energy and operational effectiveness in likely amphibious scenarios against an enemy. Chapters I and II introduce the research and the approaches made by others to model amphibious operations. Chapters III and IV cover the two simulation methodologies, namely agent based and discrete-event simulations. Chapter VI and VII cover the quantitative analysis, conclusions, and recommendations as they pertain to energy insights, operational insights, and future work.

II. LITERATURE REVIEW

A. AMPHIBIOUS OPERATIONS

There is much written from great and experienced military theorists, such as Sun Tzu, Carl Von Clausewitz, and Alfred Thayer Mahan, which the U.S. Armed Forces use to be prepared for positions of operational leadership, and to think strategically about all types of wars and the means used fight them (U.S. Naval War College, 2015). While all three theorists may not agree on how best to conduct forcible entry from the sea, Griffith's rendition of Sun Tzu's 'The Art of War' says, "attack where he is unprepared," and seabased forces provide this capability (Griffith, 1971, p. 69). Where disagreement may also arise is, which of the multifaceted technologies of today best help accomplish this mission? Undoubtedly, what is not covered by history is modern-day, complex, concept platform integration. Developments of new SSCs and armored personnel carriers (APCs) (e.g., ACVs, MPCs, etc.) can be defined in terms of specifications and system performance, typically quantified as MOPs. Yet, it is often the systems of systems that contribute toward mission accomplishment, typically quantified as MOEs. Amphibious assault, and the technological advancements made therein, present unique challenges to the adversary. Platform-intensive operations, however, significantly increase the complexity of battle. So, while belligerent nations must defend their coasts against a hovercraft that can carry a formidable force quickly from well over the horizon (OTH), this capable connector is susceptible to battle damage and breaking down. If we assume no battle damage to vehicles, and no personnel destroyed, as with most DESs and calculators, then we fail to capture what centuries of theorists have been saying not to discount—the enemy. Hence, this research considers the impact of the enemy on the mission, rather than MOPs that only focus on the isolated performance of each system.

A counter argument to logistic calculators and complex platforms is the impact of U.S. Marine Corps leadership, bravery, and experience—all of which provide a formidable edge that is unquantifiable. The Marine Corps history of amphibious operations stretches from 1776 to 2006. While the Bahamas in 1776 represent the first amphibious operation, Veracruz, in 1846, was the first major joint amphibious operation.

Marine Captain Alvin Edson led a battalion (BN) of Marines on 9 March 1846, thus executing the first joint forcible entry operation (JFEO), with the support of over 8,000 soldiers, sailors, and Marines (U.S. History., 2015). Few real-time analysis tools have been made with the modernizations of amphibious assault technology in mind. As we explore past studies, according to Clausewitz's *On War:* "Critical analysis is not just an evaluation of the means actually employed, but of *all possible means*—which first have to be formulated, that is, invented. One can, after all, not condemn a method without being able to suggest a better alternative" (Howard, Paret, & West, 1984, p. 161). To this end, this research aims to build on other work that incorporates a vast breadth of research investment into making the Marine Corps an even more capable force.

This section addresses some of the misperceptions of amphibious operations. In his memoirs, Sir Walter Raleigh wrote, "It is more difficult to defend a coast than to invade it" (Edwards, 1868, p. 239). According to Col. Theodore L. Gatchel, USMC (Ret.), "Americans can always refuse to pay for maintaining an amphibious capability, thereby giving up what Liddell Hart calls 'the greatest strategic asset that the sea-based power possesses.' If Americans should choose to take such a step, they will have, in effect, accomplished what no enemy has managed to do: defeat a modern amphibious operation" (Gatchel, 1996, p. 217). History only gives us so much as we prepare for future wars. Meanwhile, the "record of amphibious warfare in the twentieth century seems to validate Sir Walter Raleigh's assessment that defending against an amphibious operation is more difficult than conducting one" (Gatchel, 1996, p. 216). Amphibious operations include two opposing forces: the defender and the attacker. There is a common perception that the attacker in an amphibious operation incurs high risk and with that, higher numbers of casualties. Gatchel offers, this reputation is from few, notorious landings that resulted in historic levels of casualties only after the force was ashore. Amphibious operations where high casualties were incurred as a result of the amphibious operation were Tarawa and Omaha Beach at Normandy (Gatchel, 1996). Seldom are casualties attributed to the character of the amphibious operations, which is further exemplified by the safe landings at Guadalcanal and Okinawa. During both of these operations Marines encountered formidable defensive forces, not during the landing

itself, but during the taking of the island. Colonel Gatchel offers that both Guadalcanal and Okinawa fuel the misperception of amphibious assault with high casualties that were incurred long after forces were massed ashore (Gatchel, 1996).

1. *Distributed Combat Systems*

Spreading out combat power can mitigate the risk associated with amphibious operations. One way to minimize risk in land, air, naval, amphibious, and now cyber operations is through survivability distribution (Hoe, 2001). According to Captain Keith Jude Hoe, Singapore Armed Forces, and NPS student, a potential benefit to dispersed seabased operations is that multiple platforms reduce risk. For example, Captain Hoe found that staying power does not increase much with increased tonnage or size. Moreover, that a ship that displaces 7,000 tons or less requires approximately a single hit from an *Exocet* missile, while a larger, 90,000-ton ship requires only 2.3 missiles, based on a proportional increase in missiles required. This, he continues to say is a "phenomenon that poses a dilemma for naval planners" (Hoe, 2001, p. 38). Is it advantageous to build a massive ship with awesome firepower that has limited staying ability, or many smaller ships that aggregate to both massive firepower and staying ability? The Marine Corps is facing a similar challenge with SSC. Arguably, a large, lone connector, exemplified by the concept Ultra Heavy Lift Amphibious Connector (UHAC) or concept SSC, fully loaded, masses force ashore in a similar manner as the 90,000-ton ship masses firepower. Meanwhile, a smaller SSC or self-deploying Amphibious Assault Vehicle (AAV) increases survivability—and resilience—by distributing Marines across MPCs capable of withstanding a collective increase in missile strikes.

The Marine Corps is not alone in its interest in distributed operations. The Army's Future Combat System (FCS) though eventually cancelled, was envisioned for distributed operations (Unit of Action Maneuver Battle Lab [UAMBL], 2003). The FCS was an example of a major Army acquisitions modernization program with many subsystems. Some of these included weapons systems and others included communications equipment; however, all of these components were intended to network together to form a tough combat unit. The FCS brigade was designed to be both expeditionary in nature,

and able to conduct day and night distributed operations. Since the FCS represented many systems, the loss of one subsystem in battle would not mean the loss of the whole.

2. The Role of Connectors in Amphibious Operations

Ship-to-shore (sometimes called seabase-to-shore) connectors play an important role in amphibious operations, and model-based tools that provide insight about their effectiveness could be beneficial to decision makers. Few tools exist, and those that do have limitations. For example, the SSC Analysis of Alternatives (AoA) conducted in 2007 illustrates the complexity of modeling SSCs and amphibious operations coupled with the inadequacies of spreadsheet modeling (Department of the Navy, 2007). This AoA focus is on the mission of providing ship-to-shore transport of joint forces within Ship-to-Objective Maneuver (STOM) and other assault and non-assault (e.g., humanitarian, etc.) operations launched from the Seabase. The methods used in the SSC AoA "developed an EXTEND [discrete event simulation] DES model and three spreadsheet models to prepare the simulation inputs" (Department of the Navy, 2007, p. 27). The performance, loading, transport, and transport plan models were run for a baseline major combat operation (MCO) MEB scenario. The initial capabilities document (ICD) .

> identified two broad categories of materiel solutions: air cushion vehicles (ACV) and wheeled/tracked displacement craft (DC). The ACV [not to be confused with amphibious combat vehicle] solutions were the existing Landing Craft Air Cushion (LCAC), LCAC Service Life Extension Program (SLEP), new procurement LCAC SLEP, and a new technology ACV. The DC alternatives were wheeled or tracked monohulls and a wheeled or tracked catamarans. (Department of the Navy, 2007, p. ES-1)

This AoA has been heavily criticized due to unexplained or missing data, along with an entire portion that was information copied verbatim from a paragraph earlier in the report. One example of unsupported data is according to this AoA, aviation assets cannot lift "26%" to "28%" of a Heavy Brigade Combat Team (Department of the Navy, 2007, p. 1). No evidence or explanation is provided for the numbers 26% and 28%. Similarly, it is difficult to understand just what the AoA is talking about when it says, "86% of the 2015 MEB sea-based maneuver echelon (SBME) surface task forces' vehicles and equipment will need to be carried ashore via non-air (surface) assets for a STOM surface assault"

(Department of the Navy, 2007, p. 1). Why only 86%? And, why only surface assets, when much investment has been made in the CH-53K external lift capability? The AoA's unsupported numbers and vague derivations make it a point of study in Advanced Combat Modeling at NPS. What this AoA does show, however, is that accurately depicting the complex nature of amphibious operations is very difficult. Spreadsheet tools and rounded percentages (e.g., 86%) deny decision makers the benefits of *seeing things move and interact*. Since the adversary is highly adaptive, so too must be the tools produced for decision makers.

3. **Exploring the Reduction of Fuel Consumption for Ship-to-Shore Connectors of the Marine Expeditionary Brigade**

Similar limitations are evident in recent research for evaluating fuel inefficiency in the wake of vehicle modifications. An SE capstone group leveraged a fictional Marine Corps Title 10 scenario, EW 12, set in Africa 2024, in order to provide traceable analysis for the E2O. This research benefitted from observing SE's dedication of time and effort to work breakdown structure (WBS) and needs analysis. Nevertheless, according to Lieutenant Stephen "Jack" Skahen, United States Navy, Michael Boyett, Michael Brookhart, Steven Benner, and Josue Kure, since the adversary often lacks traditional warfighting methods compared to U.S. forces, technological inferiority has led nonpeer adversaries to adopt improvised explosive devices (IEDs) on the battlefield (Skahen, Benner, Boyett, Brookhart, & Kure, 2013, p. 2). Nevertheless injured and dead personnel "from IEDs in the theaters of Operation Enduring Freedom (OEF) and Operation Iraqi Freedom (OIF) increased, the amount of armor per vehicle and the number of vehicles required has grown, reducing the fuel efficiency and increasing the dimensions and weights of the vehicles that are deployed" (Skahen et al., 2013, p. 32). ExtendSim discrete-event simulation revealed that "Seabase Distance and Sea State" impact mission time and fuel; moreover, that the Landing Craft Unit (LCU) "may be able to provide better fuel economy over employment of the LCAC" (Skahen et al., 2013, p. XXIV). Still, absent from this analysis are a closer look into distributed seabased operations across both vertical and surface means of STOM (e.g., STOM-vertically [STOM-V], over

the horizon [OTH], and by STOM-surface [STOM-S]), a self-deploying Marine amphibious combat vehicle, and, above all else, battle damage.

4.   Operational Energy/Operational Effectiveness Investigation for Scalable Marine Expeditionary Brigade Forces in Contingency Response Scenarios

This study shifts the focus to evaluating fuel in an adversarial environment. "Operational Energy/Operational Effectiveness (OE2) Investigation for Scalable Marine Expeditionary Brigade Forces in Contingency Response Scenarios" is an NPS SE capstone report. The group of students that authored the capstone was called "Team Expeditionary" and their project focused on EW 12, Phase III of the Title 10 wargame. Phase III, EW 12, focuses on Humanitarian Aid and Disaster Relief (HA/DR). Previous capstone groups focused their studies on logistics and SSC, as seen with EW 12, Phase II, (Besser et al., 2013) and Phases I and II (Skahen et al., 2013). This thesis combines the collective efforts of operations research with these SE capstone projects, in order to provide an innovative tool for the future development of amphibious technology. After revisiting the stakeholder's needs after the final project review (FPR), E2O expressed an interest in a broader agent based amphibious assault simulation. The FPR to E2O concluded that a principal finding of the capstone that rated further exploration was how platforms support JFEO from the seabase. Specifically, it was insightful to realize that variations in the number of platoons of Marines ashore has great effect in necessary Quick Reaction Force (QRF) and Medical Evacuation (MEDEVAC) fuel usage from energy drivers such as the MV-22 and CH-53K. STOM-V consists of rotor and tilt rotor aircraft. Figure 1 shows energy impacts for QRF and MEDEVAC operations for platoons of size three, four, and five, which are blue, red, and green, respectively. Powering up results like those shown in Figure 1 are integral to better understanding energy drivers in amphibious operations, which are larger than patrolling operations with platoons of size three, four, and five.

	QRF/CAS Insertion	Close Air Support	MEDEVAC	QRF/CAS Withdrawal	Logistics Resupply	Ground Mission
3-Platoon	1142.68	802.51	1779.27	1142.68	333.88	23.47
4-Platoon	1755.02	787.37	1779.27	1755.02	333.88	22.37
5-Platoon	2731.15	817.65	2670.02	2731.15	333.88	29.71
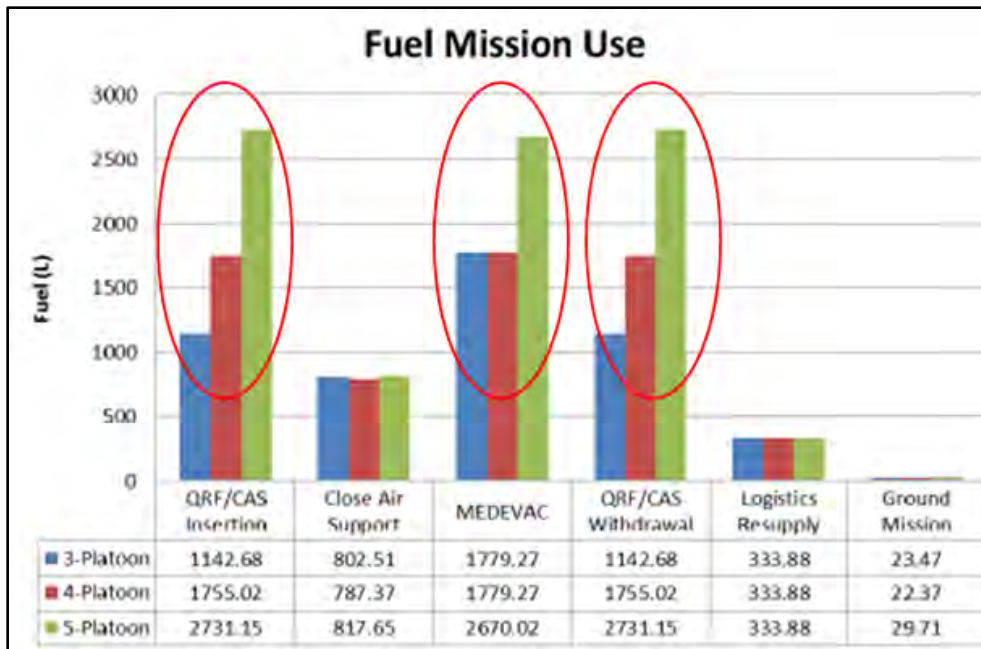
Figure 1.   QRF/Close Air Support (CAS) Insertion, MEDEVAC, and
QRF/CAS Withdrawal for 3-Platoon, 4-Platoon, and 5-Platoon have
higher Fuel Mission Use than Close Air Support, Logistics
Resupply, and Ground Mission
(from Team Expeditionary & Cohort 311-132, 2014).

Jet Propellant 5 (JP-5) is the jet fuel used by U.S. Navy aircraft and SSC. The transition from legacy platforms to new aircraft has increased both capability and fuel consumption. For every upgrade in technology (e.g., MV-22 replaced the legacy CH-46 for medium lift) there was a corresponding impact in fuel consumption. As a for instance, if there was a 300% increase in fuel consumption by the MV-22 from the CH-46—that the MV-22 is 300% more capable conducting medium lift missions. Nevertheless, the preponderance of Marine assets regularly being deployed is part of the Aviation Combat Element (ACE), which is the air component of the MEU. Exploring both split operations and disaggregate operations is a direct result and continuation of this December 2014 capstone project. Further examination of fuel usage effect on QRF and MEDEVAC operations by prepositioning ACE forces and cross decking air assets to other air-capable ships in the seabase links this thesis to the capstone project. Increased analytics will further the work and time invested in the research requested by E2O.

B.   GENERAL DESCRIPTION OF THE MARINE CORPS SCALABILITY AND AMPHIBIOUS ASSAULT

There is one tactical principal which is not subject to change. It is to use the means at hand to inflict the maximum amount of wounds, death, and destruction on the enemy in the minimum amount of time.

Gen. George S. Patton
Speech to the Third Army (1944)

The complex Expeditionary Fighting Vehicle (EFV) or Advanced Amphibious Assault Vehicle is designed to take Marines from Navy ships to the objective. The hope is to finally replace the legacy AAV-7A1 Amphibious Assault Vehicle, which provides neither the armor nor speed required today. Unfortunately, cost overruns contributed to the cancellation of the EFV in 2011. According to an Institute of Electrical and Electronics Engineers (IEEE) columnist, Robert N. Charette, "the Pentagon now spends about $21.6 million every hour to procure new military systems. As the cost and complexity of defense acquisitions programs continue to spiral out of control, many defense experts believe runaway military spending is unsustainable" (Charette, 2008, p. 1). The Marine Corps needs an affordable tool to help determine the right mixture of ship-to-shore connectors and amphibious personnel carriers to conduct JFEO.

1.   The Environment

In 2014, the nation and the Department of Defense (DOD) felt the impacts of sequestration. DOD acquisitions system for products and services can always do better, since "soldiers in the field are being denied much-need equipment, while civilian programs go unfunded" (Charette, 2008, p. 1). There are impacts from sequestration; among them, it blocks the armed forces' ability to modernize through new programs. Often such delays can further impact program budgets, creating unforeseen costs. With most government contracts, once the contract has been awarded the DOD starts paying even if the government elects to shut down. The DOD acquisitions environment is further complicated as the "tide of war is receding" (Obama, 2011, p. 2) in the Middle East and the emphasis shifts to Asia and the Pacific. Put simply, war-driven, urgent requirements

will be less and less (e.g., Mine-Resistant Ambush Protected [MRAP] vehicles needed due to IEDs) and the products and services procured during the pivot to the Pacific will be done in a fiscally constrained economy. Nevertheless, the challenge facing decision makers is achieving a better fighting force that balances force modernization, sustainment, force structure. A first steps towards addressing this challenge is leadership communicating their policy objectives. The Marine Corps has taken the lead to this end. Then Commandant General James Amos signed the capstone document for the twenty-first century USMC: Expeditionary Force 21 (EF-21). It provides direction. With this policy, the USMC will hopefully make better investments in the right capability. In his article, Dr. Axe highlights a consequence that "After an investment of 15 years and $17 billion, today the Army is still struggling to build better radios and estimates it may need to spend another $12 billion to get what it needs" (Axe, 2012, p. 1). Detailed Marine Corps policy and data-driven decisions from inexpensive simulation tools will provide insights in how to achieve powerful, future warfighting equipment.

2. Marine Corps Background

The Marines have landed and the situation is well in hand.

—Attributed to Richard Harding Davis (1864-1916)
First American correspondent to cover the Spanish-
American War and the First World War

This section covers a top-down look at the Marine Corps Title 10 obligation, namely to have an amphibious operations capability.

a. United States Marine Corps

The USMC is the United States' force-in-readiness. Required readings for all Marines are capstone publications like EF-21, called the Marine Corps Doctrinal Publications (MCDPs). MCDP 3, *Expeditionary Operations*, describes the naval and expeditionary character of Marine forces (Department of the Navy, 1998). During the past 13 years, while Marines focused primarily on MCO in Iraq and Afghanistan, concurrent amphibious operations took place aboard amphibious ships. Marines embark

aboard Navy ships and sail around the world, training host nations and supporting crisis response (CR), as they have done so often in their past. While the concept of a tailorable, scalable MAGTF may be new—the importance of being expeditionary is rooted in numerous historical examples. Furthermore, being expeditionary is *key* to the existence of and the *why* for having a Marine Corps, which includes operational maneuver from the sea (OMFTS). OMFTS and the means to get Marines ashore support "As a global power with global interests, the United States must maintain the credible capability to project military force into any region of the world in support of those interests. This includes the ability to project force both into the global commons to ensure their use and into foreign territory as required" (Dempsey, 2012, p. 2). The Marines Corps brings with it a litany of experience in amphibious operations. To name a few, Marines were embarked with the Continental Navy during the American Revolution; crossed the Gulf of Mexico during the Mexican-American War; and fought at the Battle of Hampton Roads during the Civil War, in both Europe and the Pacific during World War II, in Korea, in the Cold War, and most recently in Iraq and Afghanistan (Symonds, 1995). Less known instances where Marines have answered the "amphibious" call are Lebanon (1958), post Hurricane Katrina in New Orleans (2005), and during relief in Haiti (2010). Marines enjoy centuries of lessons learned and over a decade of recent wartime experience that can be applied in their next expeditionary amphibious operation.

b. *Marine Expeditionary Brigade*

Historically, the Marine Corps leverages a combination of embarked air and ground forces in sourcing amphibious operations. A MEB is the second largest MAGTF of approximately 15,000 Marines and Sailors. Its comprised of the four elements ground, logistics, air, and headquarters. All can vary in size to meet the commander's needs. Nominally it includes a reinforced infantry regiment, a Marine aircraft group, a combat logistics regiment, and a command group (Trickey, Benbow, & Taylor, 2010). There are three MEBs: the 1st, 2nd, and 3rd Marine Expeditionary Brigades based in California, North Carolina, and Japan, respectively. Recent operations such as Operation Iraqi Freedom, with Task Force Tarawa, and Operation Enduring Freedom, with Task Force Leatherneck, called upon Marines from 2nd MEB and 1st MEBs as part of the initial

invasions. The MEB construct has a purpose, as the scalable nature of MEBs is well-suited for addressing weak/failed states and asymmetric threat environments. While a full MEB may be used for MCO, and may first need to be embarked as part of an Expeditionary Strike Group (ESG), smaller elements (e.g., 2,000 Marines) regularly deploy as part of six-month rotations, as required. As the Marine Corps transitions away from land warfare and conducts increased amphibious operations, a smaller force that can scale up to an MEB and can regularly deploy is required. This force already exists and it is called a MEU.

c.   *Marine Expeditionary Unit*

The Marine Corps routinely projects power from the sea through forward-deployed MEUs; the principal component of the MEB. The battalion landing team (BLT) Marines and MEU supports the introduction of follow-on forces and can support special operations. The MEU is cyclical, expeditionary, self-sustaining, and able to complete a myriad of missions from the MEU Mission Essential Tasks (METs). MEUs often complete a certification period, i.e., a certification exercise (CERTEX), which enables them to demonstrate MET capabilities in completing a range of military operations (ROMO). For example, an MEU conducts numerous visit, board, search, and seizure (VBSS) and long-range raid training missions prior to attempting real-world VBSS or HA/DR operations. These "work-up" periods are six months long, providing the ACE, Ground Combat Element (GCE), and Amphibious Ready Group (ARG) with opportunities to combine and train to full operational capability (FOC). The MEU is to the MEB what the ARG is to the ESG: a smaller component of modular construct that enables tailorable force structure from the sea. To support the rotation, there are seven MEUs: three on the East Coast, three on the West Coast, and one in Japan. Additionally, two Special Purpose MAGTF-Crisis Response (SPMAGTF-CR) bases, in Spain and Africa, provide persistent forces close to areas of uncertainty, which may be reinforced and called on to support the modular nature of Marine expeditionary operations. The SPMAGTF-CR, however, does not project power from sea bases. Nevertheless, the MEU is capable of conducting OMFTS form surface and vertical sea based means deployed today.

d.   Sea Bases

A2/AD compels expeditionary bases and sites, namely sea-basing, in order to support maneuver warfare and logistics. Before cyber operations, amphibious operations were unique in that they occurred on the sea, land, and in the air. With so many unique capabilities (AAV, ACV, MV-22, F-35B, etc.) the MEU commander has a tough decision given the limited capacity aboard ships. Rarely will MEUs deploy configured the same, meanwhile "Forward-deployed ATFs are normally organized into ARGs with three amphibious warfare ships (an amphibious assault ship [general purpose] [LHA]/amphibious assault ship [multipurpose] [LHD], amphibious transport dock [LPD], and dock landing ship [LSD])" (Department of Defense, 1992, II-6). Similarly, there are limitations with well deck and flight deck capacity (with the exception of LHA-6 and LHA-7), as to how it embarks, deploys, and launches tilt-rotor aircraft, helicopters, landing craft, amphibious vehicles, etc. (USMC Amphibious Operations, 2014). The "amphib" has two variants:

> The LHD and LHA each has a full length flight deck and hangar to support helicopter, tiltrotor, and vertical/short take-off and landing aircraft [e.g., F-35B]. Well decks provide for ship-to-shore movement of landing craft and Amphibious Assault Vehicles (AAVs). The Commander Amphibious Task Force (CATF) and Commander, Landing Force (CLF) and their staffs are normally embarked on these ships. (Department of Defense, 1992, II-6)

The sea base allows for landing area selection. While the United States has invested in capital ships, adaptive adversaries have developed coastal missile defense systems, which make it no longer tactically prudent to park warships offshore.

e.   Distributed and Split Operations

ARG/MEU employment does not restrict commanders to keeping the three ships in a close, tight formation. Thus, ARG shipping may consider a wide formation and the MEU commander may elect to spread detachments of Marines across several ships, thus splitting up the force. The *split* or *disaggregated* manner increases the flexibility, capability, and scope of the MEU. Split operations are generally closer than disaggregated operations. For example, "After completing a rigorous six month work-up

cycle, the 15th MEU set sail for its western pacific deployment May 2010, during which time the 15th MEU conducted numerous operations and exercises in dozens of countries" (15th Marine Expeditionary Unit [MEU], 2012, p. 1) During this deployment, the "15th MEU's Force Recon Platoon executed the first opposed VBSS mission in Marine Corps history in 100 years aboard a captured vessel, and rescued the crew without one shot being fired" (15th MEU History, 2012, p. 1). Concurrently, the LHD responded to "torrential rains [that] ravaged Pakistan and caused major flooding…to conduct Humanitarian and Disaster Relief. While operations were conducted in Pakistan, the 15th MEU also provided air support to OEF in Afghanistan. The 15th MEU Harriers conducted over 300 close air support sorties from August until October" (15th MEU History, 2012, p. 1). Spreading the ACE and GCE force across several ships reduces the risk of losing the whole MEU if a single ship is destroyed. Splitting the ACE among the LHD and LPD, which are both air-capable ships, also decreases the density of aircraft on the flight deck.

f. Operational Maneuver from the Sea

OMFTS combines the strengths of maneuver and surprise against the adversary. In 2001, the

> Marines and Sailors of the 15th MEU, special operations capable (SOC), conducted an amphibious assault over 400 miles into the land-locked country of Afghanistan . . . and set new standards for Marine Corps amphibious doctrine. Landing at a remote airbase, 90 miles southwest of Kandahar, the Marines established Camp Rhino, America's first Forward Operating Base while maintaining the first significant conventional ground presence in Afghanistan. (15th MEU History, 2012, p. 1)

Operational maneuver is the "marriage between maneuver warfare and naval warfare" (U.S. Marine Corps., 1998, p. 28). The adversary has to decide how and where it will defend its shore. Seldom does the BLT ever really concern themselves with where, resolving that leadership will pick the right location away from the adversary. Figure 2 shows an AAV launching from the well deck of the "amphib."

Figure 2.   An AAV debarking from an amphibious assault ship USS Bataan (LHD-5). AAVs in operation today are over 40 years old (from Eckstein, 2015).

Advancements in technology, similar to the one seen in Figure 2 from so many years ago, allow both the adversary and the seabase to cover more ground. This poses new questions: What does it mean to be beachable? What does it mean to be amphibious? And, what connects the ship effectively to the shore? Types of connectors include the Maritime Landing Platform (MLP), Joint High Speed Vessel (JHSV), LCAC, UHAC, and LCU, to name a few.

g.   *Amphibious Assault*

Taking Seoul during the Korean War in 1950 is an example of OMFTS. Amphibious assault, however, implies an opposed landing. Ideally, the MEU CATF would like to conduct an unopposed amphibious landing quickly from OTH. As the LF presses inland, "from naval warfare . . . the advantages inherent in sea-borne movement, and the flexibility provided by sea-based logistics" would fuel and supply the forward line of troops (FLOT) all the way to the objective (OMFTS MCDP, 2001, p. 28). How far Marines can conduct vertical amphibious landings has changed with the advent of extended reach from the MV-22. Increased concerns from IEDs and mines have caused

unease with the legacy tracked AAV that is currently in use. Nevertheless, the AAV remains a practical means for bringing troops and equipment ashore. The AAV lacks the mobility and armor required for today's amphibious operations. Several solutions to the legacy AAV include an upgrade to the AAV, which is affordable given the state of current technology. In DOD acquisitions, technology readiness level (TRL) or procuring a system incrementally might increase the likelihood of getting the right product to the warfighter. There are four ACV prototypes in production. Unlike the acquisitions approach used with the EFV, the ACV will take an *incremental* approach, where ACV 1.0 will have different capability than 2.0. The primary difference between the two ACVs is the 1.0 variant will have to ride in an SSC, while the ACV 2.0 will be autonomous. Specifically, the ACV will build on basic shore-to-shore mobility that works well when crossing ravines and canals, as seen in Iraq. Thereafter, ACV 2.0 represents a self-deploying, ship-to-shore capability, which is similar to that achieved by the EFV. Figure 3 shows Assault Amphibian Modernization out to 2034. Figure 3 projects that approximately 700 ACVs, totaling six amphibious assault companies, are to be procured to replace the legacy AAV. Meanwhile, approximately 392 AAVs will receive an upgrade.
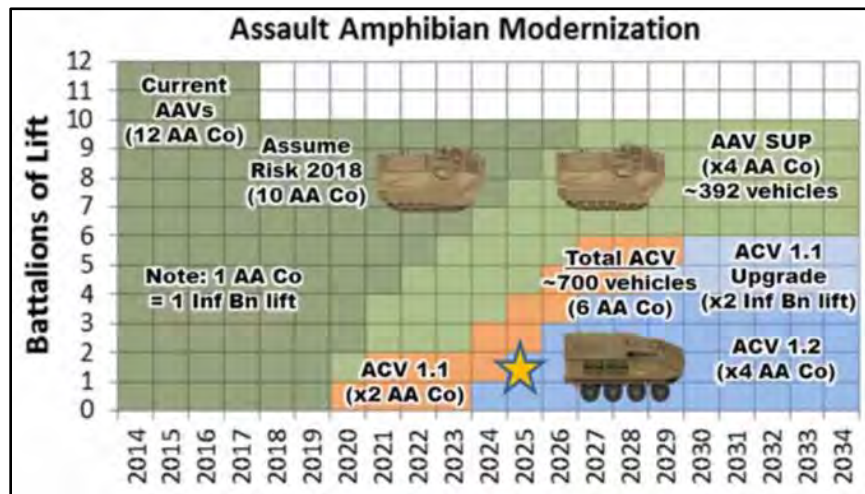
Figure 3.   Assault Amphibian Modernization projections from 2014 to 2034.
Approximately 700 ACVs (wheeled, bottom right), totaling six
companies, are to be procured to replace the bulk of the legacy AAV
(tracked, upper left). Nearly 400 of the AAVs are to receive an
upgrade (from LaGrone, 2015).

At present, decision makers heavily favor force protection (or armor) and speed. The future ACV procurement is rapidly approaching. The advent of the ACV, increased cost consciousness, and the desire for data driven decisions all make this research timely. The next amphibious procurement will play a critical role in successful amphibious assault missions for decades.

The ACV is still early in the defense acquisitions system. Procurement will depend heavily on MOPs. These MOPs are likely to reflect those ranges seen in the initial operating capability (IOC) briefed to Congress by the military ground forces specialist Andrew Feickert regarding the ACV:

- The proposed vehicle must be able to self-deploy from amphibious shipping and deliver a reinforced Marine infantry squad (17 Marines) from a launch distance at or beyond 12 miles with a speed of not less than 8 knots in seas with 1-foot significant wave height and must be able to operate in seas up to 3-foot significant wave height.

- The vehicle must be able to maneuver with the mechanized task force for

  sustained operations ashore in all types of terrain. The vehicle's road and cross-country speed as well as its range should be greater than or equal to the M1A1 [42-45mph].

- The vehicle's protection characteristics should be able to protect against direct and indirect fire and mines and IED threats.

- The vehicle should be able to accommodate command and control (C2) systems that permit it to operate both at sea and on land. The vehicle, at a minimum, should have a stabilized machine gun in order to engage enemy infantry and light vehicles (Feickert, 2014, p. 3).

What Figure 3, the Marine Corp's Assault Amphibian Modernization, does not show, is that operations and support for the ACV will extend well beyond 2034. The expeditionary nature of the Marine Corps and its Title 10 requirement to conduct operations from ships at sea inland, drives the development of technologies that seamlessly get Marines ashore. The complex nature of amphibious operations means the ACV should be designed to handle humanitarian operations all the way to forcible entry operations.

III. EW 12 SCENARIO AND MANA MODEL DEVELOPMENT

Modern threats call for the integrated application of naval capabilities in the maritime domain and beyond.

—Expeditionary Warrior 2012

This chapter begins with a general overview of EW 12 and the modeling software selected, MANA. Additionally covered are the benefits of MANA, which include why MANA's intuitive interface is so useful to DOD decision makers, as well as its limitations. Last, we review the research questions, and describe the MANA modeling, including particulars of the major agent types.

A. GENERAL DESCRIPTION

The A2/AD scenario used in EW 12 is set in fictional 2024 West Africa. The adversary is comprised of both conventional and nonconventional forces in Savanna, Africa. The threat scenario is further complicated by instability created by a weak host nation. The Free Savanna Movement (FSM), and a neighboring invasion from the West African Federation (WAF), have prompted a U.S.-led coalition (Wargaming Division, 2012). Figure 4 shows the enemy force composition and strength in opposition of Combined Joint Task Force Savanna (CJTF-Savanna). Adversary assessments concur with Figure 4, suggesting First Corp (I Corp) is moving northwest to the vicinity of Dakar, Savanna. Accordingly, CJTF-Savanna desires an amphibious operation south, near Barra, which strategically oversees the Gambie River.
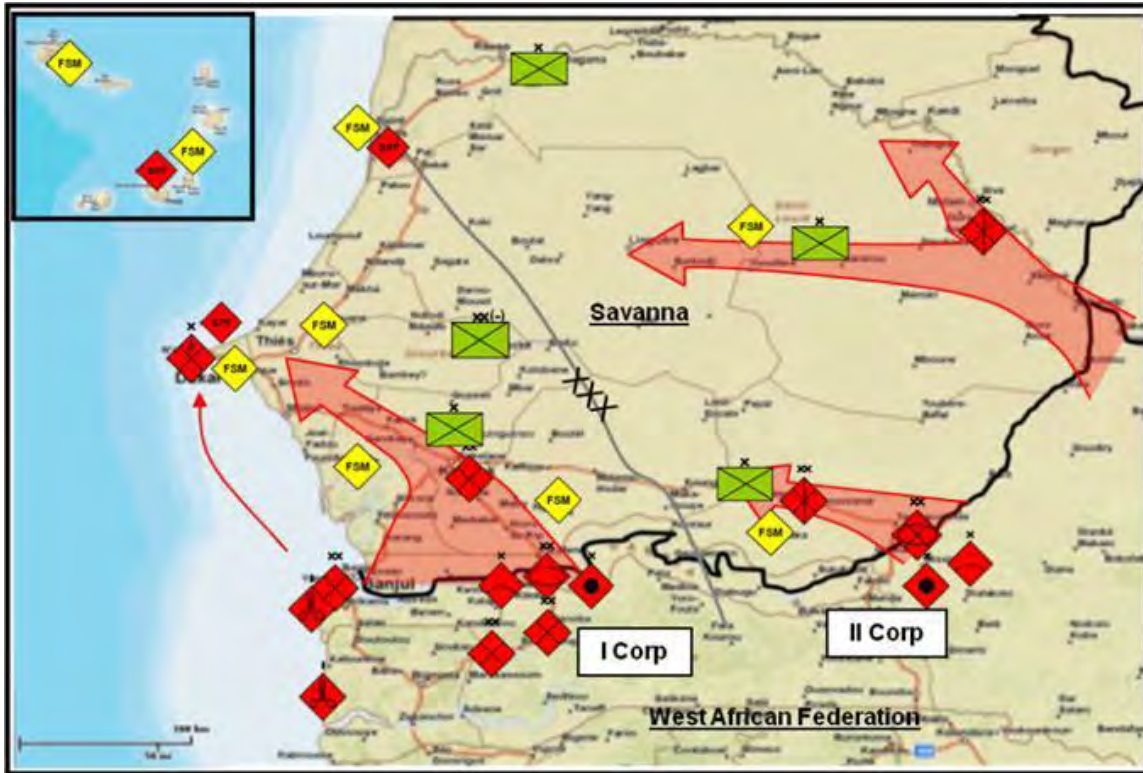
Figure 4.   Enemy ground threat situation (from Wargaming Division, 2012).

The baseline scenario follows the vignette structure of EW 12, and specifically this research explores an amphibious landing and subsequent battle once Phase I is complete. Phase I occurs after both maritime and air superiority have been achieved, which set the conditions for entry operations into Savanna. This research looks at a BLT reinforced by the MEU/MEB during Phase II, "Gain Entry." The CJTF's JFEO capabilities are to secure the city, support expansion of air points of debarkation (APODs), and sea points of debarkation (SPODs) (Wargaming Division, 2012). CJTF-Savanna agrees to conduct an amphibious assault due to the combinations of urban terrain, conventional, and nonconventional forces in Savanna.

The ARG has maneuvered to a position off the coast just OTH at 25 nm. The ARG has the full strength of the aviation and surface connectors of the MEU. The ACE is postured to provide STOM-V with MV-22s. Meanwhile four SSCs must bring waves ACVs, M1A1 tanks, combined anti-armor teams (CAATs), mobile howitzers, and infantry ashore. SSC or LCAC payload of ACV, M1A1, etc., waves can either be

22

accompanied by AAVs or a heliborne raid. In our modeling, we explore four scenarios to support the bringing of equipment ashore:

LCAC (ACV): unaccompanied
LCAC (ACV) + AAV: accompanied on wave one by AAV
LCAC (ACV) + MV-22: accompanied by a heliborne raid of MV-22
LCAC (ACV) + AAV + MV-22: accompanied on wave one by AAV and by a heliborne raid of MV-22

Figure 5 shows the CJTF Concept of Operations (CONOP), Phases I-III. Phase II uses elements of the amphibious task force (ATF) to seize CJTF objective 4.
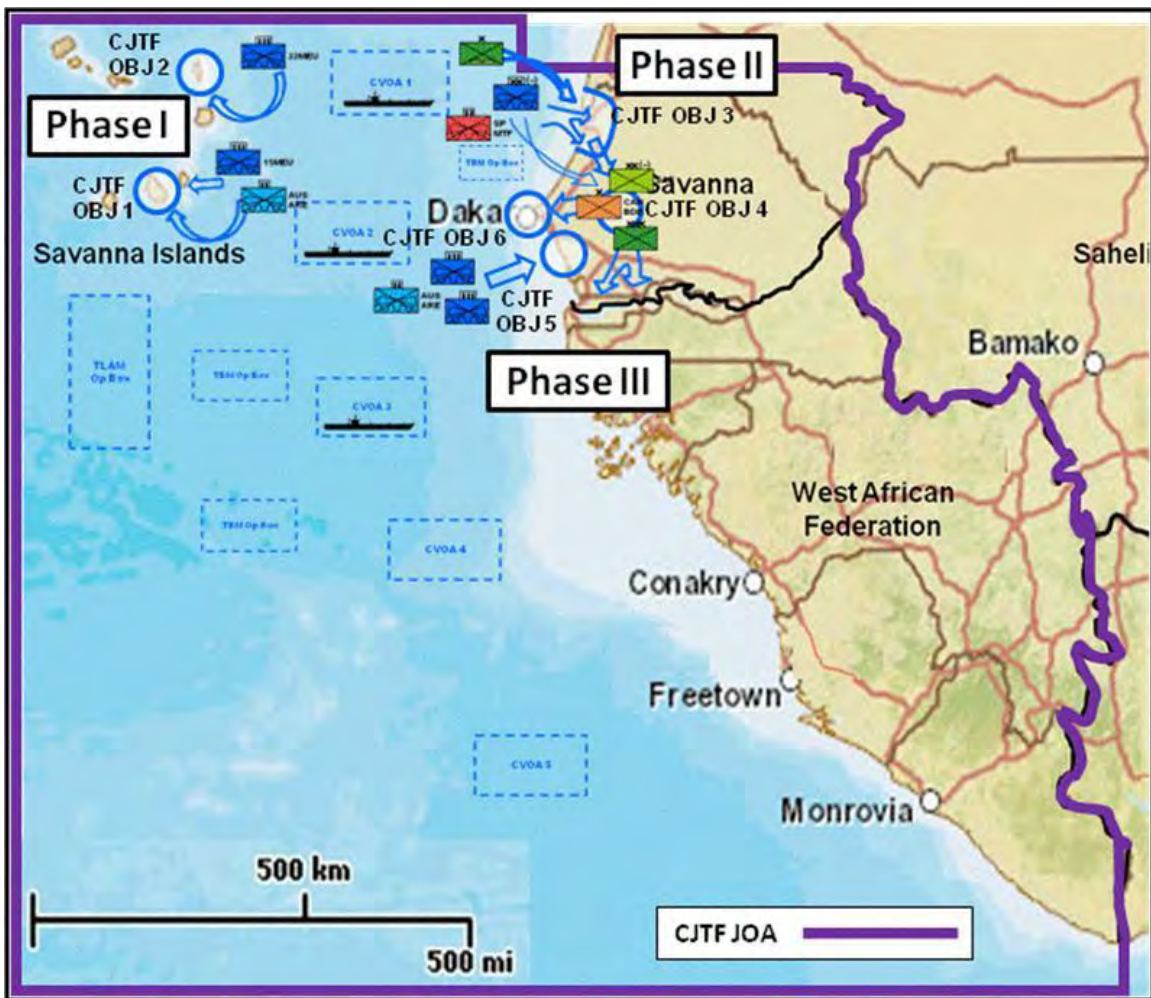
Figure 5.   CJTF CONOP, Phases I-III (from Wargaming Division, 2012).

The mission of CJTF-Savanna is to conduct Operation RESTORE SOVEREIGNTY to re-establish the territorial integrity of Savanna, neutralize the WAF's offensive capability, and transition security responsibilities to United Nations (U.N.) forces (Wargaming Division, 2012).

B.   MANA

1.   What is MANA?

This research uses Map-Aware Non-uniform Automata Version V or "MANA" software, which was deemed suitable for modeling amphibious assault. MANA was deemed suitable for this effort because it was designed for use as a scenario-exploring model that is capable of addressing a broad range of problems (McIntosh, Galligan, Anderson, & Lauren, 2007). MANA is an agent-based model that can be used to simulate combat behavior. It allows the user to create a simulated complex adaptive system for important real-world elements of combat, including change of plans due to the evolving battle, the influence of situational awareness when deciding an action, and the importance of sensors (McIntosh et al., 2007).

2.   Benefits of MANA

MANA software is fit for modeling amphibious assault because it allows for the creation of heterogeneous agent types, and is stochastic, which allows for capturing uncertainty and running the simulation multiple times using different random seeds to understand the effect of that uncertainty. MANA also gives the user:

- An ability to *watch* the simulation with adequate detail and visual icons

- An intuitive interface

- Agent-based interactions derived from their goals and objectives, the environment, and sensor and weapon performance

- And, an ability to be run in batch mode, over a variety of parameter settings

Another advantage of MANA is that it can take as input a particular *seed*, and this provides repeatability. *Seed* here is an initial value used by the pseudo-random number

24

generator to create stochastic behavior in MANA. With a large number of parameters that can be varied, a stochastic model like MANA can represent a range of military operations (ROMO) and threat levels with a single model structure and a good design of experiment.

3.   MANA: Limitations and Assumptions

These next two sections cover limitations and assumptions made in MANA. The primary limitation of MANA related to this research is that agents may one debuss/emboss one set of children. The main assumption made in MANA is logistics was not explicitly modeled.

a.   *Limitations of MANA*

The versatility of MANA is that there are many options and settings that one can use to create the desired behaviors. Deciding on the right amount of detail, however, for each parameter is a fine balance, and in some cases MANA may not be able to handle the level of detail desired for a specific feature. MANA models a force's aggregated ability to move through terrain. Details of individual Marines navigating obstacles—such as the beach-like stakes, barbed wire, and hedgehogs they encountered at Normandy—are not modeled. Below is a summary of the limitations of MANA, with regard to modeling amphibious assault:

- Sensors and weapons performance is modeled relatively simply, with range-probability pairs and concealment parameters, for example. The model does not attempt to explicitly incorporate aspects of the environment such as sea state, weather, etc. MANA includes only enough "physics" as is necessary (McIntosh, 2009, p. 2).

- The parameters for armor protection and penetration are simple.

- Computation cost increases quickly with detail.

- Agents may only debuss/embuss one set of 'children.' That is, LCACs cannot bring one wave of children (say howitzers) to the beach, then acquire another set of children (say infantry) back at the ship. To overcome this limitation, a separate LCAC agent was substantiated for every wave.

b.   *Assumptions Made in MANA*

Other simplifications are made because the operational metamodels that results from MANA excursions will eventually be linked with other software tools:

- Fuel consumption—Fuel burn is not modeled in MANA. As seen in Chapter II, the USMC has VBA spreadsheet tools to calculate fuel burn.

- Flight deck cycle—Deck cycle is not modeled in MANA. ACE is modeled via a DES in Simio.

- Logistics—Resupply of fuel, ammunition, water, etc., is not modeled in MANA. Chapter II describes models that support logistical resupply.

- Civilians—Neutrals or civilians also not modeled, as their impact to the MOP for different force configurations was deemed immaterial.

- Beach conditions, sea state, weather, and elevation are not explicitly modeled.

C.   RESEARCH QUESTIONS

This research shows the value of conducting large-scale design and analysis of experiments with MANA. Meanwhile, since this research deals with specifications for concept ACV and SSC, we seek to address the following questions:

- What are the ACV MOPs that positively contribute to the MOEs?

- What are the SSC MOPs that positively contribute to the MOEs?

Additionally, addressed in this section are EW 12 particulars which are applicable to the operational scenario, and how those were implemented in MANA. We also provide further details about the MANA implementation such as characteristics of the agents and the playboard (simulated battlefield).

D.   MEASURES OF EFFECTIVENESS

One purpose of the simulation in this research is to provide a tool to influence the future development and procurement of the ACV and SSC. To do this we explore several MOEs:

- MOE (1): Blue casualties

- MOE (2): Red casualties

- MOE (3): Time to attrite the Red Force to 1/3 remaining strength

- MOE (4): Force exchange ratio (FER), which is calculated for each run as (Red casualties +1) / (Blue casualties +1)

E. SCENARIOS

This research models a BLT-sized amphibious assault conducted four different ways by a MEU while embarked on the ARG, as described in Chapter II. This section presents the four scenarios modeled in this research. Subsequent sections present detailed modeling particulars, as well as details on friendly and adversary agents in MANA.

1. Baseline Scenario (Scenario One)

This scenario is based on the adversaries FSM and WAF. Pockets of adversary appear to be blending in with the local populace in the surrounding urban areas. A moderate force is believed to be guarding against a likely amphibious assault operation; however, they are unwilling to present overt defenses for fear of being targeted by CJTF air strikes. There are groups of adversary inland, with few willing to risk exposure by defending the coast. The enemy has 18 Red infantry, four Red medium/heavy artillery, two Red tanks, and four Red anti-tank teams. The adversary has anticipated U.S. involvement and believes that an urban avenue of approach is less likely than the landing force seeking an envelopment of the city from the north. Enemy activity has been low so an LCAC payload of ACV, M1A1, etc., unaccompanied on wave one is used to capitalize on the shore-to-shore mobility and force protection afforded by the wheeled ACV. Figure 6 shows four LCAC SSCs returning to the seabase after wave one of bringing Blue forces ashore.

Figure 6.   Four LCACs or SSCs "+" returning to the seabase after bringing Blue ashore.

2.   Scenario Two

This scenario combines the baseline with AAVs. It is more likely than the baseline scenario with LCACs operating alone. The MEU's BLT will provide the landing force for the ship-to-shore movement. As the LCACs bring waves of personnel and equipment ashore, the CJTF employs self-deploying AAVs on wave one. The AAVs remain in their approach lanes and accompany the LCACs on wave one, pressing inland to establish security while friendly forces clear the landing beach. Once tactical integrity and force consolidation are complete, the force continues with assault operations. Figure 7 shows four LCAC SSCs loaded with ACVs, M1A1 tanks, and equipment accompanied by AAVs on wave one.

Figure 7.   Four SSCs, capable of 4xACV or 1xM1A1 "LCAC loads." The
MANA icon used for the LCAC is "+," during a wave ashore, this
icon will be overlayed by numerous icons of ACVs, M1A1 tanks,
and equipment. Wave one is accompanied by AAVs.

3.   Scenario Three

This scenario combines the baseline with a MV-22 helicopter-borne raid inland. Also known as STOM-V, this form of air assault with tilt rotor aircraft require an Area of Responsibility (AoR) that does not have prohibitive air defense artillery (ADA) to rotary wing operations. The CATF benefits from the deep insert afforded by tiltrotor aircraft, which supports his overall scheme of maneuver (SOM). The CATF LCAC payload of ACVs, M1A1s, etc., accompanied on wave one by tiltrotor aircraft, provide enhanced littoral maneuver and a range of options for the landing force (Department of Defense, 1992). Figure 8 shows the heliborne raid of MV-22 aircraft from the seabase.
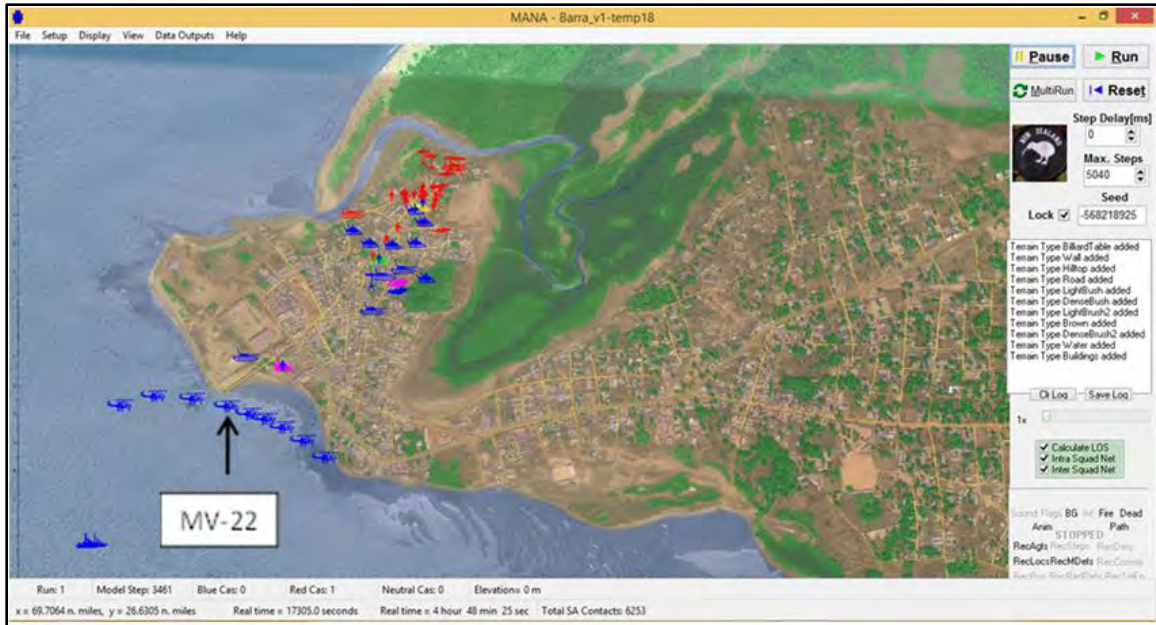
Figure 8.   Heliborne raid of MV-22 aircraft from the seabase.

4.   Scenario Four

This scenario combines AAV and MV-22 joint operations. The LCAC payload of ACVs, M1A1s, etc., is accompanied on wave one by AAVs and MV-22s. In this STOM-V and STOM-S amphibious assault the landing force (LF) takes advantage of additional amphibian firepower and the range of tiltrotor insertion. The two forces then transition from swimming and flying insertion forces to an on-land maneuver force (Department of Defense, 1992). Figure 9 shows the combination of both a heliborne raid and AAV. The necessary service craft deliver the ACVs, M1A1 tanks, and equipment ashore with an accompaniment of AAVs on wave one.
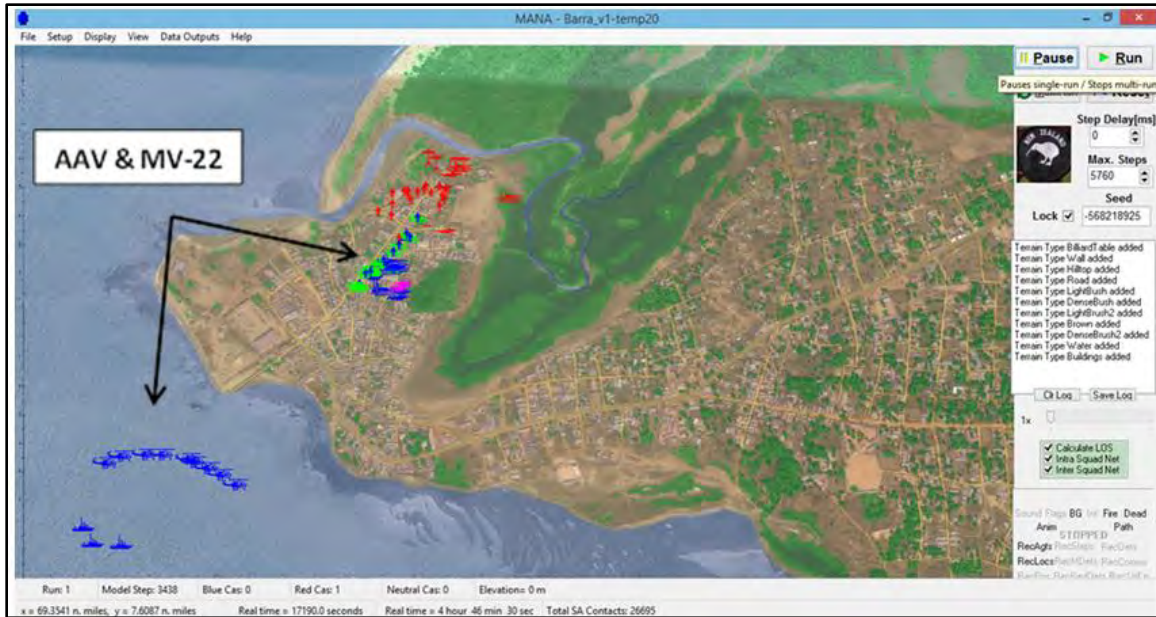
Figure 9.   Heliborne raid and wave one supported by AAVs.

F.   MODELING PARTICULARS

In this section, we provide further details on how terrain was modeled, as well as the force build-up ashore and the FLOT, all of which are vital to the CATF as discussed in Chapter II.

1.   Theater of War—The Sea, Surf, Shore, and Land

This MANA battlefield configuration has a global map size that is 70 nm by 70 nm. One time step in the model is equal to five seconds. Red and Blue agents on the battlefield are organized into groups called "squads" and are limited by both terrain and organic sensor capabilities, which together determine and what they can "see." Maneuver and placement of squads are relative to an X-Y Cartesian grid. An offshore area to the southwest supports offshore distances of 25 nm.

Three types of maps form separate layers that make up the battlefield: Background, Terrain, and Elevation. The background map is detailed imagery of the theater of war, which is commonly satellite imagery of the AoR; it does not impact the model computations, it simply serves as a background visual for the user. Meanwhile, both the terrain and elevation maps do impact model calculations. MANA uses a

Windows bitmap file to define terrain, and each pixel is assigned distinct RGB (red, green, and blue) color settings (McIntosh, Galligan, Anderson, & Lauren, 2007). Additionally, each terrain type (color) is assigned a value of "going" (how well the pixel can be traversed), "cover" (how much protection from fire the pixel provides), and "concealment" (how much protection from sight the pixel provides); going, cover, and concealment values range from 0.0 to 1.0. Figure 10 shows the RGB colors and going, cover, and concealment properties for the terrain used in this scenario.
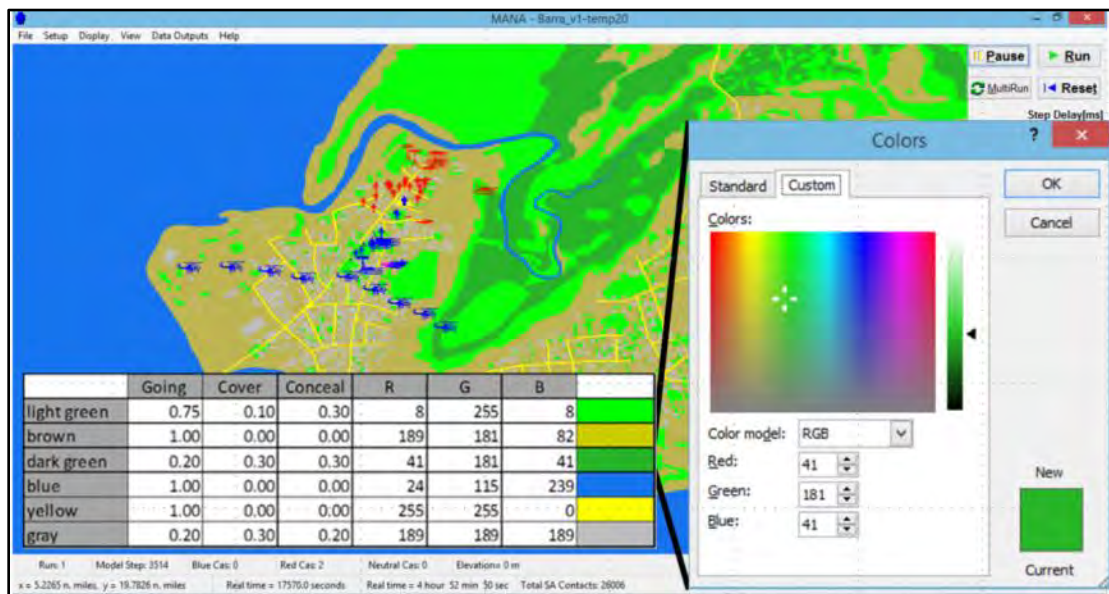
Figure 10. Terrain map, including the red, green, and blue (RGB) colors with dark green shown at right.

In MANA, the scenario editor enables the design of custom terrain not present in the defaults. An example of a default terrain is a road, which is colored with a particular color of yellow. The terrain features used in the model are light brush, sand, heavy brush, water, road, and building structure. Figure 10 shows that the road, which is colored with (255, 255, 0) "yellow," offers neither cover nor concealment, but perfect going.

Initial runs and variations were performed, and insights from these runs helped to shape the baseline scenario. A killer-victim scoreboard Excel macro was used to explore the results. These initial runs revealed the importance of massing combat power ashore prior to assaulting through the objective. When squads arrived and continued to the

32

objective without waiting for the remaining components of the ATF, the lead elements were destroyed. Initial replications also revealed the value of urban terrain. When the terrain was turned off, the ATF was more vulnerable to the adversary's artillery.

The ability to use "trigger states" in MANA is useful for specifying behaviors that should occur when certain conditions were achieved. For example, in order to achieve mass, agents in their default state release from their SSC and proceed to a predetermined waypoint, and upon reaching that waypoint, their state changes to Reach Waypoint, and in this state they wait until the rest of the force has landed ashore. Debarking agents from SSCs continue to arrive, transition inland, and wait for the final wave of the ATF. This reached waypoint state can be observed by the agent icon changing from its default blue to pink. Once the final wave arrives, a symbolic 'refueling' interaction is performed, which then triggers the entire landing force to move. Figure 11 shows the final wave arriving, disembarking, and changing their state.
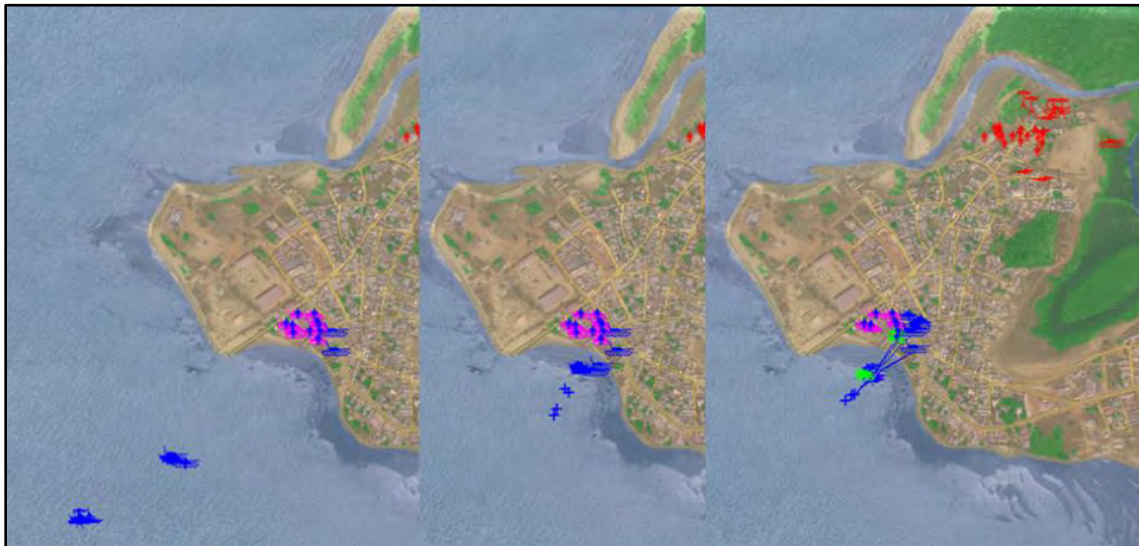
Figure 11.   In order to mass force ashore prior to moving deeper into the threat environment, agents must press inland and establish security (pink). Agents next await the final wave. As the final wave arrives squad 42, an agent representing CAAT, refuels friends, which cause the advance (green).

2. Agents

In this section, we provide a summary of the different agent types used in MANA. Table 1 provides an overview of all the agents created in MANA. From left to right it shows the agent, description, their allegiance or side, agent class, and threat level. Agent class and threat level can be used to specify sensor/weapon-target pairings.

Table 1.   MANA Agent Classifications.

Agent	Description of Blue Agent	Allegiance	Agent Class	Threat
LHD	Landing Helo dock, large air capable ship	1	99	3
LPD	Landing transport dock, L. platform/dock	1	99	3
LSD	Landing ship dock	1	99	3
LCAC	Landing Craft, Air Cushion	1	88	3
AAV	Assault Amphibious Vehicle	1	77	3
MV22	Medium lift, Tiltrotor aircraft	1	66	3
M1A1	Main battle Tank	1	2	3
LAVGrp	Light Armored Vehicle	1	4	2
AntiTank	CAAT or Anti-tank warfare team	1	5	2
BlueHowit	Short barrel mobile artillery	1	3	2
Inf	Four inf aggregated as a FT	1	1	1
ACV	ACV, wheeled	1	4	3
Agent	**Description of Red Agent**	**Allegiance**	**Agent Class**	**Threat**
RedInfant	Four Red inf aggregated as a FT	2	1	1
RedHowit	Short barrel red mobile artillery	2	3	2
RedTanks	Red Main battle Tank	2	2	3
RedAntiTank	Red anti-tank warfare team	2	5	2

There are 113 squads in the scenario file that may be activated or deactivated. Since a new squad assumes the squad number one higher than the last squad created, a deleted squad changes the squad numbers of subsequent agents. Therefore, once a squad is created it is helpful to keep it and just deactivate it in MANA so that squad numbers do not change (if, for example, you would have to make many changes to documentation if squad numbers changed).

a.   Blue Agent Properties

Table 2 contains further details for some of the Blue agents. The table contains squad numbers for individual tanks and ACVs, who their parent agent is, and the number of agents in the squad. Table 2 also contains agent class number and a run start delay. Run start delay is particularly useful when modeling agents that "come to life" and enter the scenario at different times. For example, the delays before a second, third, or fourth wave of LCACs launch. If an agent has a parent, then that agent is subject to its parent's run start. The parent of a tank or ACV represents the LCAC that carries that entity ashore. More details are provided in Appendix A.

Table 2.   This table shows the four M1A1 tanks and 19 ACVs modeled. The table also shows the LCAC squad number or parent agent that brings them ashore. For example, ACV-P-1, ACV-P-2, & ACV-P-3 and the Recovery ACV (squad 93, ACV-R-1) all have the same parent.

Squad #	Squad	Parent	# of Agents	Agent Class #	Run Start Delay
34	M1A1-1	4	1	2	0
35	M1A1-2	5	1	2	0
36	M1A1-3	7	1	2	0
37	M1A1-4	8	1	2	0
76	ACV-P-1	6	1	4	0
77	ACV-P-2	6	1	4	0
78	ACV-P-3	6	1	4	0
79	ACV-P-4	73	1	4	0
80	ACV-P-5	73	1	4	0
81	ACV-P-6	73	1	4	0
82	ACV-P-7	75	1	4	0
83	ACV-P-8	9	1	4	0
84	ACV-P-9	9	1	4	0
85	ACV-P-10	9	1	4	0
86	ACV-P-11	74	1	4	0
87	ACV-P-12	74	1	4	0
88	ACV-P-13	74	1	4	0
89	ACV-P-14	74	1	4	0
90	ACV-P-15	12	1	4	0
91	ACV-P-16	12	1	4	0
92	ACV-P-17	75	1	4	0
93	ACV-R-1	6	1	4	0
94	ACV-C-1	73	1	4	0

Blue agents all have allegiance "1." Table 2 shows a run start delay of zero for all of the squads listed here, because they are the children of LCAC agents. The agent class number allows entities to target and be targeted by appropriate types of agents. For example, infantry will target other infantry and CAAT, while CAAT will target both infantry and tanks.

Placement of Red agents was in accordance with the EW 12 scenario. At the beginning of the simulation, the Blue agents are all located at the seabase. The operations from the MLP or seabase debuss SSCs, which then debuss ACVs by waves that swim to the shore. Later, at the objective, the ACV debusses its Blue infantry. Once Red classifies Blue targets, the Red forces engage.

The subsequent sections provide additional detail regarding modeling of:

- Seabase

- SSC

- AAV (self-deployer)

- MV-22

- ACV (shore-to-shore variant)

- M1A1

- CAAT

- Howitzers

- Infantry

(1)   Seabase

The ARG is the seabase modeled in this research. While the ARG is smaller than the ESG, these three ships are indicative of the capability sailing at any given point within the three operational MEUs. The model can easily be adapted to other forms of seabases since there are many options for the seabase. In many of the likely scenarios, the seabase is OTH, postured to support low signature SSC to deploy APCs, ACVs, and AAVs close to shore during one period of darkness. The modeled three vessels that comprise the ARG seabase have the properties discussed in Chapter II. The basic model

36

structure can be modified to incorporate MLP, which can bring more LCACs and the JHSV capable of offloading ACV offshore. The JHSV and MLP programs advertise increased maneuverability and speed. Figure 12 shows the LHD agent. Figure 12 depicts the MANA graphical user interface (GUI) screen for setting agent "personality," and shows that the LHD in its default state has a personality weight of 50 toward its next waypoint. Note that all other personality weightings have been assigned a value of 0, ensuring that while in this state the LHD will only move towards its next waypoint and will not engage in other behaviors.
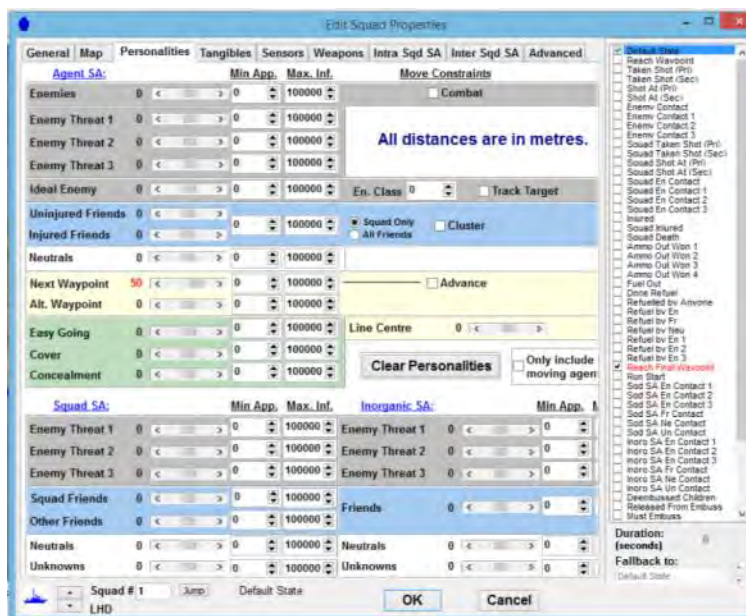
Figure 12.   LHD Agent: Depicts the GUI for in MANA. The agent icon is
located in the lower left, possible trigger states (e.g., Default State,
Reach Final Waypoint) are in a column to the right.

(2)   Ship-to-Shore Connectors

We chose to model the LCAC SSC because the service life extension program for the LCAC will continue its use through 2027, and it represents the current ARG capability. Furthermore, since LCACs presently serve as the Navy's high speed connectors, they represent a worst case. An operation requiring multiple waves also represents a worst case. It is feasible that a JHSV or UHAC loaded with ACV could

deploy a much higher volume of ACV, but that was not a focus of this research. This research took care to model a more limited and yet practical scenario with three waves of, at most, four LCACs. If a JHSV or MLP is desired, an arrival of ACV at a certain time and location offshore is easier to model in MANA than what might be required to make a similar change in a coded model (e.g., VBA). Nevertheless, an LCAC can carry approximately 120,000 lbs at speeds of 40 kts in seas with waves heights of 4.1 to 8.2 feet, averaging 6.2 feet (Department of the Navy, 2007). Figure 13 shows the three LCAC waves from the ARG. A total of four LCACs are selected, based on the new LHA and LPD configurations.
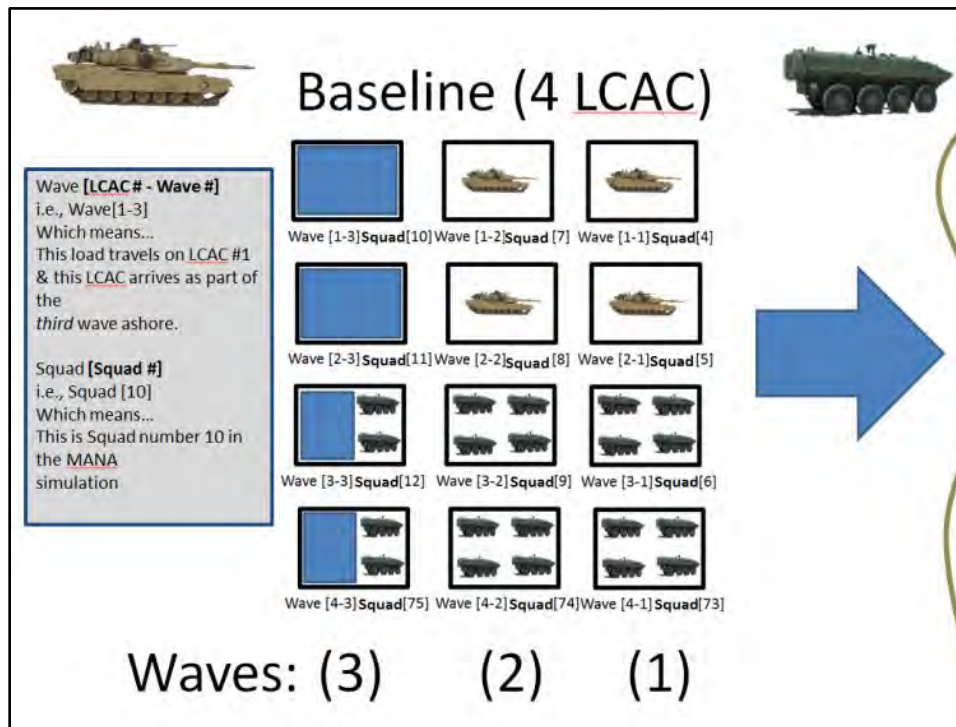
Figure 13.   Baseline factor of four LCACs as the SSC. The bottom right square shows the fourth LCAC on the first wave loaded with four ACV. The squad number is 73 for that particular LCAC. One may alter the design features of these "black box LCAC" to upgrade this modeled agent capability to JHSV, UHAC, "Mike Boats" (LCM-8), LCU, concept LCAC, etc.

Figure 13 also represents the future for this research. The "black box LCAC" can be configured to represent any possible future SSC. Modeled LCACs have the Run Start

trigger state enabled. The Run Start time includes a delay for loading and offloading vehicles and equipment. For each wave, a new set of LCAC agents are used. Chapter II described one benefit of amphibious ops is the attacker's ability to determine the time and place. Modeling waves with run start delays is reasonable, as the mission is time-driven. Figure 14 shows a negative weighting towards friendlies, and the negative weight results in squads that are more dispersed on the battlefield (McIntosh, Galligan, Anderson, & Lauren, 2007). Figure 14 also shows the Run Start trigger state in the far right column (font shaded green).
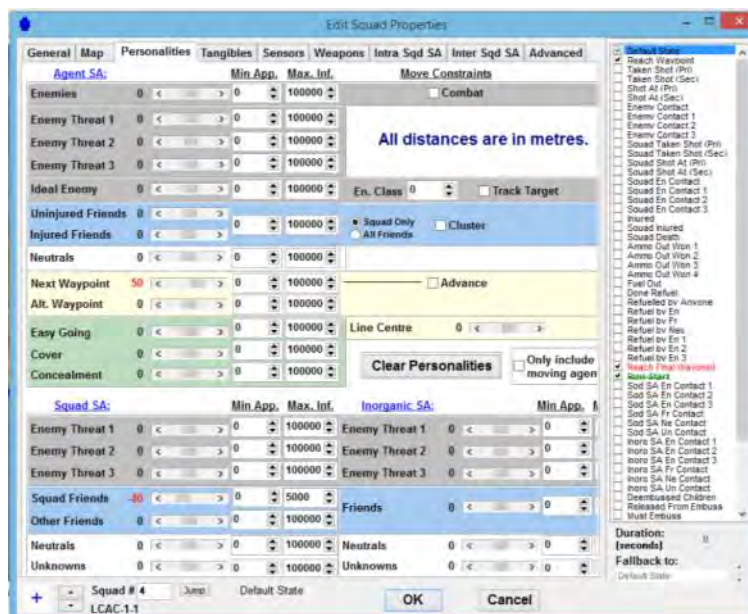
Figure 14.   LCAC Agent: Depicts the Personalities GUI in MANA. The agent icon is located in the lower left, possible trigger states (e.g., Default State, Reach Waypoint, Reach Final Waypoint, Run Start) have a check in the box. The Run Start trigger state is unique to the LCAC, as their waves are based on time.

(3)   Amphibious Assault Vehicles

The legacy AAV still deploys regularly with the MEU. Therefore, excursions using the BLT and AAVs are likely as ACVs are meant to serve as reinforcing echelons of a JFEO. Assuming that an MEU-sized force (BLT) would be first ashore; a question this research sought to answer was how the ACV as a shore-to-shore increment could be

more effective than the old AAV or previous increment. Nine AAVs were modeled for wave one, which was based on the number required for a company of lift. Shore-to-shore and ship-to-shore mobility were covered in Chapter II and represent the future life cycle of the ACV. The AAV was modeled to hold a reinforced infantry squad.

The weapon for the AAV was modeled to represent a 0.50 cal machine gun. Speeds for the AAV ranged from swim speeds of eight knots to land speeds of 40 mph. A remote weapon station (RWS) was not considered, however, it could be implemented based on the considerations outlined for the ACV and upgrades intended for this 40 year-old platform. The GUI in MANA for the AAV differs from the LCAC (Figure 14) only in that the agent icon located in the lower left is a Blue tracked APC. Possible trigger states (e.g., Default State, Reach Waypoint, Reach Final Waypoint, Run Start) remain the same as for the LCAC. This section covers the agent used to model an amphibian self-deploying vehicle comparable to the AAV. However, it is also well suited to model the EFV, ACV 2.0 increment as TRL improves.

(4)   MV-22

STOM-V provides rapid inland ranging and additional Marine FT lift capability, as required of scenario 3. The GUI in MANA for the MV-22 differs from the LCAC (Figure 14) only in that the agent icon located in the lower left is a Blue helicopter and dispersion is affected by a personality weight of –30 from other friends. The MV-22 has a 7.62 millimeter (mm) gun aircraft unit and several crew served weapon systems. These options, such as a tail gunner, limit the altitudes at which they can fly. Modeled instead are the embussing behavior of 24 combated-loaded Marines on each MV-22. The speed, vulnerability, and range of the MV-22 are modeled—weapons and the deck cycle are not.

(5)   Amphibious Combat Vehicles

Nineteen ACVs are modeled in this research: 17 normal ACVs (ACV-P[1-17]), a repair or towing variant, and communications variant. The ACV is the main Marine carrier or vehicle for this research. Two ACV can carry a reinforced Marine rifle squad and two days of supply. Since there are two ACV for what was one AAV, the ACV brings two RWS. The ACV may also be configured with a MK-19 grenade launcher,

which is not modeled, however, the RWS and increased armor is modeled—as compared to the legacy AAV. There are three crew members: the vehicle commander, a gunner, and a driver. A Marine company of lift requires 21 ACV. Two to four FTs per ACV cover the requirement that 10 to 15 Marines be onboard (8-16 Marines were modeled). The speed of the ACV allows it to keep up with the M1A1. The questions surrounding the ACV are ideal to explore with MANA. For example, armor, increased lethality in the RWS, and cross country speeds comparable with the M1A1 in A2/AD or degraded mobility, are all parameters that can be changed in MANA. Similarly, MANA supports the interoperability with connectors too. As mentioned previously, L-Class ships (e.g., LHD, LPD, etc.,) and MPF bring additional SSCs.

Four trigger states were implemented in MANA to incorporate the complexity of amphibious operations. First, the Default State covers the swim from debussing from the LCAC to a safe location ashore at distances of 5, 12, 25 nautical miles (nm). Second, Reach Waypoint stops the ACV from advancing inland. Instead they establish security, awaiting the complete force buildup. Third, as previously described, Refueled By Friend occurs once the final wave arrives (because a member of that wave refuels friendlies). Fourth, Reach Final Waypoint dismounts infantry on or near the objective, upon reaching the final waypoint. Figure 15 shows the four trigger states that are active for all the ACVs. It also shows the agent icon, which is also that of the AAV.
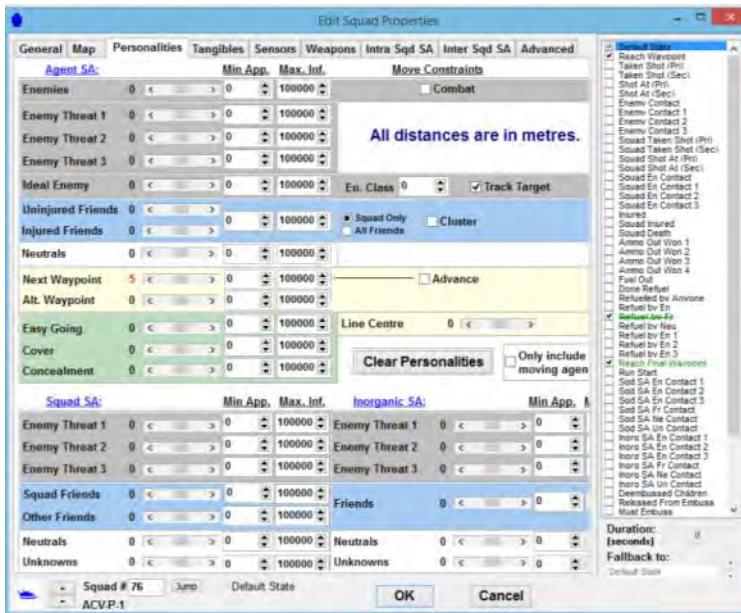
Figure 15.   ACV agent: Depicts the GUI for in MANA. Trigger states used are
the Default State, Reach Waypoint, Refuel By Friend, and Reach
Final Waypoint. Run start is not required as the ACV are debussed
from LCAC when the LCAC reaches its debark point.

The next few screen shots show the ACV squad properties:

- **Tangibles tab:** Shows movement speeds, threat, allegiance, and agent class information.

- **Sensors tab:** Provides probabilistic detection and classification range information and target class prioritization.

- **Weapons tab:** Shows round counts, reload time, maximum effective ranges, penetration, and probability of hit.
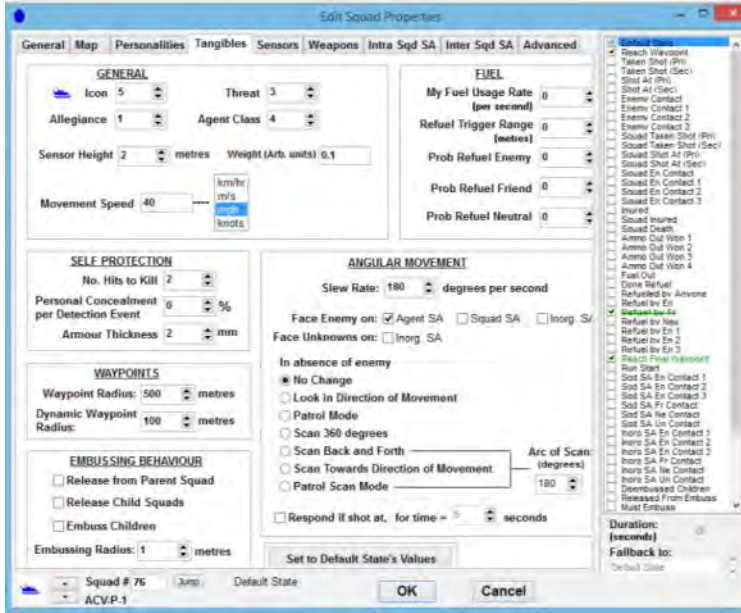
Figure 16.   ACV agent, tangibles shown are number of hits to kill, movement speed, allegiance, threat level, and agent class.
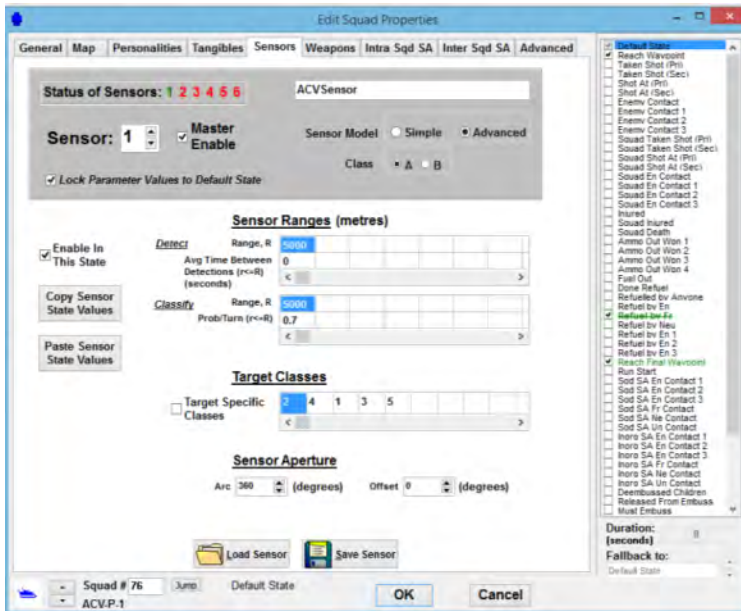
Figure 17.   ACV agent, detection and classification range and probability shown.
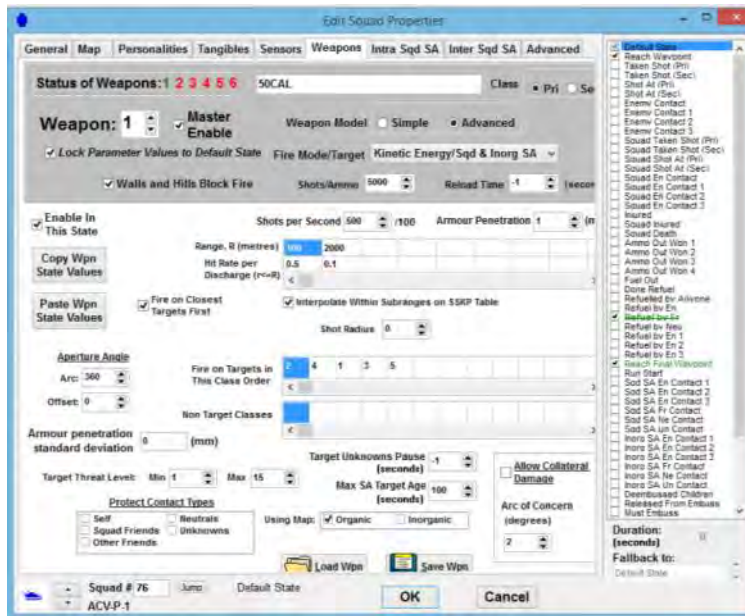
Figure 18.   ACV agent, depicts weapon ranges, probability of hit, round count, reload time, target priority list.

(6)   M1A1 Abrams Tank

The LF has four main battle tanks embarked on the MEU. LCAC modeled are only capable of waves of a single tank. The tank provides superior firepower and mobility. The tank, too, has gone through several series and upgrades. This thesis does not focus on this type of vehicle, save for the fact that many amphibious requirements are being based on keeping up with the M1A1's cross-country speed of approximately 45 mph. The M1A1 also has excellent armor. For modeling purposes, the tank's armor and number of hits required to kill it, represent an upper bound for all agents. Yet, even the M1A1 is limited by target acquisition, that is, the ability to classify an enemy. One thing to keep in mind is that the tank's 120 mm round has a higher logistical footprint, as compared to other ammunition, like that of the 0.50 cal. Therefore, if further excursions are run in MANA, the user may want to consider how to capture the additional logistical strain associated with longer battles and or increased battle intensity.

(7) Combined Anti-Armor Team

The CAAT is unique in that it both has a personality weight to move toward an ideal enemy, and that it refuels friendly agents when it arrives last, for reasons previously described in Section C of this chapter (Figure 11). Figure 19 shows a positive personality weight to target its "ideal class," Red tanks (which are agent class 2). This ensures that the CAAT will engage enemy armor units whenever possible. The modeled weapon is comparable with a tube-launched optically tracked, wire-guided (TOW) missile system. Modeling the TOW missile system provides a lower bound worst case as there are other tank missile systems (e.g., AGM-114, Spike, Javelin) that have higher probability of weapons release, probability of hit, and probability of damage given a hit, than the TOW. The CAAT have three rounds, with a delay in between attempts, but with good armor penetration.
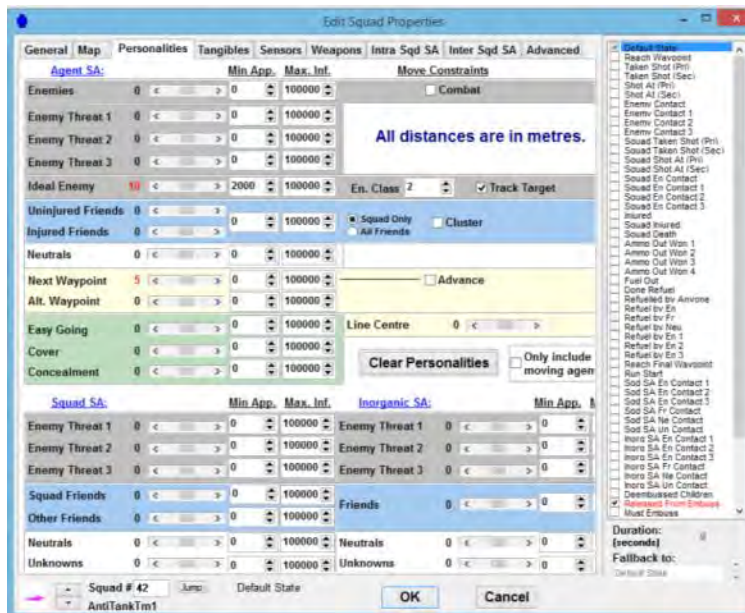
Figure 19.   CAAT agent called AntiTankTm1, represented in pink, has a personality weight to move toward Red tanks. Once released from emboss, the agent seeks to Refuel Friends (see: Section C of this chapter).

(8)   Howitzers

Howitzers are not known for their mobility. The agent name preserves the purpose of this agent—long to medium range artillery. The expeditionary fire support system (EFSS) provides expeditionary fire support. While the right mix of mobile to fixed artillery is not the focus of the research, expeditionary artillery is part of the future concepts decision makers will be considering for EF-21. The structure of the model is not currently equipped to explore the impacts of the CH-53K requirement to be able to externally load the EFSS and its vehicle. However, this model can demonstrate the impacts of mobile artillery fire.

(9)   Infantry

Infantry are loaded aboard the AAV, ACV, and MV-22. In MANA, all of the embussed infantry are secure in their APC until the infantry are debussed or dropped off at either the landing zone or the objective. That is because, in this model, there is no hostile resistance against the carriers. This could be changed in the future, if desired. Several methods can be employed to release infantry from their parent. The method used here is that the infantry are released upon the carrier reaching its objective. Dismounting infantry earlier exposes them to enemy fire, while dismounting later runs the risk of increased casualties if the entire vehicle is destroyed (e.g., from IED, artillery, etc.). A method of maintaining mass with the infantry is to preserve the FLOT until reaching the objective. Multiple waves in an amphibious assault and terrain make formulating a FLOT challenging. Terrain includes the surf, sand, and urban terrain from streets and structures.

The AAV can hold a reinforced rifle sqaud. The ACV will hold less than a complete squad of Marines. A squad is 13 Marines, comprised of a squad leader and three FT of four Marines each. The FT concept is unique to the USMC and is designed to bring increased firepower on the enemy. Some argue that a weakness of the ACV is that it potentially splits up FTs and the squad between two vehicles. Since 2007, however, Marines have ridden in combat in a vehicle that holds a payload comparable to the ACV, specifically the Mine-Resistant Ambush Protected (MRAP) vehicle. APCs designed to withstand IEDs were vital for OIF and OEF. As seen in Chapter II, Marines anticipate

enountering mines during an amphibious assualt. The size of this vehicle is now familiar to Marines, and squads have been split up while riding in High Mobility Multipurpose Wheeled Vehicles (HMMWVs) for combat operations.

b.   Red Agent Properties

This section covers modeling Red agents:

- Tanks

- Anti-Tank Teams

- Artillery

- ADA

- Infantry

Chapter II describes the advantages of the defense and the complex terrain forged by the attacker prior to reaching the enemy during an amphibious assault. This chapter covers the enemy EW 12 scenario. FSM and WAF present both irregular warfare and conventional threats. In this analysis, we find that where Red lacks platforms of varying type, model, and series—Red accounts for this by having more resources, concealment, greater maximum effective range, and increased overall situational awareness. Figure 20 shows Red's force laydown.

Figure 20.   Red tanks, anti-tank teams, ADA, and infantry.

(1)　　Red Tank

There are two heavily armored and concealed tanks for Red. Both tanks have sensors that out-range Blue tanks by 1,000 meters (m). Red tanks also have better logistics; therefore, Red tanks enjoy higher round counts than Blue. Red tanks only have one state and move so as to avoid being decisively engaged. Red tanks are superior to Blue tanks to give the advantage to the defense and make it formidable.

(2)　　Red Anti-Tank Team

There are two well-trained anti-tank teams. These teams also enjoy better concealment and logistics than Blue. The anti-tank team has personal concealment per detection event equal to 50%, which means it has a 50% chance of not being acquired by Blue. For reference, a concealment value of 100% will give a Red anti-tank team agent a 0% chance of being seen (McIntosh, Galligan, Anderson, & Lauren, 2007).

(3)　　Red Artillery, Air Defense Artillery

The Red artillery has personal concealment per detection event equal to 70%, given the FSM's ability to blend in with the local populace, or the WAF's proclivity to nest their artillery near cities or in other areas that make targeting difficult. Red artillery also models the impact of air defense artillery, as Red artillery actually prioritizes Red aircraft above infantry and CAAT.

(4)　　Red Infantry

Red infantry enjoy some of the similar befits of the defense and basic characteristics of the scenario described. Like Red artillery, Red infantry are all 70% concealed. The Red force is massed or concentrated, which creates a formidable defense for Blue. Red is also organized with a layered defense, ranging Blue as they advance toward Red's position. In MANA, every Red infantry requires 11 hits to be killed, meaning Red infantry is 11 times harder to kill than Blue. The number 11 is somewhat arbitrary, but served to provide a reasonable Killer-Victim scoreboard baseline.

IV.   DESIGN OF EXPERIMENTS

This chapter covers the design of experiment; specifically, the choice of factors and levels, robust design, and design choice. Additionally, we discuss how the number of replications was determined, as well as how the experiment was executed.

A.   GENERAL DESCRIPTION

Understanding the fundamentals of DOE is important. Without an adequate understanding, the experimenter risks wasting time and resources, and unnecessarily limiting the analysis that can be performed on the data. Our DOE considers four scenario types and 77 other factors. From the seabase, force masses ashore via one of the following configurations: Figure 21 shows the baseline scenario, scenario 1, is highlighted in white, with its major components listed in the schematic.

- LCAC (ACV)

- LCAC (ACV) + AAV

- LCAC (ACV) + MV-22

- LCAC (ACV) + AAV + MV-22
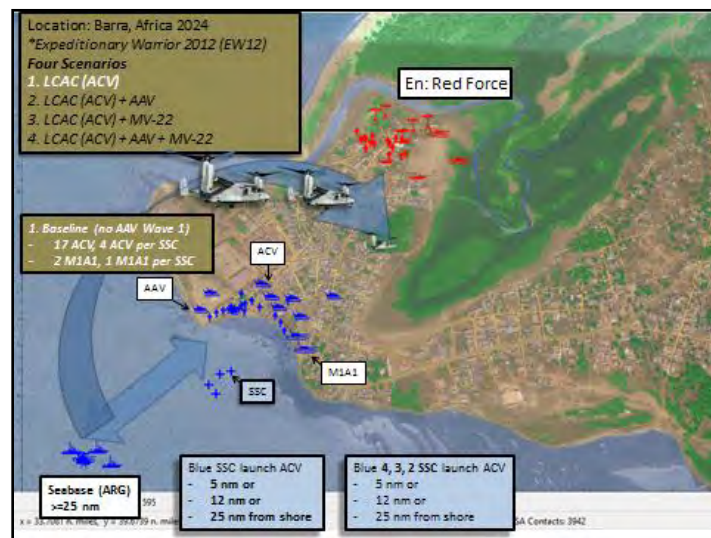
Figure 21.   Experiment setup schematic, which shows the four scenarios and two other decision factors: (1) distance from shore that ACVs are deployed from the SSCs, and (2) the number of SSCs.

Figure 21 summarizes the four scenario alternatives. The bottom left corner of Figure 21 shows the seabase. The baseline/scenario 1 consists of LCACs completing no more than four waves, bringing ashore 17 ACVs, four M1A1s, and the supporting equipment. These waves are unaccompanied by legacy AAV or MV-22 support. Scenarios two and three build on this, bringing additional forces ashore either from STOM-S or STOM-V. The factor settings listed at the bottom of Figure 21 show that the ACVs may be launched to swim to shore from 5, 12, or 25 nm, and that 2, 3, or 4 LCACs are used to transport the ACVs.

To build our efficient DOE for a MANA model, we conduct the following steps:

1.   Define decision and noise factors, and their levels/bounds
2.   Select the appropriate design
3.   Verify the design, ensuring space-filling and low correlation properties

1.   Factors and Ranges of Interest

Factors of interest cover a broad range of possible parameters; inputs that were developed in both Chapters II and III. Factors can be either continuous or discrete/categorical. Tables 3 and 4 contain complete listings of all Blue and red factors, respectively. Both Table 3 and 4 show factors other than the scenario type, a brief description, their minimum (Min), current, and maximum (Max) values (if continuous) and their levels (if discrete or categorical). The following tables are colored red and blue, which is used to distinguish threat (if Red) and friendly (if Blue). Various data in the two Min and Max columns are highlighted in yellow to break out the continuous variables from the categorical. Since we can adjust these variables they are controllable factors, which will be explained in greater detail after the table.

Table 3.   Complete listing of Blue experiment factors.

Agent	Explanation	Factor	Min	Max	Current	Unit
BLUE							
Ships	Amphib debark distance	LCDbkDist	5	25	12	nm
Ships	Amphib velocity	LCMvtSpd	10	30	25	kts
LCAC	Velocity at Default State	LCACMvtSpd	25	60	42	kts
LCAC	No. Hits to kill	LCACHit2k	1	3	1	Hits
LCAC	Number of LCACs deployed in Amphibious Ready Group	LCACQty	2	4	4	LCAC
AAV	Sensor Detection Range at Default State	AAVSnrDetRng	8000	10000	5000	meter
AAV	Sensor Classification Range at Default State	AAVSnrClsRng	1000	8000	3000	meter
AAV	Swimming Velocity at Default State in the water	AAVMvtSpd	5	42	34	kts
AAV	No. Hits to kill	AAVHit2k	1	3	1	Hits
AAV	Remote Weapon Station (RWS) Range	AAVrws	800	2000	1000	meter
AAV	Infantry carrying capacity	AAVInfCap	2	4	4	infantry
ACV	Sensor Detection Range at Default State	ACVSnrDetRng	8000	10000	5000	meter
ACV	Sensor Classification Range at Default State	ACVSnrClsRng	1000	8000	3000	meter
ACV	Sensor Classification Range at Default State, Probability	ACVSnrClsProb	0.5	0.95	0.7	
ACV	Swimming Velocity at Default State in the water	ACVMvtSpd	8	45	40	mph
ACV	No. Hits to kill	ACVHit2k	1	3	2	Hits
ACV	Remote Weapon Station (RWS) Range	AAVrws	800	2000	1000	meter
ACV	Infantry carrying capacity	ACVInfCap	2	4	10	infantry
MV-22	Sensor Detection Range at Default State	MVSnrDetRng	8000	10000	5000	meter
MV-22	Sensor Classification Range at Default State	MVSnrClsRng	1000	8000	3000	meter
MV-22	Sensor Classification Range at Default State, Probability	MVSnrClsProb	0.5	0.95	0.7	
MV-22	Velocity at Default State	MVMvtSpd	90	220	100	mph
MV-22	No. Hits to kill	MVHit2k	1	3	2	Hits
MV-22	Infantry carrying capacity	MVInfCap	5	7	6	Infantry
M1A1	Sensor Detection Range at Default State	M1SnrDetRng	8000	10000	6000	meter
M1A1	Sensor Classification Range at Default State	M1SnrClsRng	2500	8000	5000	meter
M1A1	Weapon, max effective range	M1WeapRng	1500	8000	3500	meter
M1A1	Weapon, range probability	M1WeapProb	0.4	0.93	0.4	
M1A1	Sensor Classification Range at Default State, Probability	M1SnrClsProb	0.4	0.95	0.95	
M1A1	Velocity at Default State	M1MvtSpd	30	50	40	mph
M1A1	No. Hits to kill	M1Hit2k	2	4	3	Hits
AntiTank	Sensor Detection Range at Default State	AntTnkSnrDetRng	8500	10000	8000	meter
AntiTank	Sensor Classification Range at Default State	AntTnkSnrClsRng	1000	8500	7000	meter
AntiTank	Sensor Classification Range at Default State, Probability	AntTnkSnrClsProb	0.5	0.95	0.9	
AntiTank	Velocity at Default State	AntTnkMvtSpd	3	40	25	mph
AntiTank	No. Hits to kill	AntTnkHit2k	1	2	1	Hits
AntiTank	Weapon, max effective range	AntTnkWeapRng	1000	8000	4000	meter
AntiTank	Weapon, range probability	AntTnkWeapProb	0.4	0.8	0.4	
Howitzer	Sensor Detection Range at Default State	HowitSnrDetRng	15000	19000	12000	meter
Howitzer	Sensor Classification Range at Default State	HowitSnrClsRng	10000	15000	11000	meter
Howitzer	Sensor Classification Range at Default State, Probability	HowitSnrClsProb	0.5	0.95	0.8	
Howitzer	Velocity at Default State	HowitMvtSpd	3	40	40	mph
Howitzer	No. Hits to kill	HowitHit2k	1	3	3	Hits
Howitzer	Weapon, effective casualty radius range	HowitWeapRadRng	15	30	15	meter
Howitzer	Weapon, range probability	HowitWeapRadProb	0.5	0.95	0.75	
Infantry	Sensor Detection Range at Default State	InfSnrDetRng	3000	5000	3000	meter
Infantry	Sensor Classification Range at Default State	InfSnrClsRng	1	3000	3000	meter
Infantry	Sensor Classification Range at Default State, Probability	InfSnrClsProb	0.5	0.9	0.6	
Infantry	Velocity at Default State	InfMvtSpd	2	4	3	km/hr
Infantry	No. Hits to kill	InfHit2k	1	4	1	Hits

Table 4.   Complete listing of Red experiment factors.

Agent	Explanation	Factor	Min	Max	Current	Unit
Red						
RedInf	Sensor Detection Range at Default State	RedInfDetRng	25000	30000	10000	meter
RedInf	Sensor Classification Range at Default State	RedInfClsRng	1	25000	10000	meter
RedInf	Weapon, max effective range	RedInfWpnMaxEff	250	8000	500	second
RedInf	Weapon, max effective range, prob	RedInfWpnProb	0.2	0.9	0.3	
RedInf	Movement speed	RedInfMvtSpd	3	8	4	km/hr
RedInf	No. Hits to Kill	RedInfHit2k	2	5	3	
Howitzer	Sensor Detection Range at Default State	RedHowitSnrDetRng	25000	30000	12000	meter
Howitzer	Sensor Classification Range at Default State	RedHowitSnrClsRng	10000	25000	12000	meter
Howitzer	Sensor Classification Range at Default State, Probability	RedHowitSnrClsProb	0.5	0.95	0.8	
Howitzer	Velocity at Default State	RedHowitMvtSpd	10	40	20	mph
Howitzer	No. Hits to kill	RedHowitHit2k	3	20	12	Hits
Howitzer	Weapon, effective casualty radius range	RedHowitWeapRadRng	3	25	5	meter
Howitzer	Weapon, range probability	RedHowitWeapRadPro	0.4	0.95	0.5	
RED TANK	Sensor Detection Range at Default State	RedM1SnrDetRng	8000	10000	6000	meter
RED TANK	Sensor Classification Range at Default State	RedM1SnrClsRng	2500	8000	6000	meter
RED TANK	Weapon, max effective range	RedM1WeapRng	1500	8000	3500	meter
RED TANK	Weapon, range probability	RedM1WeapProb	0.4	0.93	0.4	
RED TANK	Sensor Classification Range at Default State, Probability	RedM1SnrClsProb	0.4	0.95	0.95	
RED TANK	Velocity at Default State	RedM1MvtSpd	30	50	20	mph
RED TANK	No. Hits to kill	RedM1Hit2k	2	4	3	Hits
RED AntiTank	Sensor Detection Range at Default State	RedAntTnkSnrDetRng	8500	10000	8000	meter
RED AntiTank	Sensor Classification Range at Default State	RedAntTnkSnrClsRng	5000	8500	8000	meter
RED AntiTank	Sensor Classification Range at Default State, Probability	RedAntTnkSnrClsProb	0.5	0.95	0.9	
RED AntiTank	Velocity at Default State	RedAntTnkMvtSpd	3	40	25	mph
RED AntiTank	No. Hits to kill	RedAntTnkHit2k	1	3	2	Hits
RED AntiTank	Weapon, max effective range	RedAntTnkWeapRng	1000	8000	4000	meter
RED AntiTank	Weapon, range probability	RedAntTnkWeapProb	0.4	0.8	0.4	

a.   *Controllable Factors*

Factors in a design are classified as controllable if they can be controlled in the real world. Factors are uncontrollable if they are outside of the operator's control. There are many controllable factors associated with an amphibious assault. Operators may select from a variety of platforms. Additionally, the numbers of ACVs, SSCs, and helicopters are all controllable factors. It should be noted that some factors in a design may require changes to the structure of the simulation, and we use a translation to handle mappings and dependencies. For example, Figure 22 is a schematic that shows how the simulation's landing plan was adjusted to accommodate different numbers of LCACs.
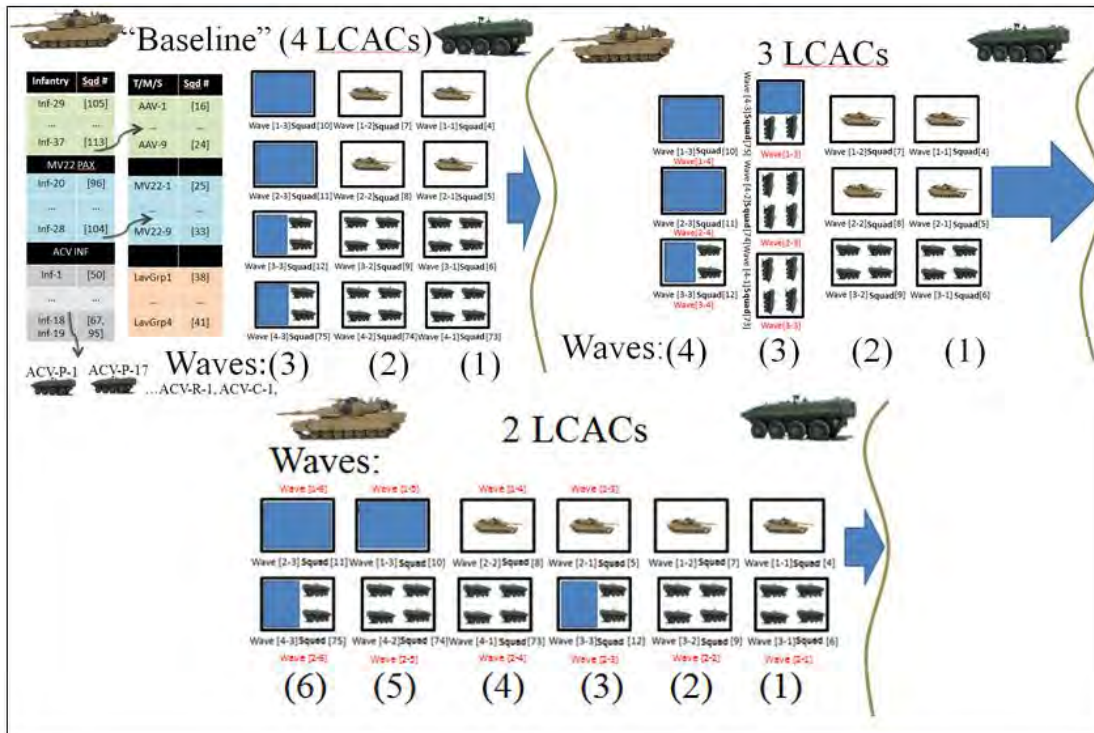
Figure 22.   A schematic of how the simulation's landing plan was adjusted to accommodate 2, 3, and 4 LCACs.

b.   *Uncontrollable Factors*

In contrast to controllable factors, uncontrollable (or "noise") factors are those that operators cannot control in the real world. In an amphibious assault, noise factors included wave height, wind velocity, and terrain. All of the rows colored in red in Table 3 represent uncontrollable factors. Noise factors are important to consider when providing a robust solution that will work in many different situations. Often, scenario-based analysis becomes too dependent upon hordes of unrealistic assumptions. While this research leverages EW 12, it is important to provide a broad analysis that considers a range of noise factors, in order to generate a robust solution. Moreover, while waves, winds, and weather are important for a higher-resolution study of the physical environment, the noise factors in our experiment are associated with characteristics of the threat. With the threat factors, we cover a broad range of possibilities for how well the enemy can sense and prosecute the incoming Blue forces with firepower.

c.   *Robust Design*

Building the ACVs and SSCs will take time and cost a lot of money. The time and cost associated with running simulation experiments is much less than making changes on the real system, and can incorporate changes more quickly than upgrading the ACV. The robust design approach was forged by Toyota engineer and statistician Genichi Taguchi (1986). In the simulation context, the simulation is a surrogate for the real system, which may realize the benefits of improved performance and decreased cost faster than the manufactured system (Sanchez, 1994). With all the factors, inputs, and alternatives for a given system, we proceed with a design process akin to simulation optimization, where the "best" answer is not overly sensitive to small changes in the system's inputs (Sanchez, 1994). Procured future equipment of the Navy and Marine Corps should be robust to a variety of missions and threats based on the approach above. Today, the adaptive adversary will change based upon technology; therefore, technology must be flexible enough to perform a variety of things well.

B.   NEARLY ORTHOGONAL AND BALANCED (NOB) MIXED DESIGNS

In this research, 78 factors, including scenario type, were varied over several hundreds of thousands of simulated amphibious assaults. Here, we take a step back and discuss how efficiency, which is the number of design points required to study k factors with m levels each, can vary considerably across possible design types. For example, to study four factors with two levels each, using a full-factorial design that investigates every possible combination, would require 2^4=16 design points. A full factorial design of four factors with four levels each would require 4^4=256 design points. Increasing the number of factors and/or levels for a full factorial design causes the number of design points needed to increase exponentially, and this is referred to as the "curse of dimensionality." A much more efficient design, developed at the Naval Postgraduate School, is called the Nearly-Orthogonal Latin Hypercube (NOLH). NOLH designs have good space-filling and orthogonality properties (Sanchez, Sanchez, & Wan, 2014). Figures 23c and 23d show a good example of the difference in coverage between factorial

and NOLH designs. Figure 23 shows a comparison of the pairwise projection plots for two factorial (if top row) and two NOLH designs (if bottom row).

a. 2^4 factorial: 16 design points   b. 4^4 factorial: 256 design points

c. NOLH: 17 design points   d. NOLH: 257 design points
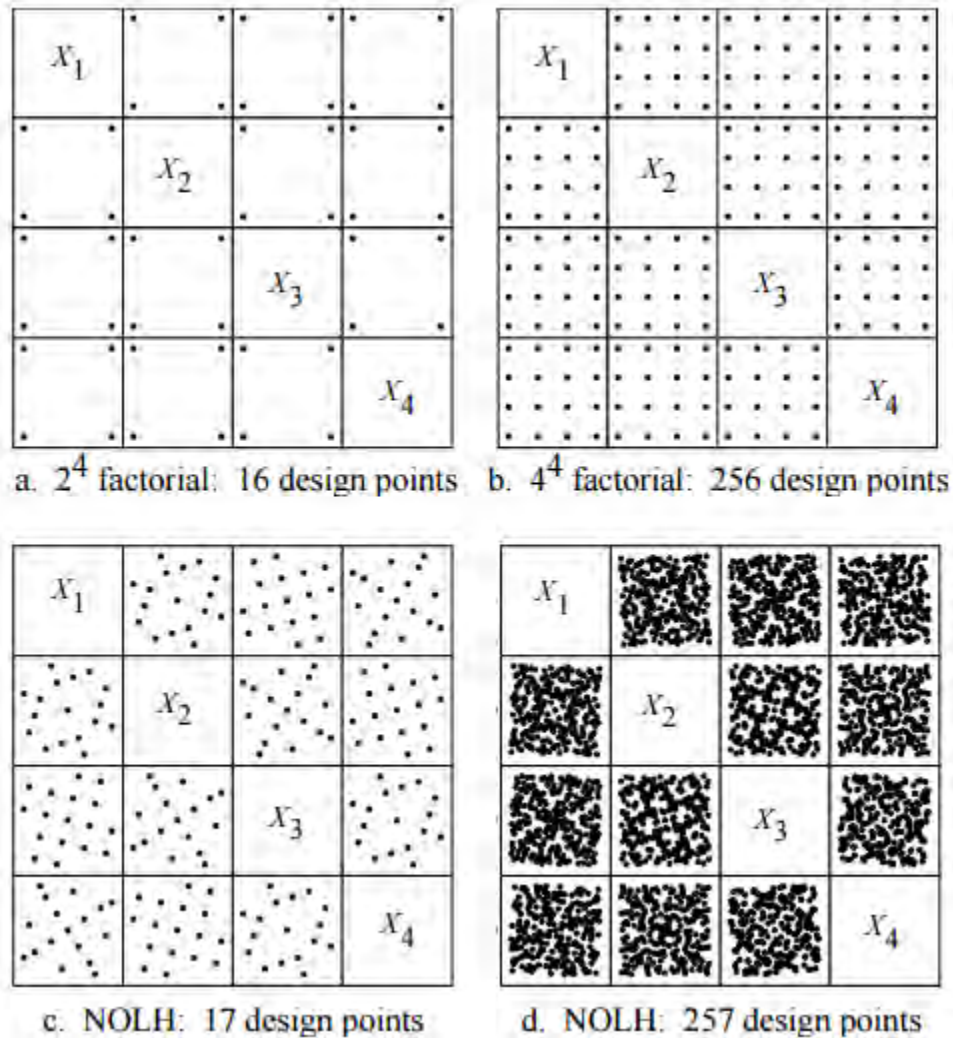
Figure 23. The top row features factorial designs and the bottom row illustrates the near-orthogonality and space-filling properties of NOLH designs (from Sanchez, Sanchez, & Wan, 2014).

The computational savings of the NOLH designs is enormous; but, the NOLH design is best suited for continuous factors. The inclusion of discrete or categorical factors can cause the pairwise correlations to increase, due to the rounding involved. Therefore, since our design contains several discrete factors, we use one of the new designs—the nearly orthogonal-and-balanced (NOB) mixed designs of Vieira, Jr.,

Sanchez, Kienitz, and Belderrain (2011, 2012). For this research, the 512-design point, NOB design template, available at http://harvest.nps.edu, is used. Figure 24 contains an excerpt of the 512-design point, NOB design spreadsheet template. Additionally, the low and high values we see in this figure are the same as the maximum and minimum values we saw in Table 3.

	GV	GW	GX	GY	GZ	HA	HB	HC	HD
4	10	25	8000	1000	5	800	8000	1000	0.5
5	30	60	1000	8000	42	2000	1000	8000	0.95
6	0	0	0	0	0	0	0	0	2
7									
8	LCMvtSpd	LCACMvtSpd	AAVSnrDetRn	AAVSnrClsRn	AAVMvtSpd	AAVrws	ACVSnrDetRn	ACVSnrClsRn	ACVSnrClsPr
9	13	58	2397	1384	38	1051	4247	5603	0.84
10	27	31	5479	2562	25	990	2767	3260	0.69
11	11	33	7493	5795	18	1366	1644	5616	0.75
12	29	53	3151	2671	18	1244	4959	2658	0.86
13	13	29	5986	4219	29	1939	4795	1493	0.6
14	28	59	4329	3274	19	1342	6753	2589	0.53
15	13	27	3479	6178	30	1195	7795	3233	0.91
16	16	32	5808	3740	32	1969	5493	3726	0.53
17	28	54	1288	6137	31	852	6247	2014	0.94
18	29	57	5055	4890	8	1620	7301	4137	0.89
19	10	32	2753	6726	16	1469	1329	6712	0.94
20	14	58	2781	1836	17	1394	2658	5288	0.85
21	24	53	2027	2315	28	1364	2836	7795	0.76
22	19	55	7014	4863	20	1361	4986	5247	0.87
23	28	35	4932	1753	30	1692	6438	3082	0.87
24	20	32	6247	7466	32	800	4726	3329	0.51
25	13	26	3548	2904	19	1303	4836	2630	0.74
26	28	48	3808	7904	31	1049	1315	6904	0.69
27	24	43	7932	6384	6	885	1219	1945	0.56
28	17	27	6438	5781	29	1925	3589	2863	0.85
29	28	58	7110	3507	19	1340	1699	4589	0.91

Figure 24.   An excerpt of the 512-design point, NOB design spreadsheet template, which allows for the investigation of the 77 factors. The template can handle simultaneous investigation of 300 factors, with discrete number levels and continuous-valued factors (after Sanchez, Sanchez, & Wan, 2014).

As previously mentioned, not only are these designs space-filling, but they also produce the near-orthogonality desired for regression analysis. All pairwise correlations are less than 0.012 in our design. A color map of correlations can be used to visualize pairwise correlations, and is shown in Figure 25. The 77 red cubes connected along the

diagonal depict the perfect positive correlation (i.e., red = 1.0) between the factor and itself, while the remaining area is shaded grey, which shows a near-zero correlation between any factors that are not the same. Appendix G shows a multivariate plot for the complete design.
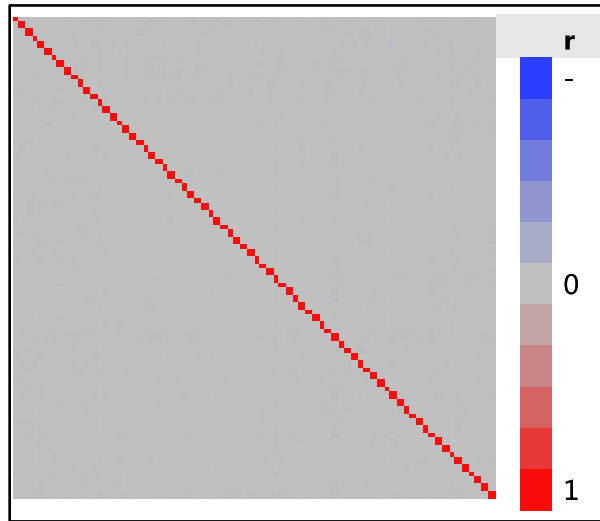
Figure 25.   Color map of the design's pairwise correlations.

C.   EXECUTING THE EXPERIMENT

The NOB design spreadsheet provides 512 design points for the 77 factors (not including the scenario type). The design for the 77 factors was then crossed with the scenario type factor, yielding a total of $4 \times 512 = 2{,}048$ design points. EW 12, MEB concept of operations, and research covered in Chapters I and II were used to guide the selection of factors, ranges, and levels. For example, E2O provided many of the ranges for factors covered, as these values were deemed interesting to the stakeholder, based on key performance parameters and objective threshold values for systems being procured. Each design point was run using 30 different random seeds. We discuss the rationale for using 30 replications in Section D.

The following section describes how the Simulation Experiments and Efficient Designs (SEED) Center configured and executed the DOE. The base case MANA scenario, in eXtensible Markup Language (XML) format, and the DOE file, in comma-

separated value (CSV) format, were entered into a software program called XStudy, written by SEED Center Research Associate Steve Upton. XStudy enables the user to map each column in the design file to a specific parameter element in MANA, using XPaths. An XPath is a reference to a specific location in an xml file. Other details about the study design, such as the version of MANA and the number of replications per design point, are also entered into this tool, yielding a single "study.xml" file. This study file is used by another program called oldmcdata, also written by SEED Center Research Associate Steve Upton, which programmatically modifies the MANA XML file, producing a separate XML scenario file for each design point. An open source software package called condor, available from the University of Wisconsin (http://www.cs.wisc.edu/condor), is used to distribute and manage the MANA jobs in parallel across a set of available processors. The oldmcdata software creates the set of submit.dat files needed by condor, one for each design point job. A job consists of a set of replications for one design point excursion. Upon completion of the runs, oldmcdata includes a data postprocessor that combines MANA summary file output from the individual design point excursions into one csv file, ready for use with any data analysis software package. This output file contains input factor settings from the DOE, the random number seed, and outputs for each replication. The SEED Center high-performance computing cluster configuration used for these runs was composed of 128 Windows processors, with 2-4 gigabytes (GB) of random-access (RAM) per processor.

D.   NUMBER OF REPLICATIONS

One replication of the base case MANA takes, on average, 10 minutes, and this computational cost must be taken into account when determining how many replications to perform. One method for determining an adequate number of replications is the data given in Equation 1. We will use this equation to estimate the sample size needed to perform null hypothesis significance testing given the Blue casualties' MOE. Our choice for alpha (α), which represents Type I error, was 0.05. The choice for power, which is 1 minus beta (β), the Type II error, was 0.95. In Equation 1, then, $Z_\alpha = 1.96$ and $Z_\beta = 1.64$. Our choice for the

practical difference we want to detect, in the denominator, was 2, and the estimate for standard deviation, based on 100 replications of the base case, was 5.86.

$$n = \left(\frac{\sigma \left(Z_\alpha + Z_\beta \right)}{\left(\mu_0 - \mu' \right)} \right)^2 \qquad (1)$$

The resulting sample size (n), given our values described above, is 112. The cost in computational power and time, however, might not support doing this many replications. We note that we could lower n to 68 by dropping power to 0.8 (a common choice), vice 0.95. We turn next to visualizing, in Figure 27, how the half-width of the confidence interval for the mean decreases as a function of the number of replications, in order to determine where diminishing returns occur. As the confidence interval half-width decreases, we achieve increased precision on our estimate of the mean. Figure 27 shows that while 112 samples might be ideal, the additional precision acquired by doing between 30 and 100 replications may not be worth the increased computation cost. This is particularly true because when we fit metamodels to the resulting output, we are able to leverage data collected from the entire design to estimate factor effects. This substantially increases the power of the statistical tests.
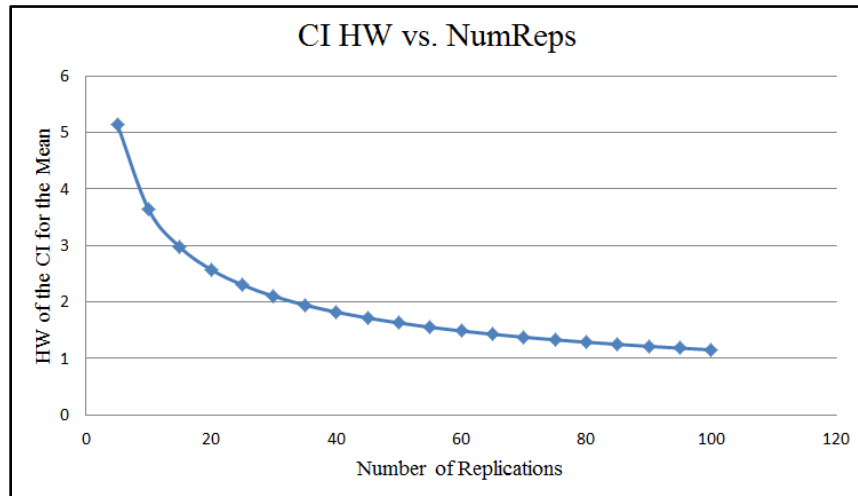
Figure 26.   Confidence interval half-width diminishing returns, based on the number of replications. It appears that the added benefit from going from 30 replications to 100 might not be worth the computational cost of running a MANA simulation that takes 10 minutes, on average, for each simulation.

59

In the end, we choose to perform 30 replications of each of our 2,048 design points, resulting in 61,440 total simulation runs. Given access to the SEED Center's 128 Windows processors with 2-4 GB of RAM each, we are able to complete the experiment in approximately 3.5 days.

V.   DISTRIBUTED FLIGHT DECK OPERATIONS AND SIMIO MODEL DEVELOPMENT

This chapter begins with a general overview of the deck cycle for aircraft on an amphibious ship, such as an LHD, and the selected DES modeling software, Simio. Additionally, it covers the benefits and limitations of Simio, which includes why DES is also useful to DOD decision makers. Finally, we will review the research questions for this first-stage model and describe the Simio modeling. This Simio model is an example of what Cioppa, Lucas, and Sanchez (2004) describe as a model that attempts to capture "the salient features of the situation without trying to model all of the details that could be considered" (Cioppa, Lucas, & Sanchez, 2004, p. 172).

A.   GENERAL DESCRIPTION

The principle finding of "Operational Energy/Operational Effectiveness (OE2) Investigation for Scalable Marine Expeditionary Brigade Forces in Contingency Response Scenarios" is that operational energy consumed from QRF and MEDEVAC air platforms launched from the seabase are the primary drivers of energy during expeditionary operations. Seabased aviation operations consume energy over both workups and the deployment of a MEU. The MEU regularly launches ACE platforms in support of a ROMO, including VBSS, HA/DR, A2/AD, etc. The launch and recovery of aircraft from the ARG is called the "deck cycle." Groupings of aircraft that launch together for a mission are commonly called "packages." In order to better understand the impacts to operational energy for a BLT force ashore, we will construct a first-stage model of a nominal air raid package required for the insertion of the screening force described in Chapter II.

The MEU's ACE consists of a parent MV-22 squadron reinforced with several detachments of light attack, strike, and heavy-lift aircraft from other redeployed units. Typically, the ACE consists of 12 MV-22s, 4 AH-1Zs, 2 UH-1Ys, 6 F-35Bs, and 4 CH-53Ks. The MEU commander may retain the ACE on the LHD or allocate aircraft to other air-capable ships (i.e., place aircraft on LPDs) during split or disaggregated

operations. These operations require coordination via a detailed flight schedule. A flight schedule is produced daily that includes both the Marine aircraft from the ACE and the Navy's search and rescue (SAR) platform, the SH-60. The flight schedule establishes when the ships will conduct flight operations ("flight quarters") and deconflict launch and recovery times of aircraft from spots. The only aircraft that requires the use of the entire deck for take-off ("deck-run") is the F-35B. Aircraft are kept on the forward and aft "slash" areas prior to being towed out to a spot for launch. A launch, like the MV-22 seen taking off in Figure 27 has a sequence of steps leading up to the actual launch:

1. Aircraft spotted – Aircraft towed from slash to spot.
2. "Chocks and chains" – Aircraft secured to the flight deck spot (i.e., chocks and chains put in place).
3. Aircraft are loaded with the mission fuel and ordnance.
4. Startup.
5. "Breakdown" – Aircraft chains and chocks are removed.
6. Arming – Ordnance crews and/or crew chiefs remove safety mechanisms from weapons and survival systems.
7. Launch – Deck crews clear the aircraft for subsequent takeoff.

Figure 27.   Figure 28 shows an MV-22 Osprey launching from a forward spot. All three aircraft, to include the CH-53E, belong to Marine Medium Tiltrotor Squadron (VMM) 265 (Reinforced) (from Achterling, 2014).

Three aircraft are shown, two MV-22s—one of which is taking off—and a CH-53. The aircraft are assigned to Marine Medium Tiltrotor Squadron (VMM) 265 (Reinforced) aboard the USS Bonhomme Richard (LHD 6) (Achterling, 2014).

Figure 28 shows two groupings of MV-22 Ospreys (circled in white), the groups are in the forward and the aft "slash." In the forward "slash" of the LHD there are four MV-22s. At least that many are stored in the aft "slash," which is located aft of the super structure. The MV-22s in the "slash" have their rotors and wings folded; an automatic process that takes approximately 90 seconds. A tug is used to pull aircraft from the "slash" and tow it over to the spot to prepare for start-up and launch. The usable spots for the LHD are spots two, four, five, six, seven, and nine. The forward "slash" prohibits the use of spot three, while the aft "slash" precludes the use of spot eight.

Figure 28.   MV-22 Ospreys with folded rotors and wings in the forward and aft
"slash" of the LHD (from Galante, 2009).

Figure 29 shows MV-22 Ospreys at night preparing for takeoff from the amphibious transport dock ship USS Mesa Verde (LPD 19). Two aircraft flying together are known as a section. This figure shows the use of expanded spots on the LPD. The

center circles are spots one and two; however, in order to allow for four aircraft to be spotted, the corner spots are used. The MV-22s with their blades turning both have red lights shining and are on spots three and six diagonally across from each other. Meanwhile, the MV-22s in their stored configuration (much like the "slash") on the opposite diagonal occupy expanded spots four and five.

Figure 29.   MV-22 Ospreys at night occupying all four of the expanded spots on the amphibious transport dock ship USS Mesa Verde (LPD 19). Expanded spots three and six have turning aircraft, preparing for launch, and expanded spots four and five have MV-22s with their rotors and wings folded. These aircraft are assigned to the 22nd MEU and the picture was taken during a composite training unit exercise (COMPTUEX) in preparation for a deployment (from Smith, 2013).

All of these aircraft serve the GCE. With the advent of the MV-22 Osprey, Marines can travel further and faster inland than with the legacy CH-46 medium-lift helicopter. Prior to sailing as an MET-capable MEU, Marines conduct several exercises to demonstrate their ability to conduct a long-range raid, far enough that forward arming

and refueling points (FARPs) are required before reaching the objective area. Figure 30 shows the GCE boarding for a long-range raid.

Figure 30.   Marine forces from the 11th MEU cross the flight deck to the five MV-22 Ospreys attached to Marine Medium Tiltrotor Squadron 163 (Reinforced). The flight deck is that of the amphibious assault ship USS Makin Island (LHD-8) (from Fuentes, 2015).

B.   SIMULATION MODELING FRAMEWORK BASED ON INTELLIGENT OBJECTS

1.   What is Simulation Modeling Framework Based on Intelligent Objects?

We start with a modeling architecture, Simio, and the goal of gaining insight about one aspect of seabased aviation—mission holding associated (Sanchez, 2007). From Appendix I, we can see both the MANA and Simio architectures side-by-side. People like Simio because it is relatively easy-to-use software for dynamic simulation (Kelton, Smith, & Sturrock, 2011). Simio uses intelligent objects, such as customers,

infantry, or aircraft, in conjunction with the physical components of the system they are in to model and reflect dynamic interactions of entities within a system. Simio works well for DES, specifically discrete event, stochastic, models for solving problems (Kelton et al., 2011). Simio was industrialized by the same people that developed Arena (another type of DES that has been widely used), but leverages early instances of *object-oriented* modeling, which grew into the Simio of today (Kelton et al., 2011).

2. Benefits of Simio

Simio is intuitive and easy to use. Once all the objects are created, they can be used in multiple simulation models. For the Marine Corps, this is highly useful because of the combined visuals, ease of use, and building-block nature to advanced modeling. Below is a list that summarizes the benefits of Simio.

- Visualization—a Simio model looks like the real system.

- As with many software programs, with Simio it is easy to build large models of increased complexity from initial *toy* models.

- Simio objects can be used for multiple models.

- Simio objects can readily be reused and combined to build process models.

- Process models can be easily adjusted and experimented with to gain insights.

- Many experiments can be run (i.e., thousands of replications) and results are collected in pivot tables that may be exported to an XML file for analysis. (Simio LLC, 2010)

3. Simio: Limitations and Assumptions

a. Limitations of Simio

Simio is limited by the level of detail provided to each object by the user and the Simio environment. In this first-stage, launch constraint, model the focus was a long-range raid and any holding that transpired during the entire operation. The aircraft agents in Simio all takeoff and "launch" with the same flight characteristics and profile. However, this is known not to be the case for MV-22, CH-53K, F-35B, etc. Therefore, a

limitation in Simio is that the modeled system might not reflect the complexity of the real system. In aviation, winds, pitch, and roll of the ship, and temperature can alter fuel consumption rates. During flight operations, naval traffic can preclude aircraft from landing until the ship alters course. Yet, all of these, to include the unique takeoff profile of dissimilar aircraft did little to inform the MOEs. Different launches and flight conditions, which could have been modeled were not, however, this model had the right level of precision to make it valid for the purposes of this broad analysis (Kelton, 2011).

b.   Assumptions Made in Simio

The primary assumptions in this Simio model are that times for mission holding and launch are distributed with a triangular distribution. The simulation is used to better understand launch constraints and aircraft flight operations.

- Triangular distributions are assigned for service times (e.g., LPD slash, fuel/arm).

- Aircraft objects – the launch process is roughly similar for all types of aircraft and they are modeled by the same process.

- A launch includes removing an aircraft from the slash to it being cleared for takeoff.

- The flight schedule launch times representative of a flight schedule are generated from a time varying arrival process with hourly granularity.

- Aircraft from the LHD require mission holding to constitute the package.

- The LPD has one slash, two spots, one fuel, Arm/De-arm, and one chains crew.

- The LHD has two slashes, three spots, one fuel, Arm/De-arm, and one chains crew.

C.   RESEARCH QUESTIONS

This first stage model is valuable as it generates realistic inputs to the MANA second stage model. Additionally, one may adjust the first stage model independent of the larger amphibious model, which may be useful for energy-specific insights related to air operations. While this Simio model focuses on the flight-deck cycle, one could easy apply a first stage model like this to explore other key areas in amphibious assault. One

such application is instead of using aircraft launching from the flight deck, use ACV departing the LCAC, or infantry departing the ACV.

The questions guiding this first stage model are:

- Are there OE2 benefits to conducting distributed ops?

- Are there OE2 benefits to conducting split ops?

Addressed in this section are EW 12 aviation-seabase-related particulars that are applicable to the deck cycle, and how those were implemented in Simio. We also provide further details about the objects in Simio and an overview of the system.

D.   MEASURES OF EFFECTIVENESS

The purpose of this simulation is to provide a specific look into the OE2 of the ACE launching from the seabase in support of amphibious operations. Here, our MOEs include:

- MOE (5): Mission Holding

- MOE (6): Mission Total Time

E.   SCENARIOS

Modeled is a 14-aircraft package launched in support of a long-range raid, which requires a FARP. There are three available spots on the LHD and two expanded spots on the LPD. The SAR aircraft is required throughout flight operations, and the SAR SH-60 must have a free spot to land on at all times.

Covered here are:

- The three scenarios modeled in Simio: All-LHD, Split, and Disaggregated Operations (Ops).

- Modeling particulars.

- Details on the Time Varying Arrival Rate Table ("flight schedule"), servers, and objects.

F. MODELING PARTICULARS

1. Source

The source node for this long-range raid creates a maximum of 14 total aircraft to be launched from the ARG. The source is used to initiate launches according to a time-varying rate table and these launches may be probabilistically assigned to ships according to the scenario modeled. Aircraft may launch from either of the two ships: the LHD and the LPD. Aircraft may also be pulled from either the forward or the aft slash on the LHD to support the required package. The Marine ACE holds when launched from the LHD. The ACE aircraft are:

- A single SAR SH-60.

- A section of AH-1Z Super Cobras (attack and escort).

- A section of F-35B (attack and escort).

- A command and control UH-1Y (air mission commander platform).

- Six MV-22 Ospreys providing the required lift for the minimum required force and go criteria for the GCE.

- A section of CH-53Ks for the FARPs.

Table 5 lays out how many deck spots, slash areas, and crews are modeled in the three options described to compare the resources available. Split and disaggregated ops in the context of Table 5, are split ops 12/14 aircraft on the LHA and disaggregated ops 10/14 aircraft on the LHA.

Table 5.   The three options modeled are: all aircraft launching from the LHD, the split, and disaggregated operations. Aircraft launched from the LHD have two slashes (forward and aft), three spots, and one crew to facilitate the launch sequence. No LPD slash, spots, or crew are available in "all from LHD" operations.

Operations	Prop_LHA	Slash		Spots		Crews	
		LHD	LPD	LHD	LPD	LHD	LPD
All from LHD	1.0	2	0	3	0	1	0
Split	12/14 = 0.857	2	1	3	2	1	1
Disaggregated	10/14 = 0.714	2	1	3	2	1	1

The mission modeled is a long-range raid. The composition is 14 aircraft launched in any of the three operations listed in Table 5. The model focuses on the origination options, which may either be all from the LHD, the split, or disaggregated.

A requirement (to satisfy it being a long-range raid) is a FARP. From the origination options described, aircraft hold as required to constitute the package, transit to the objective area, and then FARP. The FARP mission is the responsibility of a section of CH-53Ks. The FARP has four fuel points, capable of providing gas to running aircraft in four fixed spots (a "hot static FARP"). The CH-53Ks are likely FARP platforms since they provide internal fuel stores that support bulk refueling.

The single-ship SH-60 facilitates the SAR mission, serving as the SAR aircraft. This aircraft is required for rotary and tilt-rotor operations. Of note, spot two on the LHD is dedicated for SAR operations and cannot be spotted with ACE aircraft.

Two AH-1Zs, one UH-1Y, and two F-35Bs provide escort, command and control, strike, and close air support. These aircraft all safeguard the GCE flying aboard six MV-22s. Thus, with the originations described, 2 AHs, 1 UH, 6 MVs, 2 F-35s, 1 SH, and 2 CHs, totaling 14 aircraft, are modeled.

Link weights are used to facilitate spilt and disaggregated operations. A link weight of zero bars split operations, forcing all 14 aircraft to launch from LHD. For this, a numeric property was assigned to the path connecting the source node to either the LPD slash or the transfer node, leading to the LHD forward and aft slashes.

2. Time-Varying Arrival Rate Table

The flight schedule was created to support the package described. The real-world process modeled is the initiation of the launch process for individual aircraft. This is modeled from a time-varying arrival rate pulled from a rate table. Table 6 shows the Time-Varying Arrival Rate Table.

Table 6. This Time Varying Arrival Rate Table shows the launch of a section of AHs within the first 30 minutes of flight operations, followed by the GCE aboard six MV-22s in the next 30 minutes, followed by the SAR, FARP, and command and control aircraft, until, lastly, the F-35Bs are launched.

Starting Offset	Ending Offset	Rate (events per hour)
Day1, 00:00:00	Day 1, 00:30:00	2 AHs
Day1, 00:30:00	Day 1, 01:00:00	6 MVs
Day1, 01:00:00	Day 1, 01:30:00	1 UHs, 1 SHs, 2 CHs
Day1, 01:30:00	Day 1, 02:00:00	2 F-35Bs

Another reason for the rate table is that the F-35B requires a deck run, and the sequencing of aircraft from and to the spots is dictated this way in practice.

3. Seabase

Scenarios include split and disaggregated operations (with the LPD), and all from LHD operations (without the LPD).

a. *Launch Process: LHD*

(1) Forward Slash

Subsequent to the initiation of a launch, the time required to position the aircraft is a random variable draw from a random triangular distribution that "draws" with a minimum of 15 minutes, mode of 30 minutes, and maximum of 50 minutes. We represent this distribution the following way: *T~Tri(x,y,z)*, where the forward slash is *S~Tri(15, 30, 50)*. Thirty minutes is a commonly accepted length of time to tow an aircraft out of the slash and bring it to its spot.

(2) Aft Slash

Follows the same parameters as the forward slash: *S~Tri(15, 30, 50)*.

(3) Resource Node

Following aircraft being spotted to the initiation of takeoff, the time required for fueling, breaking down the chocks and chains, arming, and the launching of an aircraft once they are spotted is a random variable draw from a random triangular distribution that "draws" with *L~Tri(3, 5, 10)* for the LHD. This modeled Simio is a limited resource

71

that has one fixed capacity and First In, First Out logic. This embodies the limitations of ordnance and fueling crews available to service one spot on the flight deck at a time.

(4)   Mission Holding

Following takeoff, the holding time required for creating the flight package is a random variable draw from a random triangular distribution that "draws" *H~Tri(5, 10, 20)*. Disparate aircraft traveling on different routes after takeoff from the LHD hold linkup for the subsequent transit, objective area, and FARP portions of the mission.

b.   LHD

(1)   Slash

Follows the same parameters as the forward and aft slash of the LHD; however, they are distributed as *SL~Tri(2, 5, 7)*. Aircraft slashed on the expanded spots are more readily available for prelaunch procedures than those aboard the LHD once flight quarters are sounded. Flight quarters occurs when a ship may is postured to safely conduct flight operations. Removing them from the LPD slash often does not entail any aircraft movement at all (see Figure 30).

(2)   Resource Node:

Spotted aircraft on the LPD perform the launch sequence, which is a random variable draw from a random triangular distribution that "draws" with *LL~Tri(2, 3, 5)* for the LPD.

c.   Transit to the Objective Area, Objective Area Time on Station, FARP Time and Sink

After the package is constituted, aircraft depart the rendezvous point and transit to the objective area and FARP location with transit time, TT, where *TT~Tri(40, 60, 120)*. The subsequent objective area time on station, TOS, where *TOS~Tri(20, 30, 45)* and FARP time, FT, where *FT~Tri(15, 20, 45)* support disparate aircraft, traveling on different routes, of varying times, over a broad range of likely missions. All three (transit time to the objective area, objective area time on station, and FARP time) follow random triangular distributions.

Upon completion in the FARP, aircraft depart the process. In Simio, objects check out of the system via a sink node. At 10 hours, the simulation ends, with the package of aircraft all having arrived at the sink.

Figure 31 shows a screen shot of the final simulation effort done in Simio.
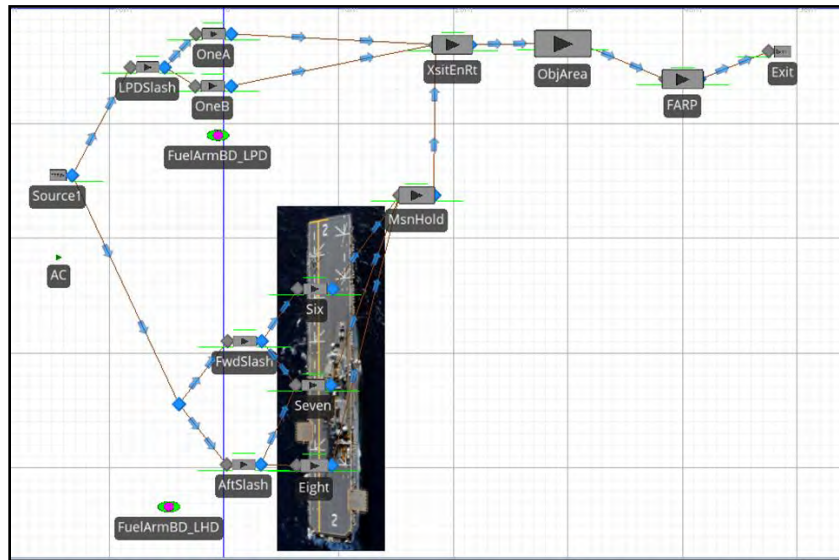
Figure 31.   Screen shot of the Simio simulation.

In summary, this section reviewed Simio and its usefulness for discrete event simulations, particularly aircraft launch constraints. We saw a varying arrival rate table operationally simulates the flight schedule. Finally, we learned about how agents, arrival times, resource nodes, and servers were used to model a long-rang raid evolution that included a FARP.

THIS PAGE INTENTIONALLY LEFT BLANK

VI. DATA ANALYSIS AND RESULTS

Gatchel sums up a sea power's advantage this way: In spite of the availability of modern ground and air transportation to defenders today, navies continue to maintain their traditional mobility advantage…no army can move with enough combat power to repulse a major assault before the landing force has established itself ashore.

—CAPT Wayne P. Hughes, Jr., USN (Ret)

In this chapter, we analyze the data generated from the experiments described in the previous chapters, and present main insights.

A. JMP DATA ANALYSIS TOOL

JMP is statistical analysis software that provides the capability for analysts to visualize and analyze data, including metamodel fitting. JMP can also be used for data manipulation prior to analysis. For example, data was concatenated, sorted, and organized in JMP. The tools in JMP can create interactive linked graphs, display data histograms and statistical summaries, as well as perform regression analysis and other multivariate methods. JMP also has a useful journal feature that allows the user to save and organize artifacts of the analysis. One of the most attractive features of JMP is its intuitive, context-dependent, menu-driven interface (Suite of Analytics Software [SAS], 2014).

B. ANALYSIS OF AMPHIBIOUS ASSAULT EXPERIMENT

First we present the four MOEs used in this analysis.

- MOE (1): Blue casualties

- MOE (2): Red casualties

- MOE (3): Time to attrite the Red Force to one-third remaining strength

- MOE (4): FER, which is calculated as (Red casualties +1)/(Blue casualties +1)

Let us now review our scenarios as they relate to the results:

- 1. LCAC (ACV) only

- 2.   LCAC (ACV) + AAV

- 3.   LCAC (ACV) + MV-22

- 4.   LCAC (ACV) + AAV + MV-22; combines scenarios 2 and 3

1.   Histograms

Histograms are commonly used to display the distributions of numeric data and indicate features of the data such as central tendency, spread, skew, and modality. The following histograms are not distributions of the raw output data—the data come from different design points averaged together. The results in this section are the means of the 30 replications at each of the 512 design points.

a.   MOE (1): Blue Casualties

Figure 32 contains four histograms from left to right: scenario 1 (baseline), scenario 2, scenario, 3, and scenario 4.
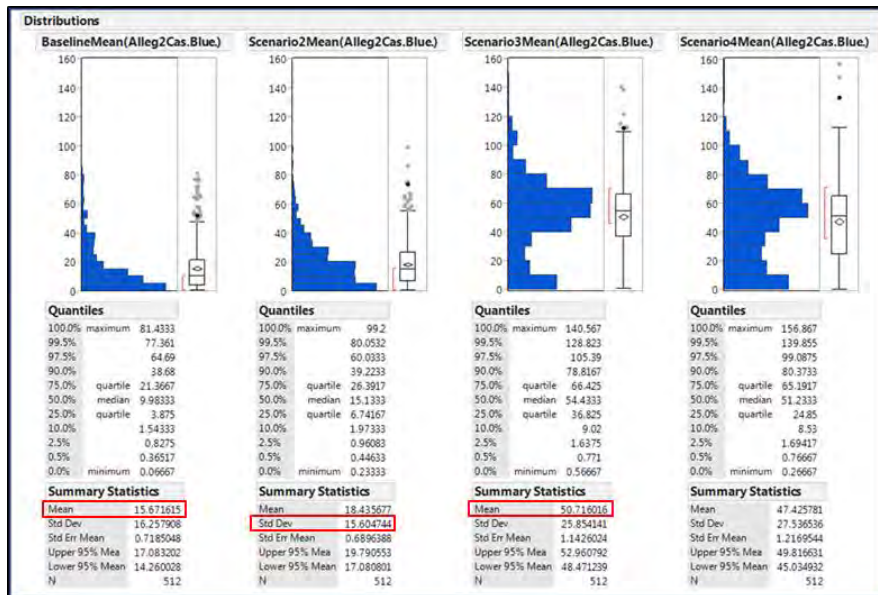
Figure 32.   Histograms of Blue casualties by scenario. The highest mean of Blue casualties occurs for scenario 3. Recall that scenario 3 conducts STOM-V, with a wave of MV-22s. Scenario 4 combines scenarios 2 and 3, so it also shows a high mean number of casualties compared to scenarios 1 and 2.

To the right of each histogram is a box plot. Box plots will be covered in Section 2. Below the histograms are quantiles and summary statistics, including the means. Scenario 3 has the highest average Blue casualties and scenario 1 has the fewest. We note that standard deviation is the smallest during scenario 2. The first two scenario histograms are positively skewed. Scenarios three and four are bimodal, with peaks near 50 casualties and 10 casualties.

Blue casualties are greatest in scenario 3, when Blue is brought in via MV-22s, which means that infantry are more vulnerable than when they are entirely inside ACVs. Scenario 4, which combines scenarios 2 and 3, is associated with greater numbers of casualties than either the ACV or ACV and AAV scenarios.

b. MOE (2): Red Casualties

Figure 33 contains histograms, box plots, and summary statistics for Red casualties.
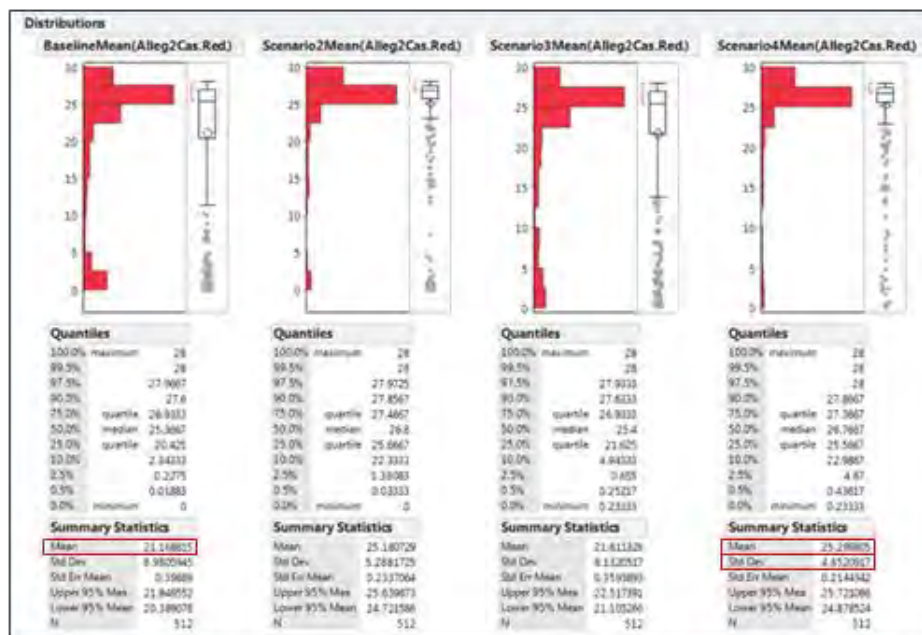
Figure 33. Red casualties are greatest when Blue attacks with ACVs and AAVs in both scenarios 2 and 4. Red's survival is better when Blue does not use the AAVs. Red casualties experience little change from scenario 1 to 3. Scenarios 2 and 4, each have waves of AAVs accompanying ACVs onboard LCACs.

The highest mean Red casualties occur with scenario 4; however, scenario 2 has a slightly higher median number of casualties. In any case, scenarios 2 and 4 are very similar. Scenarios 1 and 3 are also similar with respect to this MOE. Red casualties are greatest when Blue attacks with AAVs and ACVs in both scenarios 2 and 4. In scenario 4, Blue attacks with a combined force from AAVs/ACVs and infantry brought in from MV-22s. This scenario's strength does not appear to be the MV-22, based on the insignificant increase from scenarios 1 to 3, but rather the AAV. All four scenarios, interestingly enough, are negatively skewed, as evidenced by the long tails toward low casualties (circled in the figure) Nevertheless, Red casualties are lower, with a higher frequency when the AAV is not present, as in scenario 3.

c. MOE (3): Time to Attrite the Red Force to One-Third Remaining Strength

Figure 34 contains the histograms, box plots, and summary statistics for time to attrite the Red force to one-third remaining strength, where the fastest mean time occurs with scenario 4.
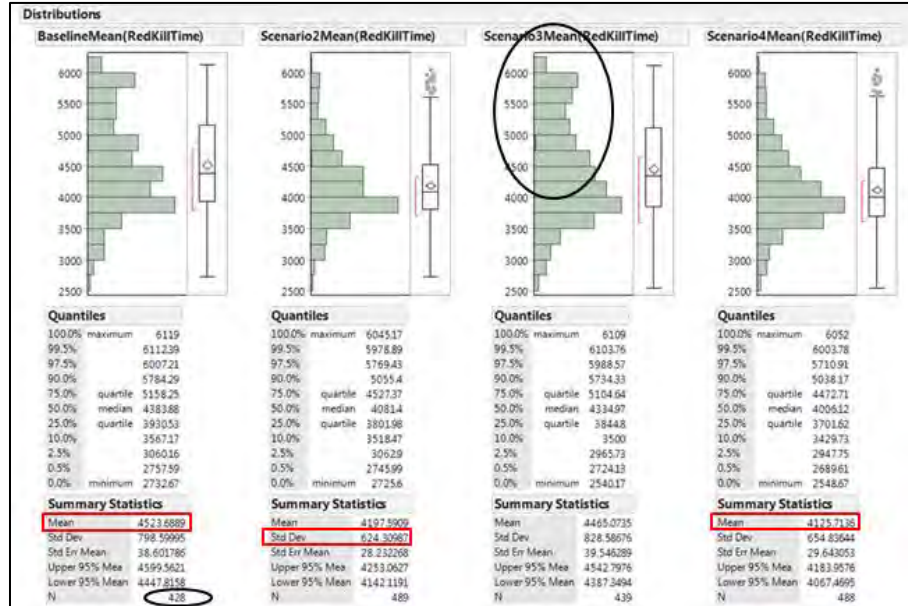
Figure 34. Time to attrite the Red force to one-third remaining strength, where the fastest mean time occurs with scenario 4. This objective is not met 84 times with scenario 1 (512 – 428 = 84). Meanwhile, scenario 2 has the lowest standard deviation and higher times can be expected with scenario 3, seen in the circled portion of the data.

78

There is, however, overlap, as seen with scenarios 1 and 3. The greater frequency of long times for scenario 3 makes sense, given the scenario 3 Blue casualty numbers. It is important to realize, in general, that achieving one-third remaining strength might not always happen. This explains why N is less than 512 for each of the scenarios. We achieve this MOE the fewest times during scenario 1—namely, that Blue is slower to mass and attrite Red.

There is good cause for us to revisit the raw output data, since if one design point attrites the enemy in only half of the replications—but when it does, does so quickly—a low Mean (RedKillTime) only tells part of the story. Therefore, a wise approach is to create a column next to the FER in the full data that is a binary result, where success is attriting Red to one-third of its remaining forces. Figure 35 shows the probability of attriting Red to the desired level.

.
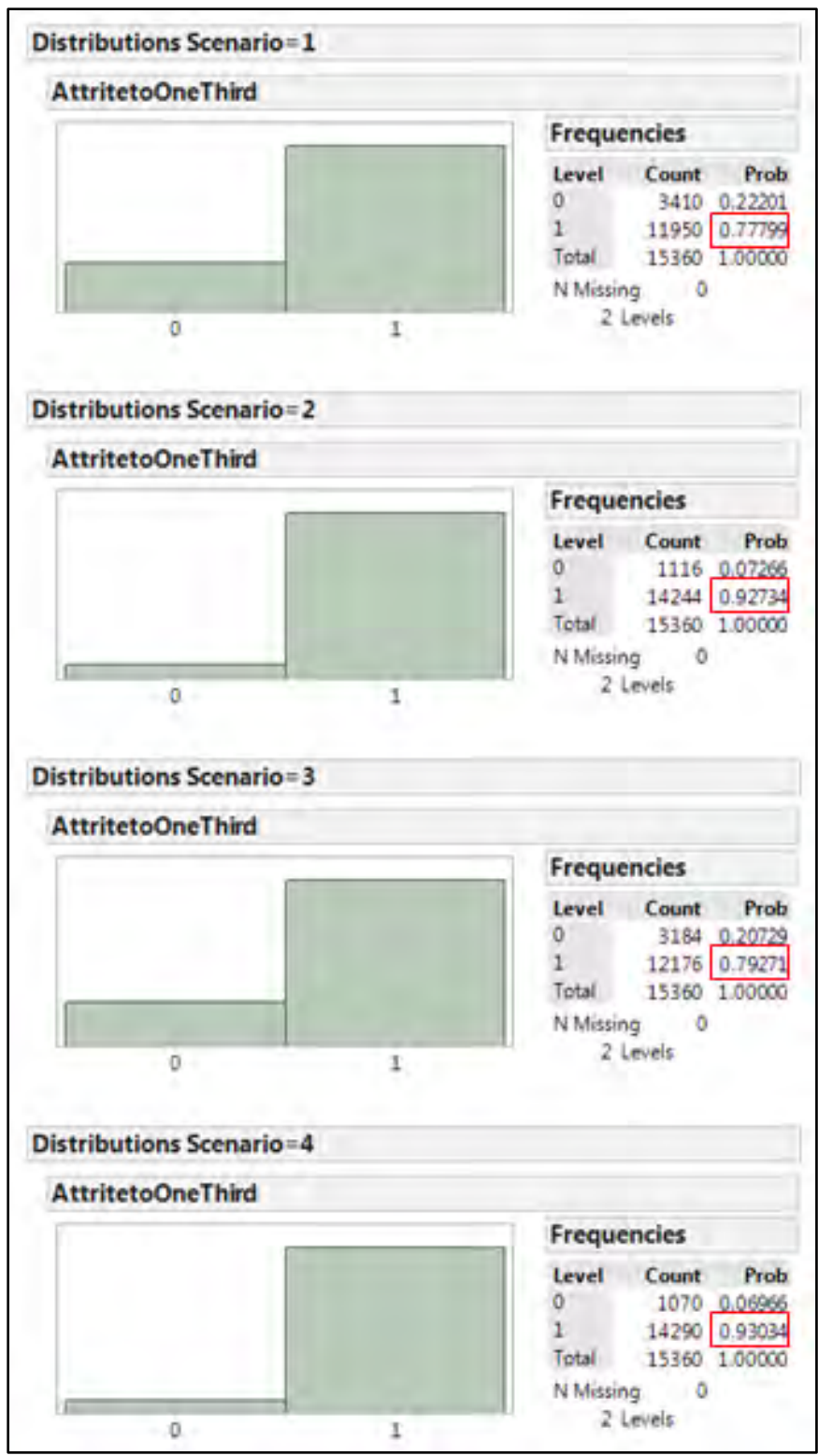
Figure 35.   Realized probability for attriting Red to one-third of its remaining forces.

The highest probability occurs in scenario 4. There is a significant jump in probability from scenario 1 to scenario 2, and then little gain thereafter from scenario 4. In the context of number of assets fighting on the battlefield, there is support that scenario 2 gives the best bang for the buck.

d. MOE (4): Force Exchange Ratio, Which is Calculated as (Red Casualties +1)/(Blue Casualties +1)

Figure 36 contains the histograms, box plots, and summary statistics for the FER MOE.
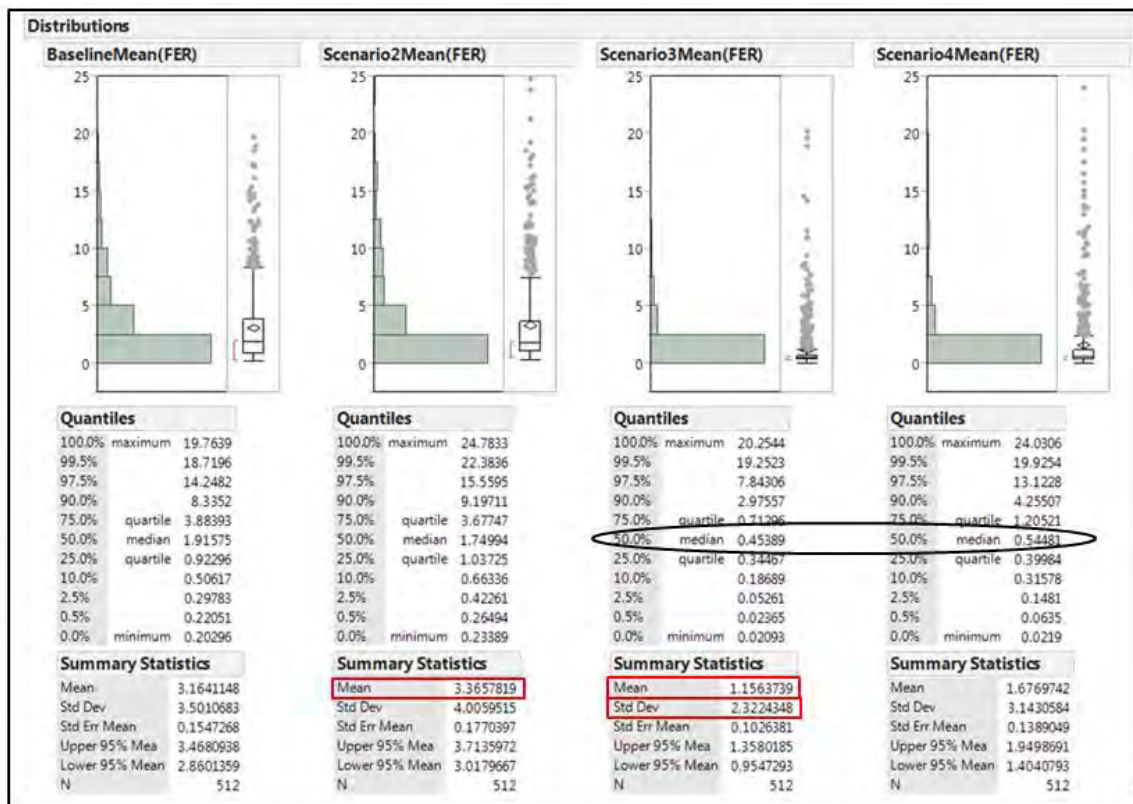
Figure 36.   FER MOE. This is calculated as (Red casualties +1)/(Blue casualties +1) with the raw data. Higher values imply that Red experienced greater casualties than Blue. Blue achieves the highest FER with scenarios 2 and 1.

Recall that the FER is calculated as the ratio of Red forces lost to Blue forces lost, where 1 is added to both the numerator and denominator in the raw output data. After it is calculated, then FER is averaged over the replications. So, for our analysis,

higher is better. If the FER is high, as it is in scenario 2, that means that Blue is losing far fewer casualties than Red. The FERs for scenarios 1 and 2 are similar, and the FERs for scenarios 3 and 4 are similar. Nevertheless, when Blue is inside vehicles, Red loses casualties at a larger rate than Blue, as evidenced by the higher FERs in scenarios 1 and 2. The impact from bringing forces in via helicopter exposes infantry earlier in the amphibious assault and makes them more vulnerable, resulting in more Blue casualties and fewer Red casualties.

FER is another example where the raw output data may provide insights that could perhaps be lost during means analysis. Figure 37 shows the scenarios with the highest mean FER (scenario 2) and lowest mean FER (scenario 3).
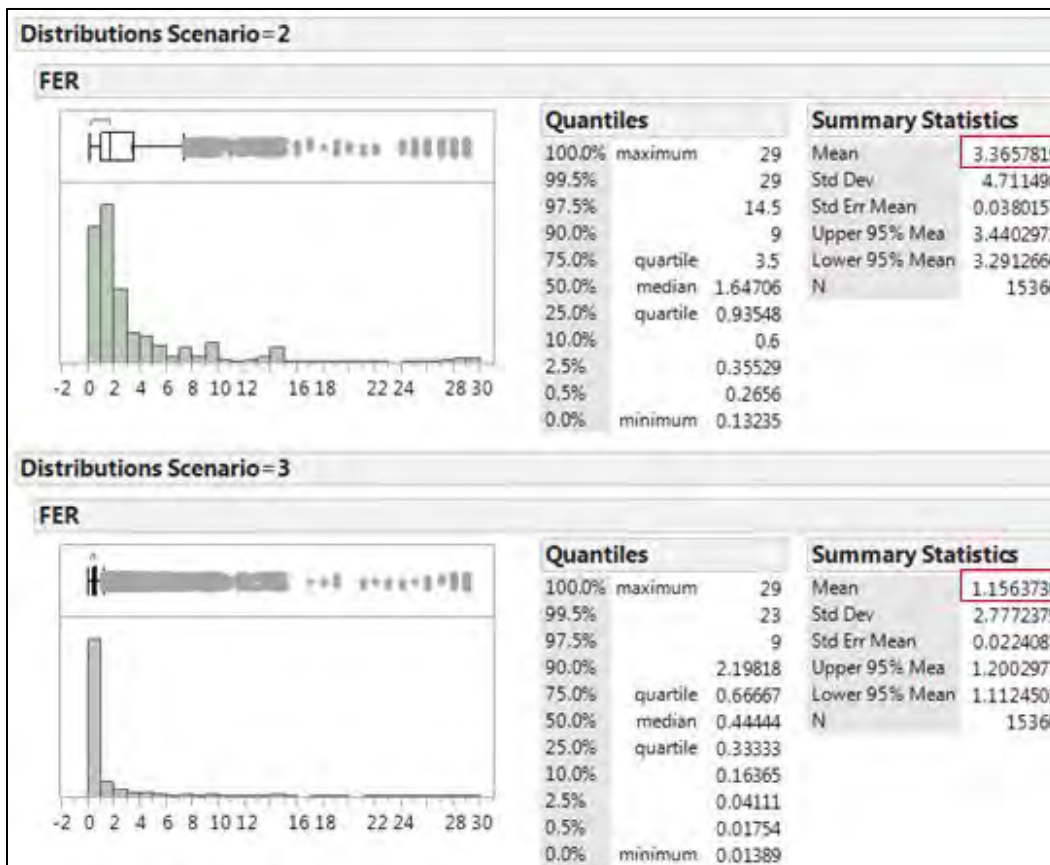
Figure 37.   FER MOE with raw output data. Highest is scenario 2 and the lowest is scenario 3.

One final comparison can be made between the FER and Blue casualties. Analytically, we observe that since Blue casualties are in the denominator of the rational fraction, that a higher FER signals a greater loss ratio of Red to Blue. Figure 38 shows Blue casualties on the y-axis, with the scenario across the bottom, and FER across the top.
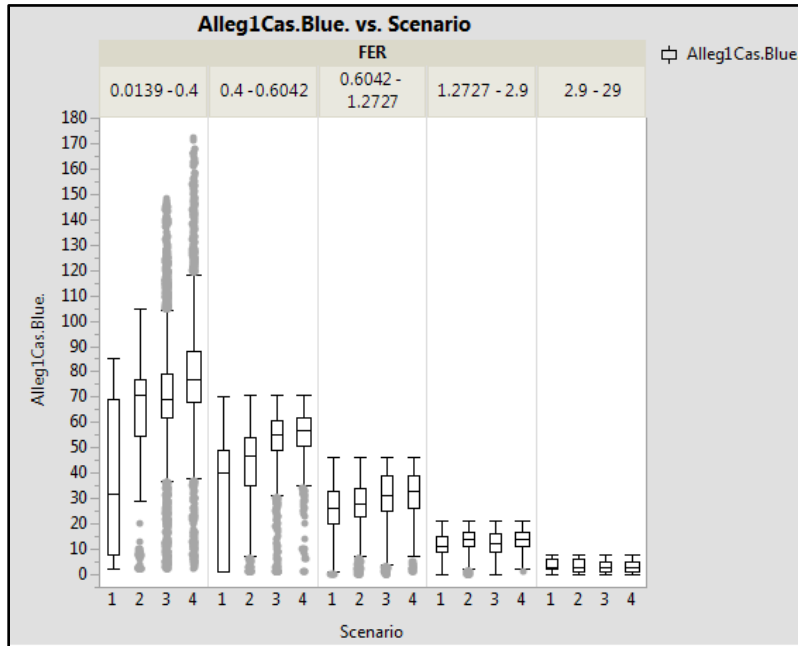
Figure 38.   Relationship between Blue casualties (y-axis) and FER (top), by scenario. Higher Blue casualties are seen at the far left when FER is the lowest.

2.   Box Plots

Next, we look at the output with box plots. Although they were part of the output in the previous section, we will cover them more in depth in this section. It can be useful, for example, to display box plots grouped by levels of a categorical variable. Figure 39 shows an illustration of box plot.
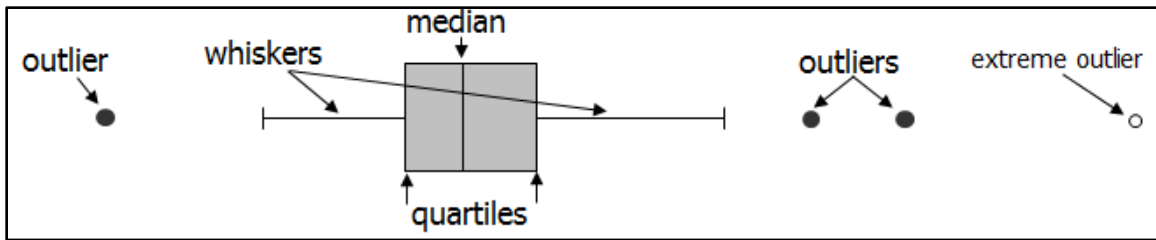
Figure 39.   Depicted is a box plot. Box plots in JMP have whiskers that extend out to 1.5 times the interquartile range (IQR). The boxed region shaded in gray represents the IQR, bounded by the 25th and 75th quantiles. JMP depicts outliers with large dots that fall outside of 1.5 times the IQR (from Lucas, 2014).

a.   MOE (1) and MOE (2)

Figure 40 shows a side-by-side comparison of Blue and Red casualties.
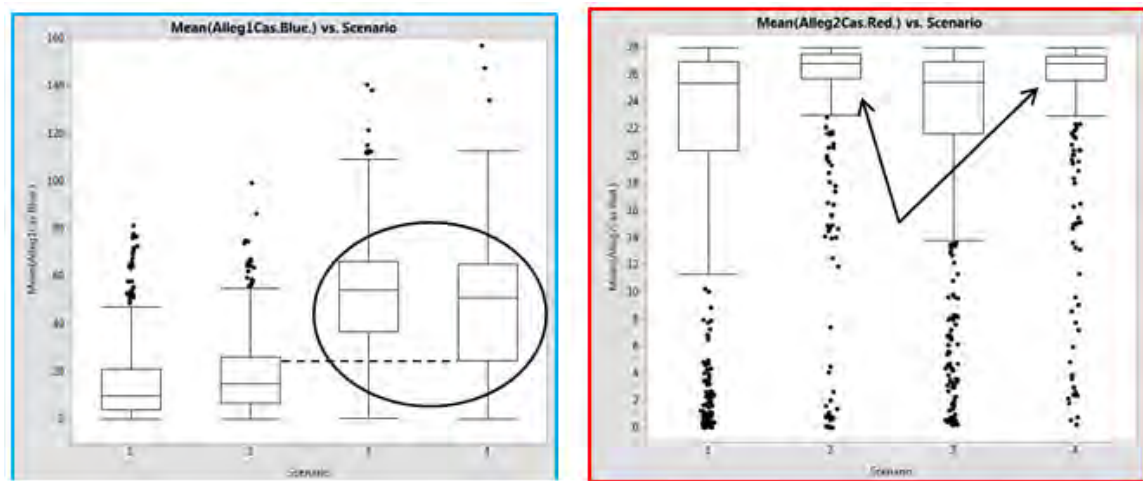
Figure 40.   This figure shows that there is little difference for Red between scenarios 2 and 4, while Blue incurs many more casualties in scenarios 3 and 4.

Note that the vertical axes on the two plots are different. These plots confirm that scenarios 3 and 4 have higher Blue casualties, but that scenario 4 has an IQR that covers more of the lower-casualty range. Similarly, Red incurs fewer casualties in scenarios 1 and 3, and more casualties in scenarios 2 and 4.

Figure 41 contains box plots for Blue casualties' MOE and Red casualties, this time grouped by scenario, number of LCACs (right vertical axis), and debark distance (across the top).
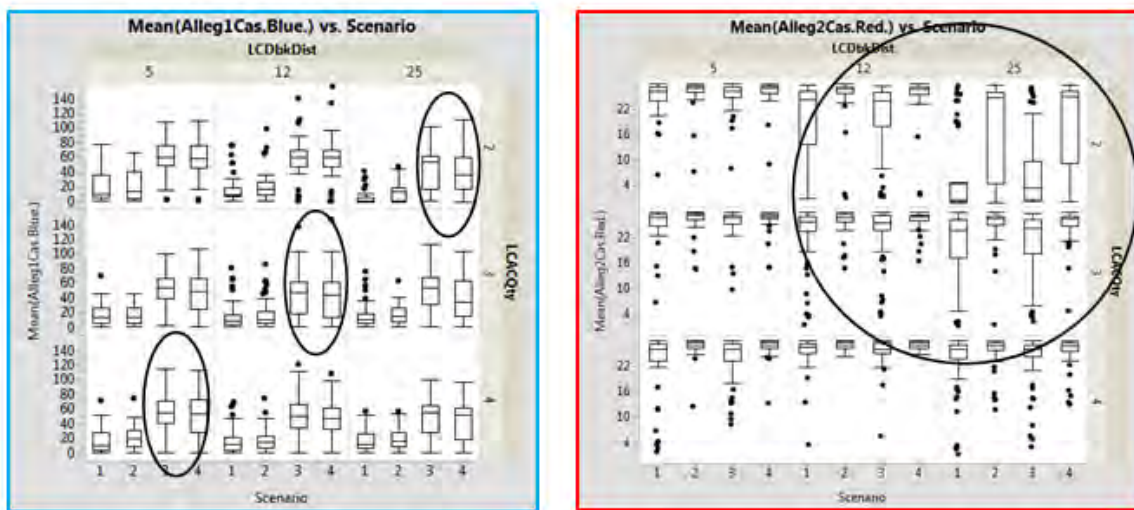
Figure 41.   The Blue casualties' plot on the left shows that Blue casualties are more influenced by scenario than by debark distance or number of LCACs. The Red casualties' plot on the right shows that Red casualties are influenced by debark distance, LCAC count, and scenario.

The plot on the left shows Blue's casualties from scenarios 3 and 4 are higher for all nine possible configurations. Further, Blue casualties do not seem to be affected by the number of LCACs. Meanwhile, the plot of Red casualties on the right shows that they are the highest when Blue debarks from less than five nm and greater than three LCACs (outside the circle). Casualties for Red are less with higher frequency inside the circle.

In order to get a better understanding of Blue casualties, we plot the mean number of Blue infantry squad casualties by scenario and squad number to gain insight into which

infantry squads are being hit the hardest. Figure 42 shows increased Blue casualties from the MANA squads representing dismounted infantry from scenario 3.
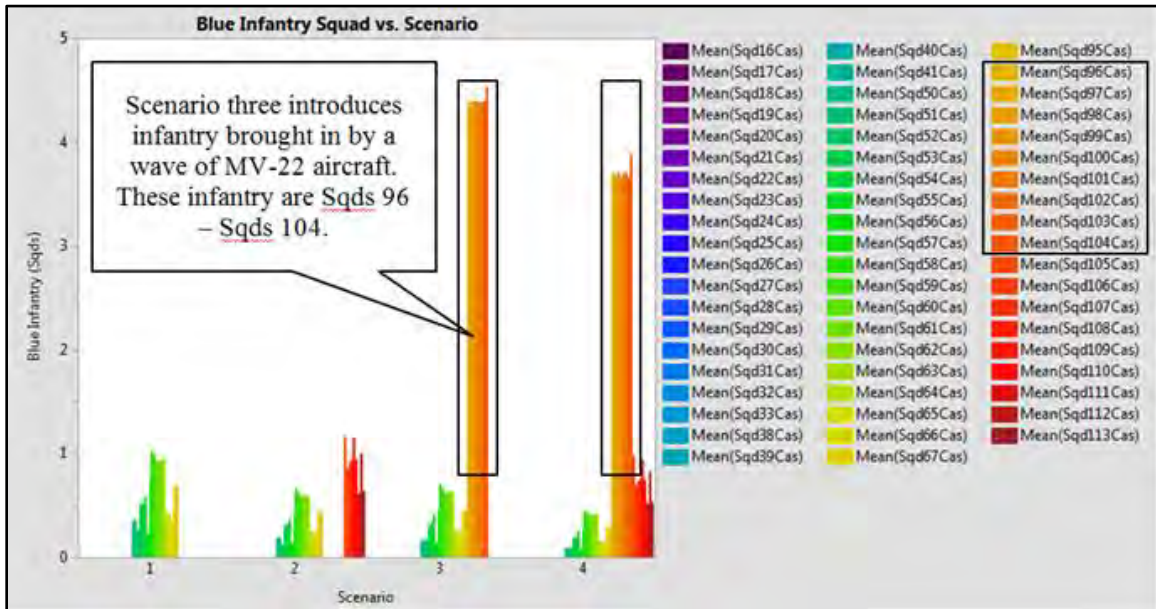
Figure 42.   Blue casualties during scenarios 3 and 4 are attributed mostly to those infantry arriving via MV-22s, STOM-V.

3.   Statistical Tests to Compare Scenarios

In this section, we further explore the differences between scenarios, this time through the use of statistical tests. Additionally, we will cover hypothesis testing:

- Define hypothesis testing

- Define p-value

- Two-Sample t-Test for equal means: analytically and with JMP

- Paired comparison

A Hypothesis (H) is a statement or claim about a population or populations, often concerning their parameters. The **null hypothesis** H_0, is the claim initially assumed to be true. Next, is the H_a or the **alternative hypothesis** which is the assertion, contrary to H_0. In a two-sample t test, the null hypothesis is $H_0 : \mu_1 - \mu_2 = 0$. We state the alternative hypothesis as $H_a : \mu_1 \neq \mu_2$, which is to say that the difference between the two means is

86

not equal to zero. In other words, we claim that the means are the same and research whether this is the case. Often the H_a is called the *research hypothesis*; however, the burden of proof required is to disprove H_0. Proof is measured by evaluating the p-value. **P-value** is the probability of seeing data this extreme or more extreme, assuming that the H_0 is true. The proof in this section will be shown graphically, calculating it analytically requires the appropriate test statistic value. The two-sample t test for the means test statistic analytical formula (see, e.g., Wackerly, Mendenhall, & Scheaffer, 2008) follows:

$$t = \frac{\bar{x} - \bar{y}}{\sqrt{\frac{s_1{}^2}{n_1} + \frac{s_2{}^2}{n_2}}}$$

Paired testing compares the outcomes between two scenarios under the same conditions. This is why it is often called **paired comparison**, which is a one-sample test on the differences of the data. For example, a paired comparison between scenario 2 and scenario 4, with the response "Red casualties" MOE, would subtract the Red casualty outputs from scenarios 2 and 4, respectively, at each of the 512 design points. The histograms showed high variability across many of the MOEs by scenario. If we detect higher variability from averaging, then the associated two-sample problem may not reflect the detail we seek, which is why a paired comparison between scenarios 2 and 4, without incorporating the differences from it *being* scenarios 2 and 4, is preferred. The analogy for paired comparisons with multiple samples is to treat each design point as a *block* when performing ANOVA.

a. Scenario: Two-Sample t Test; One-Way Analysis of Variance of Red Casualties by Scenario

Figure 43 contains an excerpt of the result of the Analysis of Variance (ANOVA) procedure of mean Red casualties by scenario. The y-axis is the mean number of Red casualties, the x-axis represents the scenario, and a horizontal line at 23 represents the overall mean of the response. We report the results without blocking on design point, and note that blocking reduces p-values (showing higher levels of statistical significance) but does not change the qualitative conclusions. Appendix C contains the full results of the ANOVA procedure of mean Red casualties by scenario. In addition, Appendix D contains the study for the raw output data.
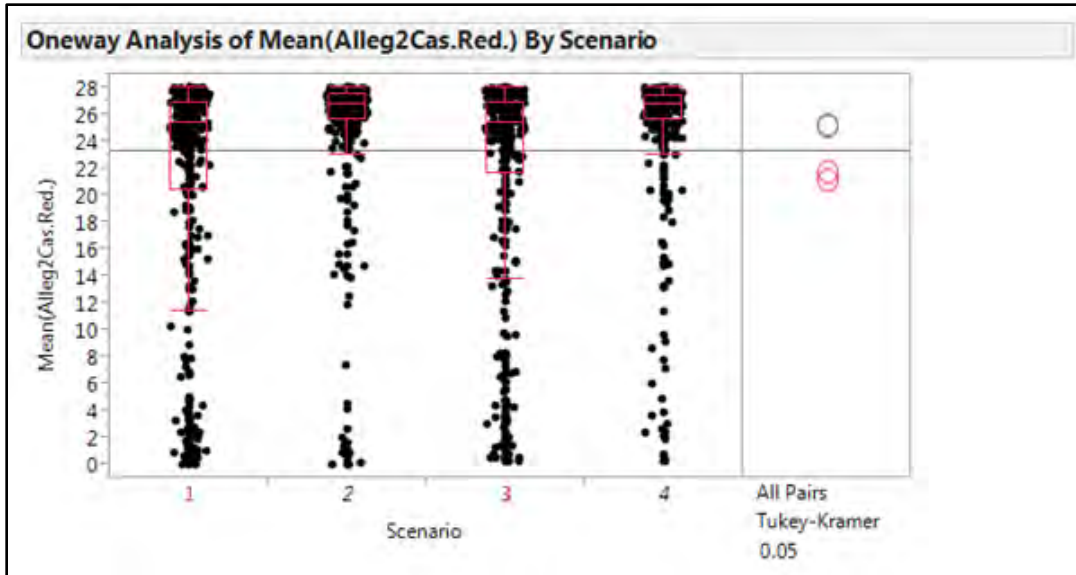
Figure 43.   This plot shows a one-way analysis of the summarized output (2,048 rows) for "Red casualties" by scenario, with the number of Red casualties on the vertical axis. In red, we see overlapping circles for scenarios 1 and 3. Scenarios 2 and 4 have similar boxplots and circles which are "overlapped."

Figure 44 shows a Connecting Letters Report and the confidence level used. Scenarios 4 and 2 are designated with "A" and scenarios 3 and 1 are designated with "B."

Figure 44.   Connecting Letters Report at the 95% confidence level.

88

Another way to summarize the comparison of the mean number of Red casualties across scenarios is with an Ordered Differences Report. In this report, the difference between each pair of scenarios is summarized with a mean difference, as well as a confidence interval and p-value. What is valuable about this report is that it shows ranked differences between scenarios, with scenarios 4 and 1 being the most different and 4 and 2 being the least. Figure 45 shows the ordered differences report, and the red box shows the dissimilar scenario groupings.

Ordered Differences Report

Level	- Level	Difference	Std Err Dif	Lower CL	Upper CL	p-Value
4	1	4.130990	0.4400472	2.99956	5.262415	<.0001*
2	1	4.011914	0.4400472	2.88049	5.143340	<.0001*
4	3	3.488477	0.4400472	2.35705	4.619902	<.0001*
2	3	3.369401	0.4400472	2.23798	4.500827	<.0001*
3	1	0.642513	0.4400472	-0.48891	1.773939	0.4620
4	2	0.119076	0.4400472	-1.01235	1.250501	0.9931
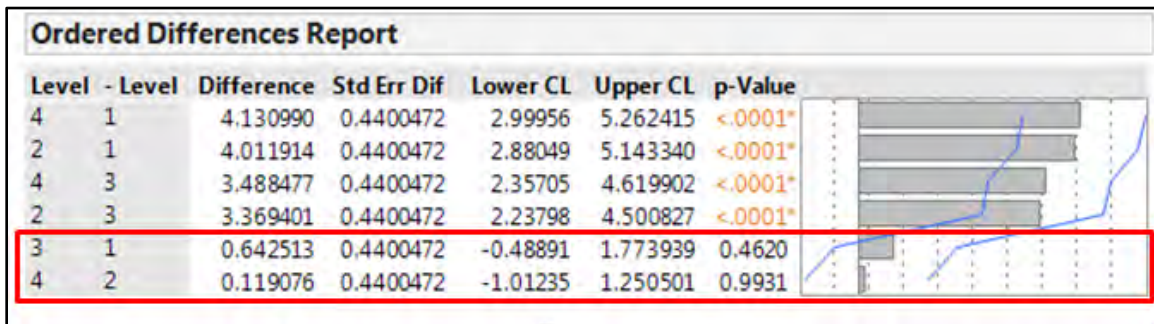
Figure 45.   The Ordered Differences Report.

We now repeat the ANOVA using the full set of output (using data from all design points and replications), vice just the 2,048 points, where each design point was summarized by its mean. Figure 46 shows the result of the ANOVA test on the full output. This result is similar to the previous result, except that this time, scenarios 3 and 1 (connecting letters B and C) are deemed significantly different.
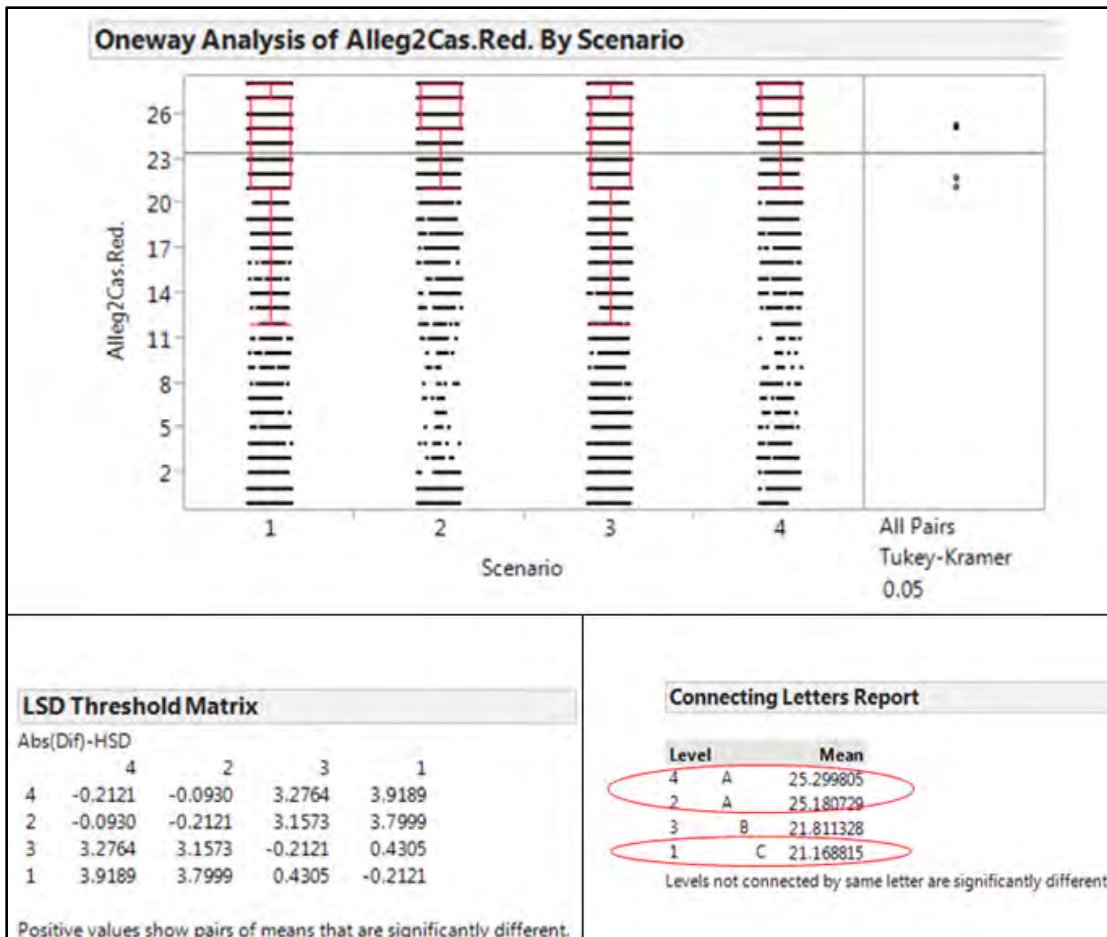
Figure 46.   One-way analysis of Red casualties, based on the full set of outputs.

We note, however, that there is still not much practical difference between the means. It is important to remember that not all statistically significant differences are considered practically significant. From Appendix H similar results can be seen with the student t-Test.

4.   Multiple Linear Regression Analysis

We now turn to multiple linear regression analysis to explore the relationship between our MOEs and the experiment factors. We start with a summary of the technique.

Simple linear regression is a model with a single regressor, x, that has a relationship with the **response** y. The model is: $y = \beta_0 + \beta_1 x_1 + \varepsilon$. The response y is a random variable. The parameters β_0 and β_1 are unknown and must be estimated with data.

To transition to multiple regression variables or regressors you add more terms. Here we will also consider interaction terms ($x_1 \times x_2$) and polynomial terms to degree two (x_1^2). Equation 2 shows the full second-order **fitted** multiple linear regression model for two regressors, x_1 and x_2.

$$\hat{y} = \hat{\beta}_0 + \hat{\beta}_1 x_1 + \hat{\beta}_2 x_2 + \hat{\beta}_3 x_1 x_2 + \hat{\beta}_4 x_1^2 + \hat{\beta}_5 x_2^2 \qquad (2)$$

How well the model fits the data is measured with R Squared, root mean squared error, and plots of the errors (ε) from our actual versus predicted values. R Squared indicates what percentage of the variability is explained by the regression model. If our interest were prediction, additional model adequacy checks could involve assessing the whether the errors are distributed normally with constant variance (σ^2). Fortunately, the estimated regression coefficients are robust to departures from normality and constant variance, so the regression models can be used to identify the most important factors and identify the nature of the relationship between these factors and the response.

a. Main Effects

The first fitted model is the main effects model for Blue casualties. This model was fit using the stepwise functionality in JMP. Both "mixed" and "forward" were used in model generation. Between BIC and p-value with p < 0.01 to enter and exit the model, p-value seemed to give the better models. The selected mode using Standard Least Squares and effect screening has an R squared of 0.53. The model has 17 terms, with the most important factor being scenario 3. Figure 47 shows the summary of fit for the full output and the most important parameters in the sorted parameter estimates $\left(\hat{\beta}s\right)$.
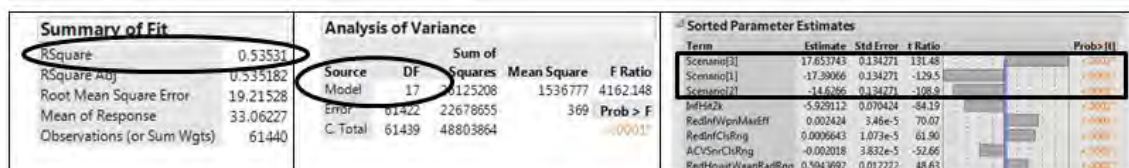
Figure 47.　Full uncompressed output, "Blue casualties." Scenario 3 increases "Blue casualties," while scenarios 2 and 1 decrease "Blue casualties."

91

Figure 47 shows that "Blue casualties" are heavily influenced by scenario 3. As a matter of fact "Blue casualties" are higher in scenario 3 than in scenarios 1 and 2. Increases in InfHit2k (i.e., infantry hit to kill) decreases "Blue casualties." *Not listed is anything pertaining to speed*.

Figure 48 shows that "Red casualties" increase with ACV speed, LCAC count, LCAC speed, and scenario 2. "Red casualties" decrease with ACV debark distance, scenario 1, and scenario 3. *Not listed in is anything pertaining to force protection or hits to kill*.
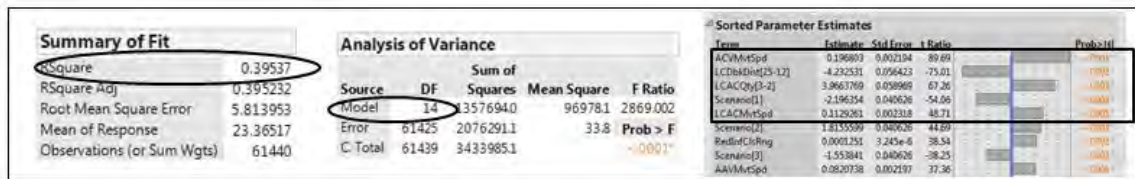
Figure 48.　Full uncompressed output, "Red casualties" depend on ACV speed, debark distance, LCAC quantity, and LCAC speed.

Figure 49 shows the prediction profiler for "Red casualties." The figure on the left supports fast LCACs, AAVs, and ACVs. The plots on the right support larger numbers of "Red casualties" with scenarios 2 and 4; however, they make a case for debark distances of 5 nm and 12 nm, and three or more LCACs.
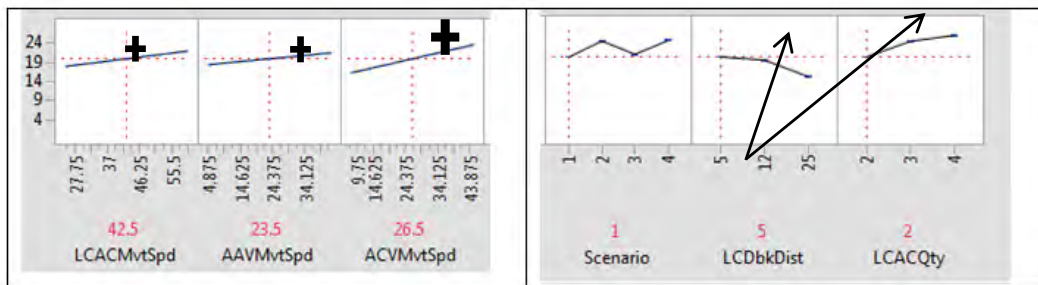
Figure 49.　Red casualties increase with all three speeds: LCAC, AAV, and ACV. Similarly, scenarios 2 and 4, and LCAC quantities of three and four increase the number of Red casualties. "Red casualties" decrease when the ACVs are debarked further than 12 nm from the shore.

The most important factors for "Red casualties" continue to be speed, quantity, and scenario dependent, which perhaps is justification for pursuing further "Red casualty" MOEs.

Finally, we look at the "time" MOE. In a main effects only model, with 12 terms, the "time to attrite Red to one-third remaining strength" is affected, as one would expect, by speed and distance. The speed that contributes most to the MOE is the ACV speed, not the LCAC speed. LCAC speed and LCAC quantity all decrease the "time" MOE. Meanwhile, debark distance and scenario 1 increase it. Figure 50 shows the "time" MOE summary of fit. A partition tree (not shown) of the probability of attriting red to one-third of its original forces gives similar results: ACV speed and debark distance are the two most influential factors.
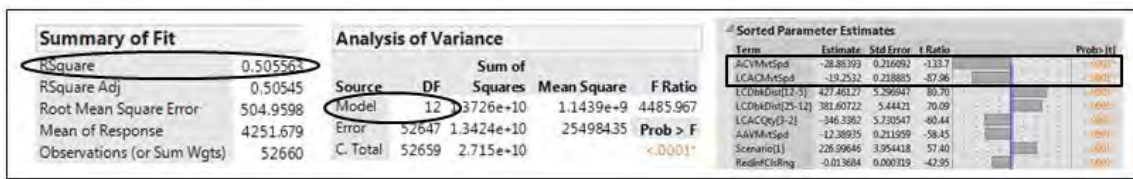
Figure 50.   "Time" MOE. ACV speed contributes most to reducing the "time to attrite Red Force to one-third remaining strength." Debark distances and scenario 1 take longer to attrite Red to the desired level.

With regard to the number of LCACs and the debark distance, Figure 50 shows the following added benefit and importance:

- Being at 5 nm is extremely important.

- Scenarios 2 and 4 are preferred.

- Going from 2 to 3 LCACs helps much more than going from 3 to 4 LCACs.

Thus, for the "time" MOE, it increases with distance; however, the benefit of going from two to three LCACs is much greater than from three to four. Figure 51 shows the prediction profiler for scenario, debark distance, and LCAC quantity.
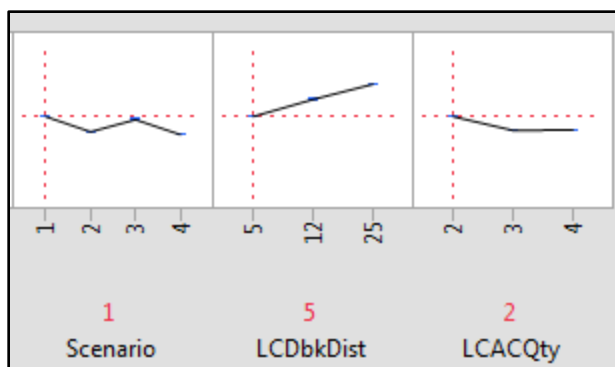
Figure 51.   The "time" MOE and how scenario, ACV debark distance, and
LCAC quantity compare.

b.   *Comparison of Main Effects*

In this section we fit simple main effect models for the MOEs. These models reflect the primary variables, and support general insights. The summary of fit and the sorted parameter estimates are provided below. Figure 52 shows Blue casualties" on the left and "Red casualties on the right.
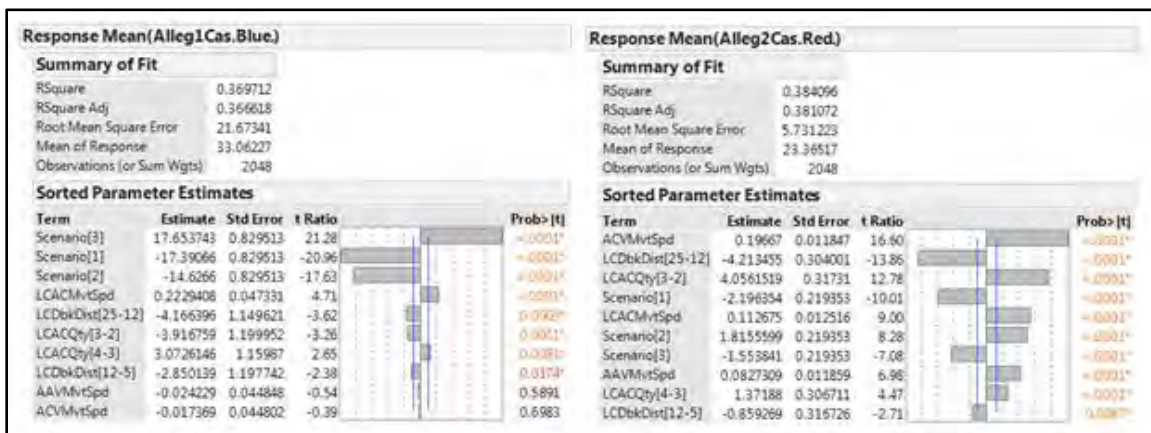
Figure 52.   The main effect models for Blue and Red casualties.

At the top of the figure are the R Squared values that measure how much of the variance is explained by the model below. This measure of observed variance is often referred to as goodness of fit. Meanwhile, the sorted plots below show the model in a ranked column that depicts most influence to least. Each term has an estimate, standard error, t-ratio, shaded horizontal bar, and Prob >|t|. First, the estimate signals that the

"Blue casualties," for example, will increase by 17.6 casualties if in scenario three. The most significant factor for Blue is scenario, while for "Red casualties" it is ACV speed. Significance is seen from both the t-ratio and Prob >|t|. In another example, seen with "Red casualties" there are nine terms that have t-ratios greater than four, likewise "Blue casualties" only has four. Also, for Blue those four are really just levels of scenario and LCAC speed. Figure 53 shows the main effects models for FER and "time" MOE.

Response Mean(FER)

Summary of Fit

RSquare	0.100852
RSquare Adj	0.096438
Root Mean Square Error	3.261382
Mean of Response	2.340811
Observations (or Sum Wgts)	2048

Sorted Parameter Estimates

Term	Estimate	Std Error	t Ratio	Prob>|t|
Scenario[3]	-1.184437	0.124824	-9.49	<.0001*
Scenario[2]	1.0249707	0.124824	8.21	<.0001*
Scenario[1]	0.8233036	0.124824	6.60	<.0001*
ACVMvtSpd	0.0400463	0.006742	5.94	<.0001*
LCACQty[3-2]	0.5315573	0.180567	2.94	0.0033*
LCDbkDist[25-12]	-0.477594	0.172993	-2.76	0.0058*
LCDbkDist[12-5]	0.3587584	0.180234	1.99	0.0467*
AAVMvtSpd	0.0064733	0.006749	0.96	0.3376
LCACMvtSpd	0.0033912	0.007122	0.48	0.6340
LCACQty[4-3]	-0.065304	0.174535	-0.37	0.7083

Response Mean(RedKillTime)

Summary of Fit

RSquare	0.516343
RSquare Adj	0.513705
Root Mean Square Error	520.0062
Mean of Response	4317.937
Observations (or Sum Wgts)	1844

Sorted Parameter Estimates

Term	Estimate	Std Error	t Ratio	Prob>|t|
ACVMvtSpd	-30.55424	1.165088	-26.22	<.0001*
LCACMvtSpd	-19.27639	1.205596	-15.99	<.0001*
LCDbkDist[12-5]	439.98584	29.3215	15.01	<.0001*
LCDbkDist[25-12]	416.20826	29.79944	13.97	<.0001*
LCACQty[3-2]	-352.3507	31.33752	-11.24	<.0001*
Scenario[1]	241.65785	21.56314	11.21	<.0001*
AAVMvtSpd	-12.72147	1.159937	-10.97	<.0001*
Scenario[2]	-170.4752	20.61656	-8.27	<.0001*
Scenario[3]	174.50158	21.36172	8.17	<.0001*
LCACQty[4-3]	-13.12048	28.52872	-0.46	0.6456

Figure 53.   The main effect models for FER and "time" MOE.

(1)   Discussion

From the summary of fits, we see that the highest R Square is attained with the time it takes to attrite red to one-third strength. Other R Squares are 0.38 or less with the lowest being FER. Depending on the MOE selected above at most 50% of the variability could be explained by these main effects, while the worst is 10%. Combat is inherently difficult to predict, which means that these values are actually doing well, but should be used for comparison rather than prediction.

For Blue casualties, there are benefits to ACV debarking at closer distances (e.g., "LCDbkDist [25-12]"), namely that Blue benefits from being inside 12 nm. However, this benefit is nothing compared to that of being in scenarios one and two. One might make many more replications to support the impact from "LCACMvtSpd" or LCAC speed.

Indeed, "Red casualties "increase with and decrease with varying signs through nine different parameters. ACV speed, LCAC quantity, speed, and scenario two are increase Red casualties. Scenarios one and three decrease casualties.

(2)   Most Important Factors

- Blue: The most important factors are *scenario and distance*. It is not clear that Blue experiences a benefit from speed. As a matter of fact we see that LCAC speed and scenario three with fast aircraft, increase Blues losses. Blue vehicles are arriving to the objective and dismounting infantry. A byproduct of the design that was not anticipated was that with scenario two there are more vehicles which increase both the weapons and armored personnel carriers to distribute the force across.

- Red: *Speed and quantity* increase red casualties most. Incidentally ACV and LCAC should be made fast before the AAV. Debark distances beyond 12 nm and scenario 1 decrease casualties more than scenario 3.

- FER/time: With differing information for MOE one and two, we turn to FER and the "time" MOE. The two most important factors seen from FER and "time" to give Blue an advantage are *scenario and speed*. Blue might seek to get into scenario 2 most often and initially explore investments in *speed in the ACV*.

(3)   Insights

Two general insights are discovered from the evidence presented from the main effect models.

- FLOT speed: The basic concept is that speed works to a certain point. Blue infantry arriving in MV-22 outpace the time required to mass force ashore. In the "time" MOE we get a sense for the right pace. ACV speed, LCAC speed, and multiple connectors create a good pace.

- Force protection: What is not seen is a mention of infantry hits to kill, concealment, or number of agents. Red consists of a formidable force of 28 agents. To give the defending force the advantage 18 Red infantry require 11 hits to kill, and are 70% concealed. The force in the defense has increased staying power and defensibility. Force protection is nested in the increased casualties from scenario 3; however, it is not explicitly influential to the attacking force.

A battle is challenging to predict. R squared captures that stochastic behavior of agents interacting and responding to what their sensors are telling them. This research does incorporate 77 of the prominent tangibles associated with amphibious assault;

however, it does not capture intangibles such as breakdowns, Marine leadership, and luck.

(4)   Major Conclusions and Findings

Dismounts and infantry arriving to the objective incur greater casualties. A self-deploying capability similar to the AAV increases the number of vehicles that Blue brings to the fight, which in turn increases fire power and distributes the force to absorb risk from enemy fire. Channelizing terrain, obstacles, and ambush locations can fix the attacking force for defending artillery. Conversely, urban terrain does limit line of sight and trajectory for common projectiles. The risks of urban terrain are not covered here. Marines will use the next AAV and ACV in a way that must be robust. The AAV was to gets people ashore safely and efficiently. The solution is not one parameter. Amphibious assault uses a system of systems, where several parameters are determined and then reassessed. If an LCAC is attrited the seabase might have to maneuver within 12 nm. Stochastic models provide results that afford simulation that may return different solutions, but its ability to predict combat and battle is labored at best.

c.   *Partition Trees*

Another analysis method is partition trees. In these models the dependant variable is still a MOE. JMP splits on the most influential factor based on "distance" between points in the collapsed output. Incidentally, this distance is the variance—and for the Marine Corps' next combat vehicle baseline and desired values are going to drive the eventual procurement. Key performance parameters are those items that a program like the ACV will be assessed against to see if it is proving the warfighter with what is required.

(1)   "Blue Casualties" Partition Tree

While Figure 54 does not show all 77 potential candidate factors, what it shows was the first and most important split was scenario.
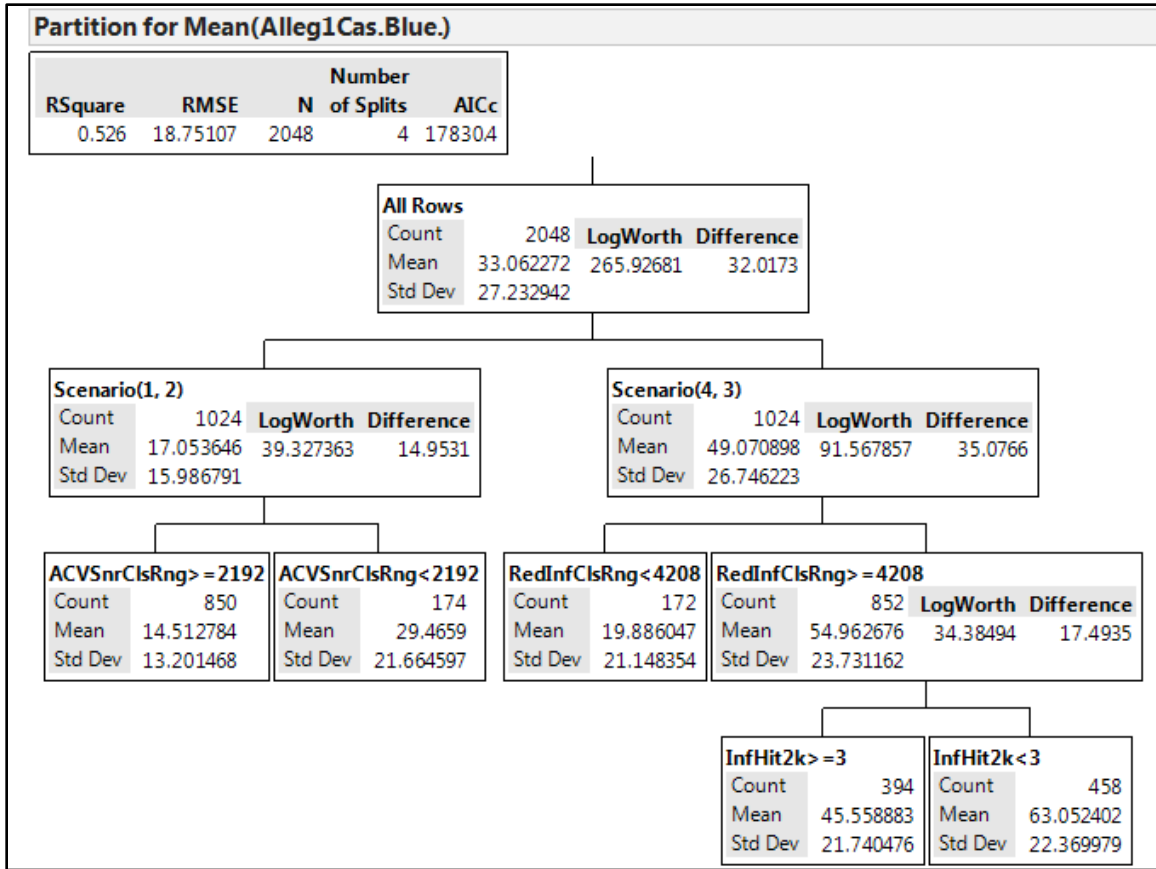
Figure 54.   "Blue casualties" partition tree.

Furthermore, we are doing a better job explaining the variability in just four splits with an R Squared of 0.53. A key threshold after splitting on scenario 1 and 2 is ACV sensor range at 2,192 meters. A less effective sensor increases casualties. Likewise, if Blue must choose scenario 4 or 3, and if Red infantry can classify targets at distances greater than 4,208 m, then the ACV and the infantry inside require increased force protections. Figure 55 shows the split history with R Square value on the y-axis and number of splits on the x-axis.
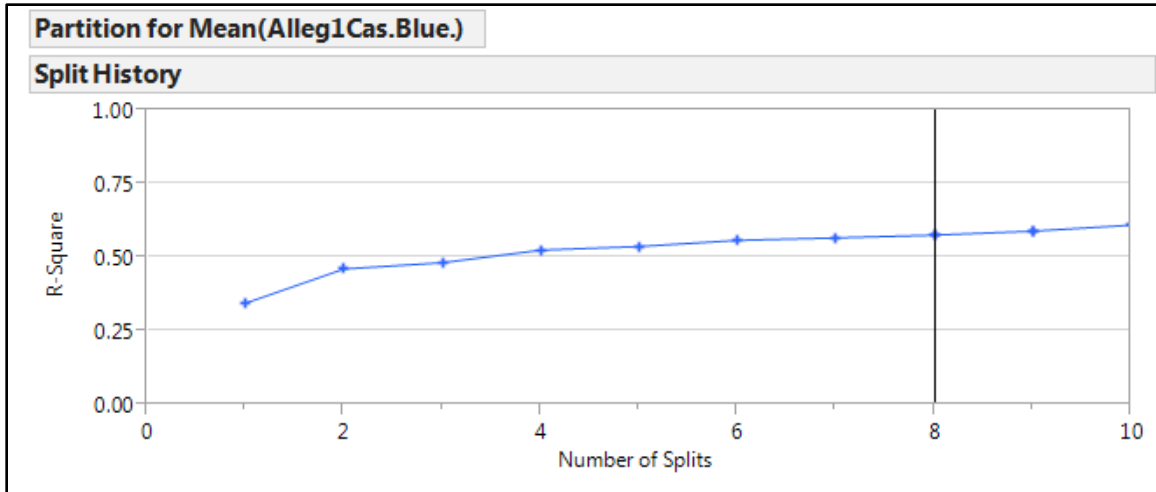
Figure 55.   Blue casualties' partition tree, split history for mean Blue casualties,
the black vertical line at eight splits shows little increased R squared
from the four splits show previously.

(2)   "Red Casualty" Partition Tree

The "Red casualties" partition tree show shown in Figure 56 indicates ACV speed is the most important factor. This tree shows an excellent example of a mitigation that might arise in the acquisitions process of the ACV or the next SSC.

Partition for Mean(Alleg2Cas.Red.)

All Rows
Count 2048 **LogWorth Difference**
Mean 23.365169 83.762441 6.43603
Std Dev 7.284963

ACVMvtSpd<16
Count 416 **LogWorth Difference**
Mean 18.236458 33.86494 9.71362
Std Dev 9.6677425

ACVMvtSpd>=16
Count 1632 **LogWorth Difference**
Mean 24.672488 58.118223 -4.348
Std Dev 5.8656565

Scenario(1, 3)
Count 208
Mean 13.379647
Std Dev 9.4080582

Scenario(2, 4)
Count 208
Mean 23.093269
Std Dev 7.1739335

LCDbkDist(5, 12)
Count 1064 **LogWorth Difference**
Mean 26.185777 63.354118 2.12922
Std Dev 2.4383517

LCDbkDist(25)
Count 568 **LogWorth Difference**
Mean 21.837735 67.304629 10.8754
Std Dev 8.6877015

ACVSnrClsRng<3562
Count 384
Mean 24.825
Std Dev 3.2743033

ACVSnrClsRng>=3562
Count 680
Mean 26.954216
Std Dev 1.2735936

LCACQty(2)
Count 164
Mean 14.102439
Std Dev 11.514614

LCACQty(3, 4)
Count 404 **LogWorth Difference**
Mean 24.977805 63.189417 7.66356
Std Dev 4.2813707

RedInfClsRng<3083
Count 52
Mean 18.300641
Std Dev 5.4462415

RedInfClsRng>=3083
Count 352
Mean 25.964205
Std Dev 3.0257302

Figure 56.   "Red casualties" partition tree, most import split ACV speed greater than 16 knots (18 mph).

What if technology readiness level cannot get the ACV to swim and maneuver on-land at speeds comparable to our top capability, commonly referred to as the speed of the M1A1? First, the speed of ACV speed splits at 16 knots (18 mph), which is less than half of the M1A1s speed. Second, the fighting in convention with scenario 2 and 4 in a slow ACV gives about the same MOE as fighting in a fast one inside 12 nm. The complexity of amphibious assault and the system of connectors, amphibians, and threat make the problem tough to break down. This is one approach to refine and quantify what matters most, when it is all important. Figure 57 shows the split history with R Square value on the y-axis and number of splits on the x-axis.
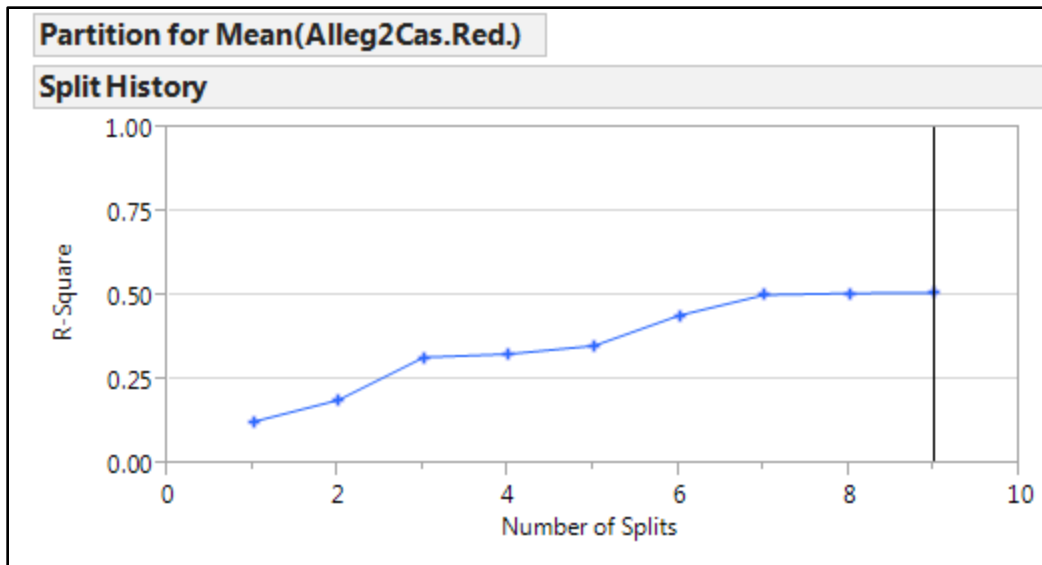
Figure 57.   Red casualties' partition tree, where more splits might explain more
of the variance.

(3)   Main Effects and Partition Tree Comparison of Most Important Factors

The partition trees reflected specific speeds and sensor ranges. The main effects gave ranked significance levels. Still, the models in the main effects did not satisfy normal residuals to confirm significance. For the main effects models the most important factors were not the same. Blue leaned heavily on scenario and Red on speed. For Red casualties, what was a ranked list of many important factors, now tells a story.

- Red casualties: for this MOE there are three important factors, which are ACV speed, scenario, debark distance, ACV censor range, and LCAC quantity.

- Blue casualties: Emphasis is still on scenario; however, ACV sensor, Red infantry's sensor, and force protection are both quantifiable and highly influential.

d.   *Multiple Linear Regression Models*

As a result of our main effect models we will now explore interactions and non-linear regressors. Recall that each experiment uses 512 design points. The modeling approach in JMP is a stepwise one that examines the p-value against 0.01 to enter the model. The entire surface for both two-way interactions and polynomials to degree two were examined for each of the MOEs.

101

The next side-by-side comparison gives a good depiction of the non-linear effects of increased degrees of freedom from additional parameters. In other words, there are diminishing returns to highly complicated models. Figure 58 and Figure 59 show side-by-side comparisons for all MOE. We see we are able to best explain the variation in the "time" MOE shown in Figure 59. For "time," "Blue casualties," and "Red casualties" with approximate 10 parameters we can expect R squared values of 0.5. Figure 59 shows that we are able to best explain the variation in the "time" MOE.
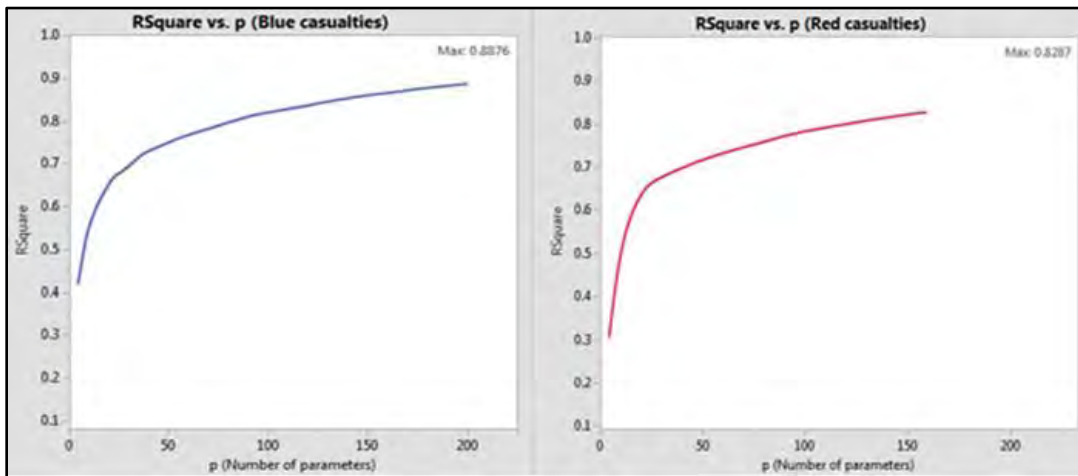
Figure 58.   R square vs. p (number of parameters) for "Blue casualties" on the left and "Red casualties" on the right.
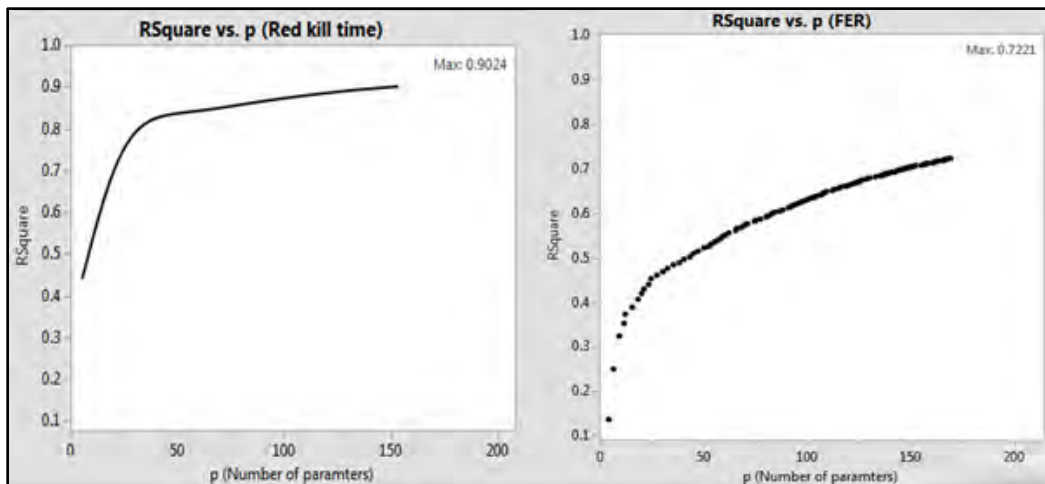
Figure 59.   R square vs. p (number of parameters) for "time" on the left and "FER" on the right.

For "time," "Blue casualties," and "Red casualties," with approximate 10 parameters, we can expect R squared values of 0.5 The R Square analysis shows that while many parameters might increase R Square that we achieve R Square 0.5 or great with few terms. Each plot shows the max attainable R Square in the top right. Knowing the best R Squared and is useful in determining a good multiple linear regression model. Approach for determining multiple regression fitted models:

- Select input parameters and choose the entire response surface for main effects, quadratic, and two-way interactions.

- Compare stepwise results with R Squared and degrees of freedom.

- Inspect p the number of parameters in conjunction with R squared, and adjusted R squared.

Here, the objective is to decrease the amount of parameters in the final model, while ensuring we find the "best" fit model. As mentioned previously, a slightly higher R squared is not worth the addition of factors that unnecessarily increase the complexity of the model. Hierarchy is when we chose to keep main effects terms if quadratic and two-way interactions contain a factor that might not otherwise have been as influential or significant to the model.

First, we look at the multiple linear regression for "Blue casualties." Figure 60 shows an actual by predicted plot. Additional graphs and results for the parsimonious multiple linear regression models for each MOE are provided in Appendix E.

Response Mean(Alleg1Cas.Blue.)

Actual by Predicted Plot
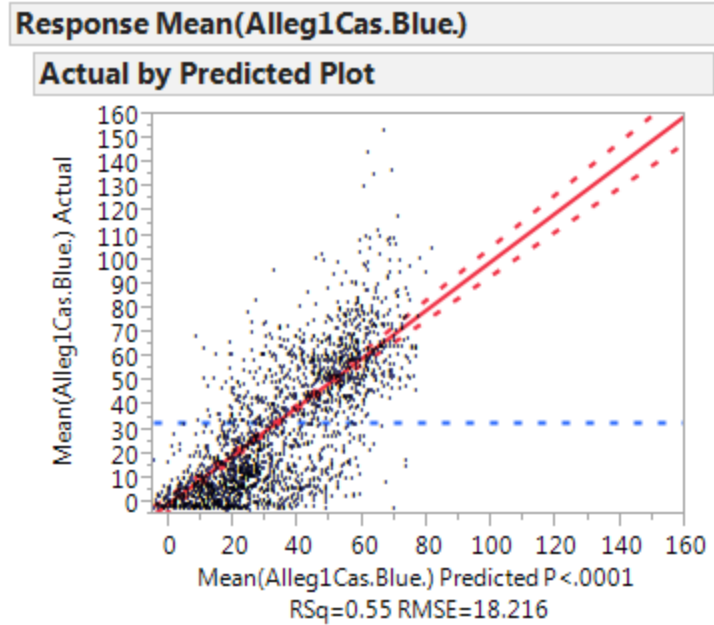
Figure 60.   Predicted mean blue casualties, with actual observations shown with black dots. The dashed blue line depicts the average blue casualties.

In Figure 60, the red line represents the predicted mean blue casualties compared to the observed black dots. The dashed blue line depicts the average blue casualties. This plot shows that there are many outliers and that blue experiences, out of many simulated amphibious assaults, casualties in the range from zero to 90. These results do not provide normal residuals, which are one of our required assumptions; however, give effective insights to concept platforms such as the future ACV.

Second, Figure 61 shows the summary of fit and R squared.

Summary of Fit	
RSquare	0.554979
RSquare Adj	0.552575
Root Mean Square Error	18.21607
Mean of Response	33.06227
Observations (or Sum Wgts)	2048

Figure 61.   Mean "Blue casualties" summary of fit. The R squared is 55%, and the R squared adjusted is 55%, implying that over half of the variation is explained by this model.

Third, after we are satisfied with the R squared, we next see a ranked list of the model's factors. Figure 62 shows the sorted parameter estimates for this advanced regression model.

Sorted Parameter Estimates

Term	Estimate	Std Error	t Ratio		Prob>|t|
Scenario[3]	17.653743	0.697189	25.32		<.0001*
Scenario[1]	-17.39066	0.697189	-24.94		<.0001*
Scenario[2]	-14.6266	0.697189	-20.98		<.0001*
InfHit2k	-5.933821	0.364311	-16.29		<.0001*
(RedInfClsRng-12500.5)*(RedInfClsRng-12500.5)	-1.293e-7	8.618e-9	-15.00		<.0001*
RedInfWpnMaxEff	0.0024399	0.00018	13.59		<.0001*
RedInfClsRng	0.0006656	5.567e-5	11.96		<.0001*
ACVSnrClsRng	-0.00212	0.000199	-10.65		<.0001*
Scenario[2]*(InfHit2k-2.42969)	1.7760961	0.630787	2.82		0.0049*
Scenario[1]*(InfHit2k-2.42969)	1.4707151	0.630787	2.33		0.0198*
Scenario[3]*(InfHit2k-2.42969)	-1.25082	0.630787	-1.98		0.0475*

Figure 62.   Mean "Blue casualties" sorted parameter estimates.

Most notably is the quadratic factor for Red infantry classification range. The implication there is that if Red classifies an agent as enemy (i.e., Blue), then Blue casualties decrease. Though there is an advantage to correctly classifying the enemy, the affect is Red engages earlier, which in turn exposes Red agents to Blue fire power. Nevertheless, if Red's maximum effective range for their weapon system is increased, the estimate suggests that it would have to be increased greatly to achieve an increase in Blue casualties.

Next, is the prediction profiler in JMP that is used to form prediction intervals based on adjusting the default levels in the fields provided. The following factors are displayed: infantry hits to kill (i.e., force protection), ACV sensor range, Red classification range, Red max effective range, and scenario. The prediction profile is highly useful because it depicts changes in MOE based on the main effects. The concave down or bent curve for the Red infantry sensor peaks at a range that covers the 3 km of transition from the sea to the shore from the location of Red's defense.
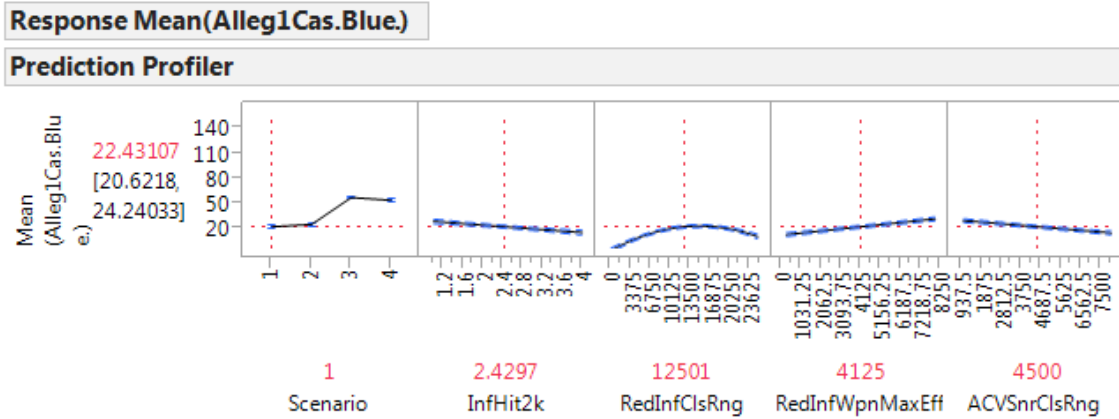
Figure 63.   Mean "Blue casualties" MOE, prediction profiler. Force protection and ACV sensor range reduce Blue casualties and scenario increase the number of casualties. The x-axis is the number of hits, range (meters), and scenario for the main effects. The y-axis is the mean number of casualties.

The R squared graphs of all four principal MOE show that we could explain more variance with increased degrees of freedom. Due to the experiment size this could be readily done in JMP, however, additional terms become less intuitive and confound what is highly specific an interesting. The force protection contributes slightly the MOE, however, having a decent sensor, the right mission scenario, and the ability to reduce signature during the transition to shore are vital to keeping Blue casualties low. What's nice is many of these can be support by sound operation planning and digital interoperability of systems. An example of interoperability is the ability to view the sensor feed from another asset.

Last, is the Pareto plot, which is a highly useful illustration that shows whether or not additional terms should be added to the model. The curved line flattens vertically towards the bottom or last factor, which is a two-way interaction between debark distance and LCAC quantity. The finding here is that no additional terms are required. Figure 64 shows the Pareto plot for "Blue casualties."

106

Response Mean(Alleg1Cas.Blue.)

Pareto Plot of Transformed Estimates

Term	Orthog Estimate	
Scenario[1]	-11.22679	
Scenario[3]	10.19239	
InfHit2k	-6.63249	
(RedInfClsRng-12500.5)*(RedInfClsRng-12500.5)	-5.83116	
RedInfWpnMaxEff	5.49481	
Scenario[2]	-5.35337	
RedInfClsRng	4.78823	
ACVSnrClsRng	-4.28659	
Scenario[1]*(InfHit2k-2.42969)	1.35469	
Scenario[2]*(InfHit2k-2.42969)	0.91993	
Scenario[3]*(InfHit2k-2.42969)	-0.79818	

Figure 64. Pareto plot for "Blue casualties." The curved line supports that little additional variance will be gained with increased degrees of freedom or more parameters.

(1)   Insights

All combinations of quadratic and two-way interactions were considered for the first four MOEs, nearly three thousand (i.e., $\binom{77}{2}$). The interactions between quantity of LCAC and debark distance, Red classification and Red max weapon range, and debark distance and ACV speed list a few. The SSC, ACV, and AAV upgrades represent three developing systems that will interact. This interaction in their development cannot be overlooked.

Consequently, an analysis for all MOE 1-4 confirm the challenges with designing a robust system that works for all scenarios. While scenario type being significant for all MOE is a function of the model, it also shows that what must be attained—namely, a family of systems that work well together. Additionally, since scenario affects Blue and not Red, it seems reasonable that Blue could provide an operating procedure that mitigates casualties. Yet, the debark distance showed strong significance for MOEs "Red casualties" and "time," but not "Blue casualties." The reason for this, which is inherited by the model, is Blue masses force ashore prior to proceeding to the objective. While

there are risks with increased distance between waves of SSC with ACV and support, the range from the threat and blue staying power appears to provide a defensible force that is not too affected by how far ACV swim inland. What's more is that this was across the slowest ACV and fastest ACV designs. Incidentally, ACV speed is necessary to swim, cross terrain, maneuver, and quickly close with the objective.

Table 7.   This is a summary of the multiple regression models explored for MOEs 1-4.

MOE	Advanced Regression			Main Effect		BIC Comparison		
	R sq.	Adj R sq.	p	R sq.	Adj R sq.	R sq.	Adj R sq.	p
Blue cas.	0.55	0.55	12	0.36	0.36	0.57	0.56	12
Red cas.	0.48	0.47	14	0.38	0.38	0.48	0.47	17
Time	0.59	0.58	14	0.516	0.513	0.59	0.58	14
FER	0.34	0.33	12	0.10	0.09	0.34	0.33	12

(2)   Conclusion

Both "time" MOE models have the same "top four" influential factors, placing particular emphasis on speed. *ACV speed, LCAC speed, debark distance, and LCAC quantity* are the most influential factors in two different modeling approaches each with good fit.

Many of the procurement decisions today are made with protecting Marines in mind, particularly the vehicles that transport infantry. Most of the casualties occurred after dismounting their armored ACV. Force protection cannot be overlooked since the risks associated with combat, and the decision as to when to dismount infantry from inside vehicles is a tough call, which is highly situation dependent.

- "Blue casualties" – In the main effects model LCAC speed and debark distance are most applicable. In the advanced model force protection was more important, as was a quadratic relationship in Red classification range. Had we looked at main effects only, force protection would have been missed.

- "Red casualties" – Both models support a heavy reliance on speed. Most important was ACV speed. The advanced model identified that the interaction between debark distance and the quantity of LCAC is significant. In the model when LCAC are either lost due to maintenance or

effective fire the remaining gear is transitioned ashore by the number of LCAC. Thus, two LCACs paying the cost of long transits for each wave ashore do less to attrite Red as well as more LCAC.

- "Time" – This particular MOE does a few things well (Appendix E). Both the main effects and the advanced model each fit well, as seen by their summary of fit data and the summary table.

- "FER" – This MOE shows that the warfighting potential with the baseline is rather good, since subsequent scenarios like scenario 2 show a less significant increase in MOE. Additionally, of the models, the FER regression model does poorly compared to other MOEs at explaining the variability in amphibious assault.

5.   Simio: Discrete-Event Simulation

First, we review the MOE for the first stage model:

1.   MOE (5): Mission Holding
2.   MOE (6): Mission Total Time

In this section, we cover findings for our last two MOES, "Mission Holding" and "Total Time." For these, 1,000 replications were run with the following experimental design:

Scenario			Replications		Controls	Responses
✓	Name	Status	Required	Completed	prop_LHA	Response 1 (Hours)
✓	no_LHA	Idle	1000	1000 of 1000	0	6.46456
✓	all_LHA	Idle	1000	1000 of 1000	1	7.04099
✓	splitOps	Idle	1000	1000 of 1000	0.857	6.99462
✓	disagg…	Idle	1000	1000 of 1000	0.714	6.95743

Figure 65.   The Simio experiment had three primary scenarios, run with 1,000 replications, one control "prop_LHA," a response. The response is "Mission Total Time."

The Simio experiment was comprised of 1,000 replications. The probability that aircraft launched form the LHA was determined by the type being either split (12/14 aircraft to be launched from the LHA) or disaggregated (10/14 aircraft to be launched from the LHA). Results came in the form of over three million rows of data (3,917,160).

(1)   MOE (5): Mission Holding

Figure 66 shows an excerpt of the results provided in the pivot table in Simio.

Category	Data Item	Statistic	all_LHA Average	Minimum	Maximum	Half Width	disaggOps Average	Minimum	Maximum	Half Width
HoldingTime	TimeInStation	Average (Ho...	0.1942	0.1450	0.2379	0.0009	0.1938	0.1444	0.2416	0.0011
		Maximum (H...	0.2860	0.2091	0.3312	0.0016	0.2769	0.1803	0.3307	0.0019
		Minimum (Ho...	0.1173	0.0847	0.1886	0.0012	0.1226	0.0842	0.1848	0.0013
Throughput	NumberEntered	Total	14.0000	14.0000	14.0000	0.0000	10.0060	5.0000	14.0000	0.1112
	NumberExited	Total	14.0000	14.0000	14.0000	0.0000	10.0060	5.0000	14.0000	0.1112

Figure 66.   Pivot table in Simio, the category "Holding Time" had to be extracted from the entire data set for all scenarios only all aircraft launching from LHA and disaggregated operations being show (all_LHA and disaggOps).

Subset and data cleaning techniques in JMP were applied to extract 39,567 rows of useable mission holding data.

Mean mission holding was highest when aircraft were all made to launch from the LHA. When launched from the LHA, all 14 aircraft experienced holding as prescribed in the model. Savings were 10% when performing split operations and 12.5% from disaggregated operations. Figures 67-69 show the mean holding and results from the 14 entities represent aircraft conducting the long-range raid.

Distributions Scenario=all_LHA

B_Value

Quantiles			Summary Statistics	
100.0%	maximum	1.49257	Mean	0.3288941
99.5%		1.33988	Std Dev	0.3405674
97.5%		1.26398	Std Err Mean	0.0034466
90.0%		0.59295	Upper 95% Mea	0.3356501
75.0%	quartile	0.51518	Lower 95% Mean	0.322138
50.0%	median	0.1818	N	9764
25.0%	quartile	0.08745		
10.0%		0.02007		
2.5%		0.00516		
0.5%		0.00123		
0.0%	minimum	9.84e-7		
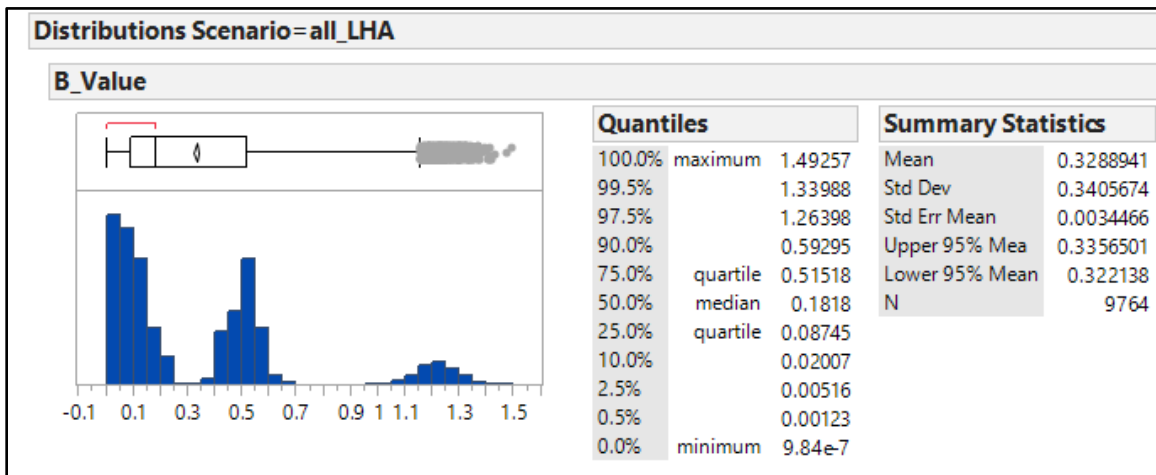
Figure 67.   Mean mission holding hours for 14 aircraft launching from the LHA only, 0.32 hours.
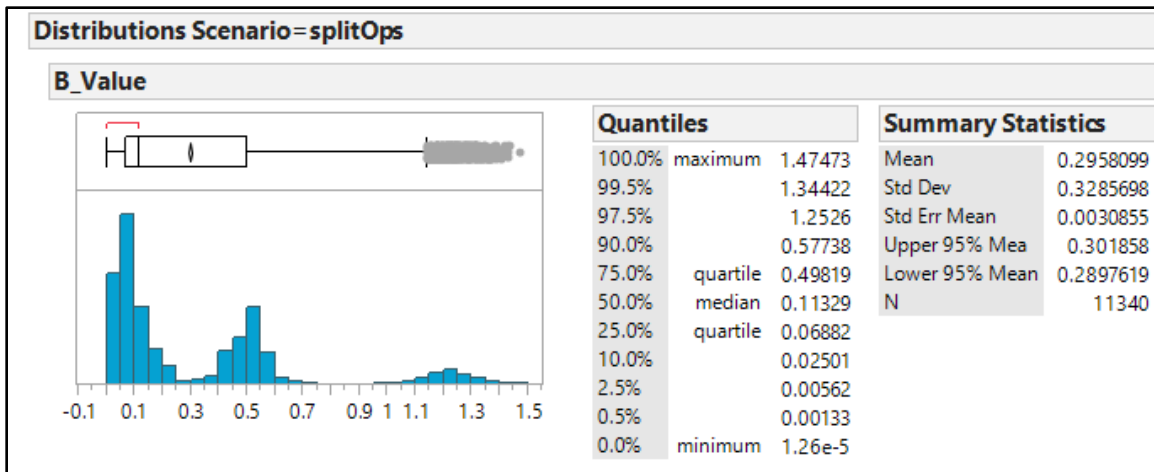
Figure 68.   Mean mission holding hours, all aircraft, during split operations, 0.29 hours.
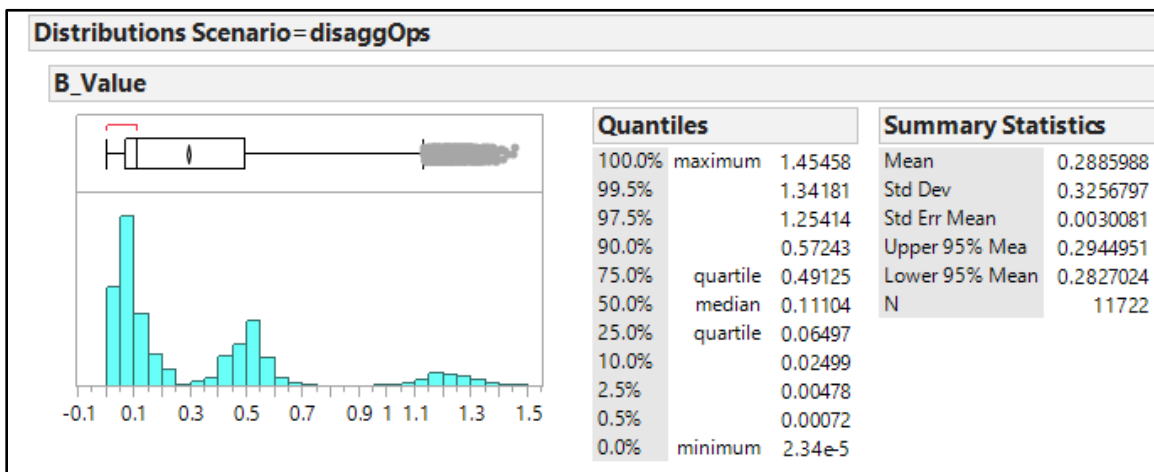
Figure 69.   Mean mission holding hours, all aircraft, during disaggregated operations, 0.28 hours.

Mission holding consists of three groupings consistent with the triangular distribution. High frequencies of mission holding occurred at six minutes, 30 minutes, and some as high as an hour. Average holding for disaggregated operations was 16.8 minutes, where all LHA operations had close to 20 minutes (19.2).

(2)   Insight

Our MANA model, scenario three showed increased casualties. Figure 70 shows the percentage increase from the baseline in casualties from scenarios 2, 3, and 4.
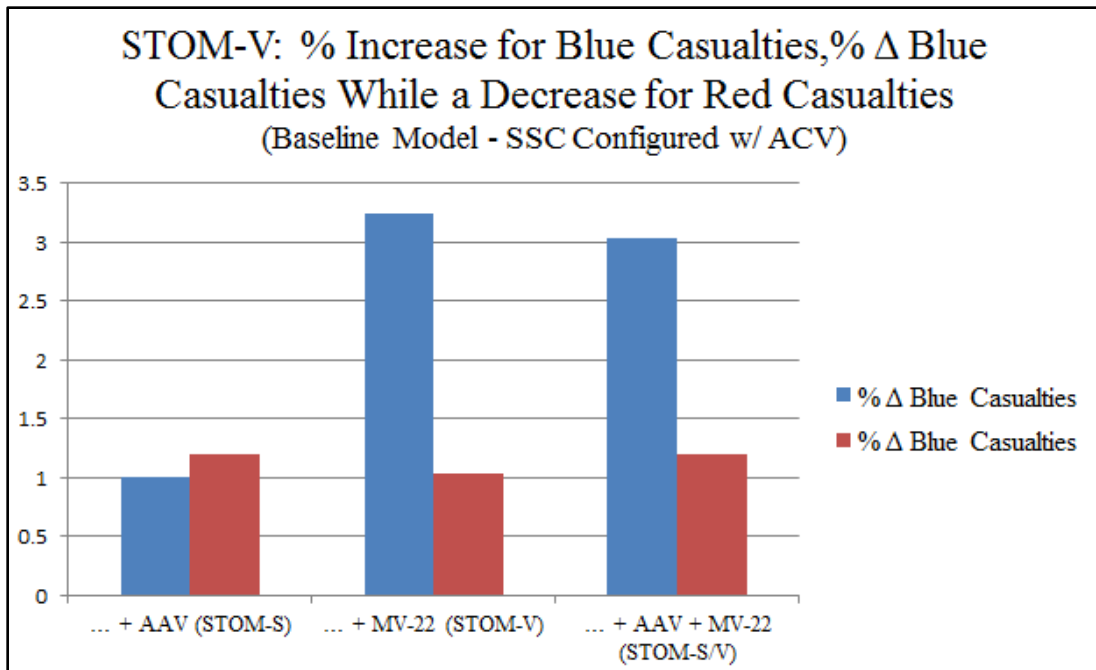
Figure 70.   STOM-V graph of increased casualties with scenario 3.

Aviation insight about increased casualties from dismounted infantry. Operationally, it is almost always planned for to hold after inserting infantry for contingencies such as CASEVAC/MEDEVAC and emergency extract (Team Expeditionary & Cohort 311-132, 2014). The amount of holding generated by the Simio model is a best case. Calculations here, however, will only account for holding associated with the launch of aircraft and should be seen as the lowest total savings.

Spreadsheet calculations are made to transform holding data into potential savings in energy and money. First, we combine average mission holding and burn rates for the principal drivers of energy the MV-22 and CH-53. We look at just these two platforms because the F-35B does not join the MEU until it sails and this research wishes to incorporate energy savings during the length workup period.

Table 8. The top line has all LHA, split, and disaggregated operations. Below are the low, operational planning, and high end burn rates in one table (i.e., "lo," "Planning," and "hi"). These numbers provide a range for a decision maker.

	ALL "LHA"	"Split"	"Disaggregated"	
Mean Holding (hrs)	0.328	0.295	0.288	
	Low (lo)	**Planning**	**High (Hi)**	
Burn Rate MV-22	2,500	3,200	4,700	pounds/hour (lbs/hr)
Burn Rate CH-53K	2,900	3,600	4,900	lbs/hr

Another calculation is made to convert mission holding (hours) and burn rate (lbs/hr) in to pounds of fuel burned per mission. Figure 71 shows pounds of fuel burned from the three scenarios at three potential levels.
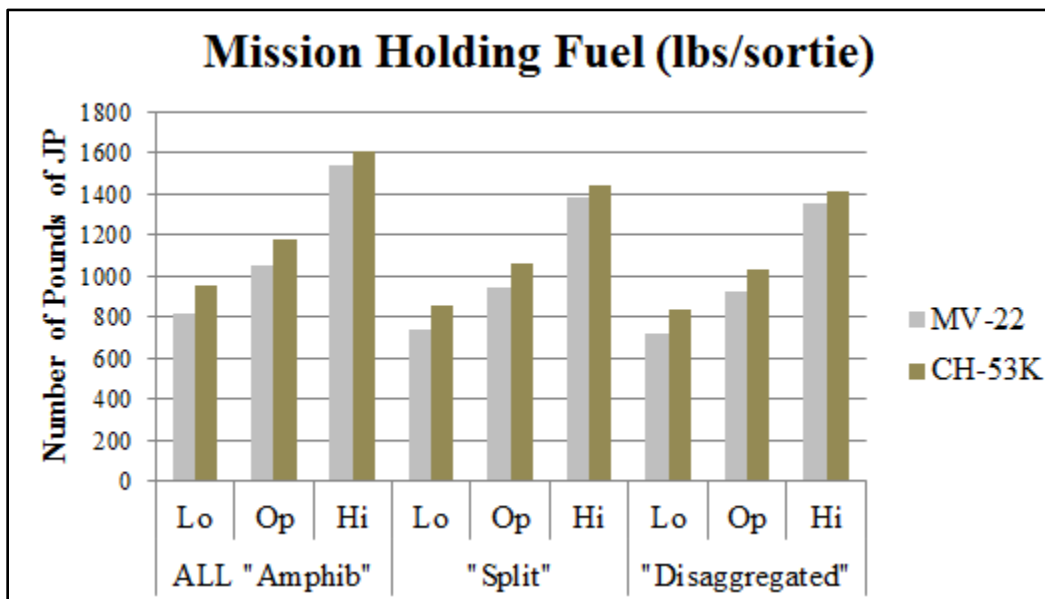
Figure 71. The bar graph shows pounds of fuel burned per sortie. A sortie is defined as one hour of flight launched from a ship.

Thus, the combined assault mission holding fuel for both the MV-22 and the CH-53K can be calculated. For the six-month workup period, there are eight long-range raids given for a MEU, which either has a low, operational planning, or high number of raids. After raids done for training on workups, there are additional "real-world" raids complete. For the six-month MEU deployment, we look at three levels of deployment

intensity consisting of 6-, 24-, or 48-raid missions. Figure 72 shows the impact of assault mission holding for the MEU based on deployment intensity.
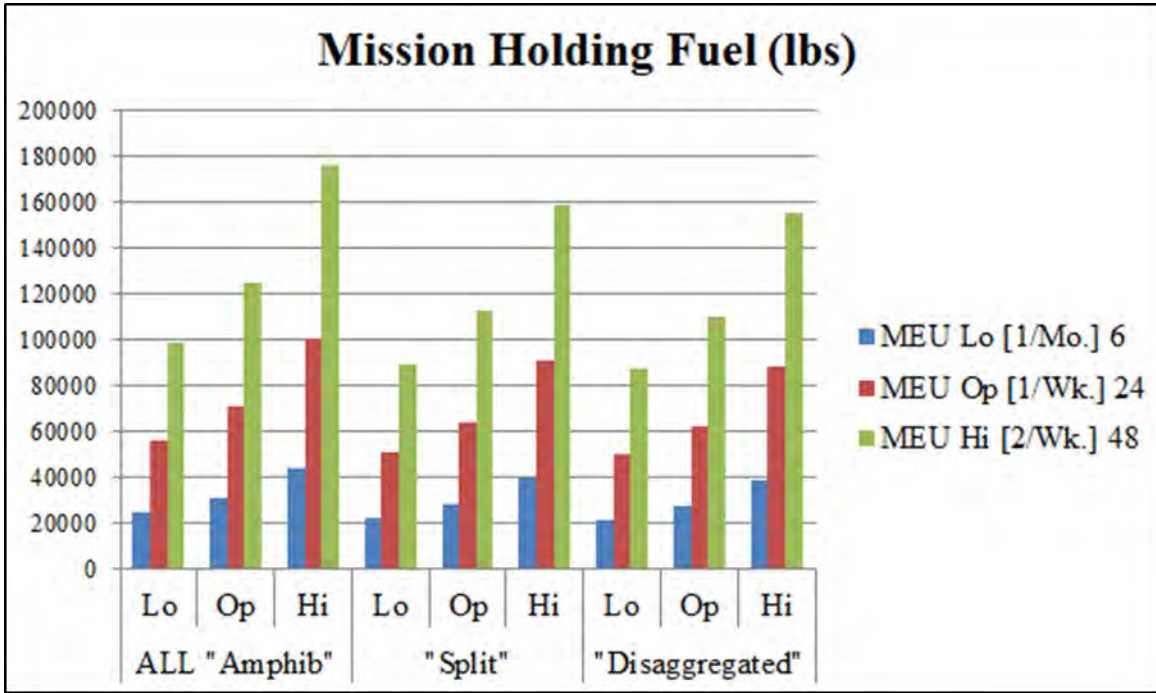
Figure 72.   Assault aircraft on a MEU deployment at three levels of deployment intensity consisting of 6-, 24-, or 48-raid missions.

For the purpose of this research a mission is a long range raid. Workups consist of two missions for each at sea training period prior to the actual deployment. With four training periods (e.g., certification exercise [CERTEX]), eight missions are added in with whether the MEU is conducting a mission every month, week, or twice a week. Figure 73 shows the money saved after 10 years of operating either split or disaggregated. To convert the mission holding fuel to dollars, again we use spreadsheet calculators.
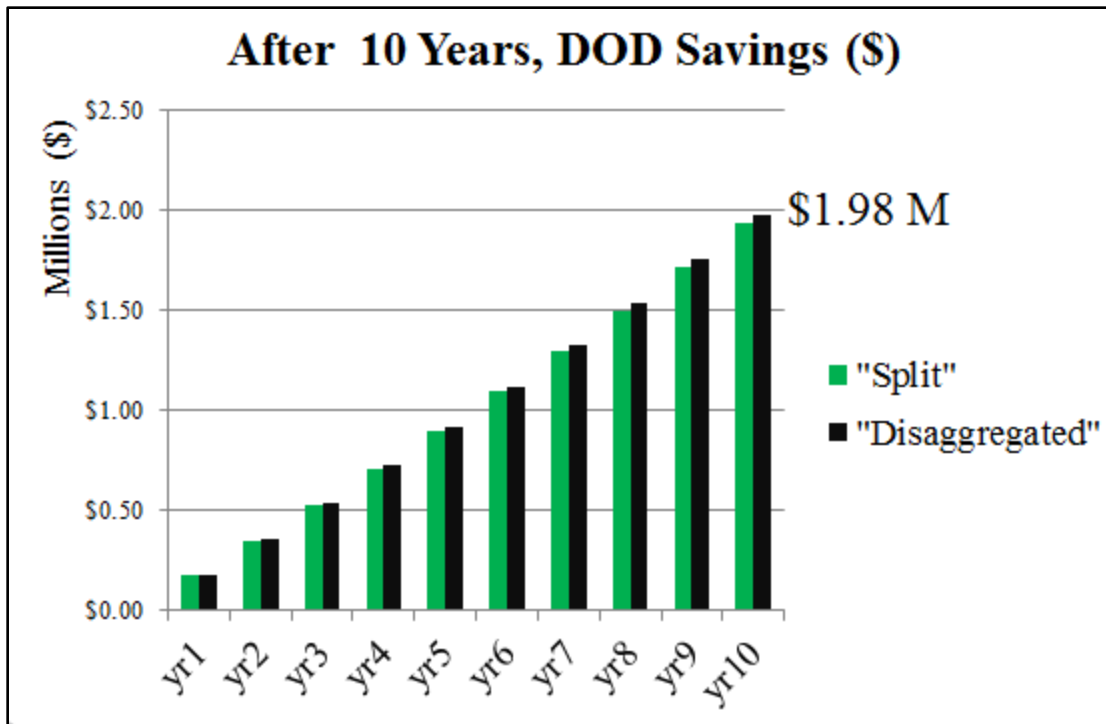
Figure 73.   After 10 years, potential DOD savings from fuel. Interest rate of return 3 %. Annual savings for split and disaggregated, $1.93 M split and $1.98 M for disaggregated.

Plot shows the monetary value of distributed operations. The difference between mission holding all on the LHA versus split and distributed was calculated in dollars. An average MEU, including workups, convert to gallons, multiply by $3.64 per gallon of JP-5. At nominal interest rate of 3%, Figure 73 shows the lost potential savings from mission holding. Two million dollars in fuel savings may seem insignificant; however, when one considers the logistics required to transport additional fuel for "holding," then this result can be magnified many times over. During the recent conflict in Iraq and Afghanistan, the cost to transport fuel to isolated bases cost up to 400 times the original cost of the fuel (Rosenthal, 2010).

(3)   MOE (6): Mission Total Time

The time that it takes to complete the long-range raid is unencumbered by the distributing of ACE aircraft from between the LHA and the LPD. The LHA has several spots and crews to mitigate the increased launch demands of large packages of aircraft.

As previously described we made the LHA worst case with regard to spot availability, restricting total numbers of spots and crews for the LHA.
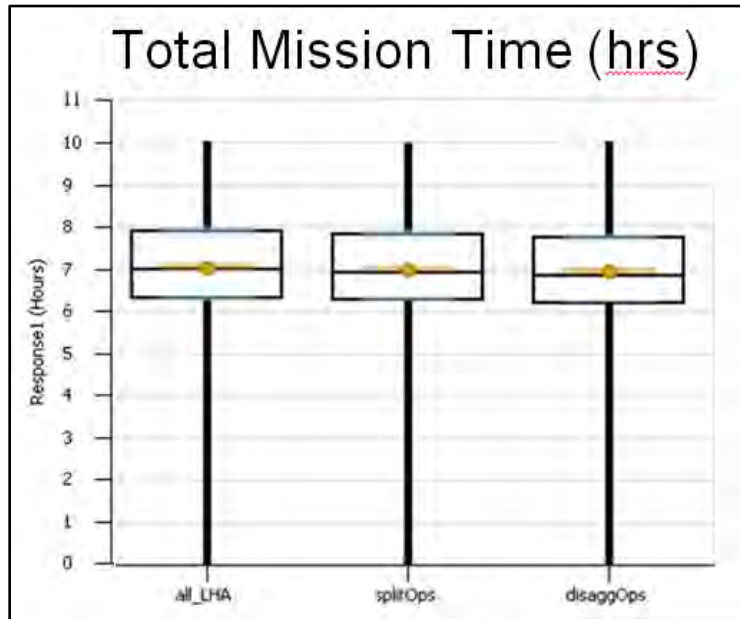
Figure 74.   After 1,000 replications, practically no significant effect on mission time.

(4)   Conclusions

Multiple air capable ships mitigate the risk of any one platform fouling an entire operation. Distributing forces on many platforms may be cheaper from smaller less complex systems and provide numerous redundant parts. Total mission times may be reduced by positioning air capable ships closer to the objective. There was no change to total mission time from distributed operations, however, a change in operating procedures may decrease mission holding, which might translate into significant monetary savings.

VII. CONCLUSIONS AND RECOMMENDATIONS

Americans can always refuse to pay the price for maintaining an amphibious capability, thereby giving up what Liddell Hart calls "the greatest strategic asset that a sea-based power possesses." If Americans should choose to take such a step, they will have, in effect, accomplished what no enemy has managed to do: defeat a modern amphibious operation

—Col Theodore L. Gatchel, USMC (Ret)

This research develops a two-stage model, where we found the most important factor to be speed. While this model is by no means the end-all, it provides verification and validation for other ACVs, SSCs, AAV upgrades, and amphibious operation models. This research supports operationally effective ACVs that operate at speeds much less than 40 or even 30 mph. These speeds align closely with the M1A1 tank land speed, and are often cited as the top U.S. capability that any future amphibian must meet. The vision for the future amphibious fleet has vehicles launching from ranges of 25 nm, 12 nm, and 5 nm off shore. Speeds, ranges, and quantities of SSCs were all varied in an efficient DOE to better understand the complex trade-space of amphibious assault.

A. OVERVIEW

In the aftermath of the EFV, the Marine Corps identified a new top acquisition priority in the ACV, which is a wheeled, amphibian designed with lessons learned from more than 13 years of combat operations. Even with an increasingly fiscally constrained force, the vehicle of complementary platforms of SSC must bring Marines to objectives quickly and safely. Currently, there are four prototypes being tested. This research uses agent-based and discrete-event simulation modeling, combined with a state-of-the-art, nearly orthogonal-and-balanced DOE to model an end-to-end amphibious assault. An overview of the model-test-model approach is provided in Appendix J.

B. ENERGY INSIGHTS

This research builds on previous SE graduate-level work that found advanced platforms like the MV-22 and CH-53K embarked with Marines provide great capacity, yet consume great quantities of fuel. This research models a long-range raid complete with MV-22s and CH-53Ks, which is one of the most taxing evolutions for not only the deck cycle, but for the ACE. The DES in Simio within this document shows the benefit to split and disaggregated operations. Specifically, operating procedures exist that *may reduce mission holding* and can be done in a way with *no effect on total mission time*. Meanwhile, several analytical methods and the MANA simulation show that the ACV, AAV, and the next SSC should be designed to meet the following specifications:

- ACV speed: 16 kts/18 mph

- ACV debark distances of 5 nm and 12 nm

- LCAC quantities should be greater than two or have operating speeds > 44 kts

In summary:

- A disaggregated and split operation is one way to mitigate excessive mission holding.

- The SSC, ACV, and the AAV upgrade need not be as fast as a tank is on land in order to be mission effective and meet requirements.

C. OPERATIONAL INSIGHTS

The ability to conduct STOM-V and STOM-S in a variety of ways allows for a landing to quickly mass forces and support ashore. During an amphibious assault, the defending force has an advantage of concealment and artillery, yet the attack can choose the time and place to land to select an advantageous avenue of approach. Operationally, SSCs have consisted of AAVs that capably brought many Marines ashore to Kuwait. Having amphibious vehicles allows for river and canal crossings, as was the case in Iraq. This is not, however, an opposed landing. During an amphibious assault vice an amphibious landing, a bigger force is required. More armor is required to defend the landing force against the variety of weapons that can be brought to bear during the launch, swimming, transition through the surf, and movement inland—all of which

cannot happen slowly. Heavily armored vehicles that might hold more may also have decreased performance and be vulnerable, compared to medium-sized ACVs.

This research also looks at the MEU contribution from nonamphibious assault landings, when forces are brought in to a secure landing zone. Figure 75 shows Blue and Red casualties by scenario.
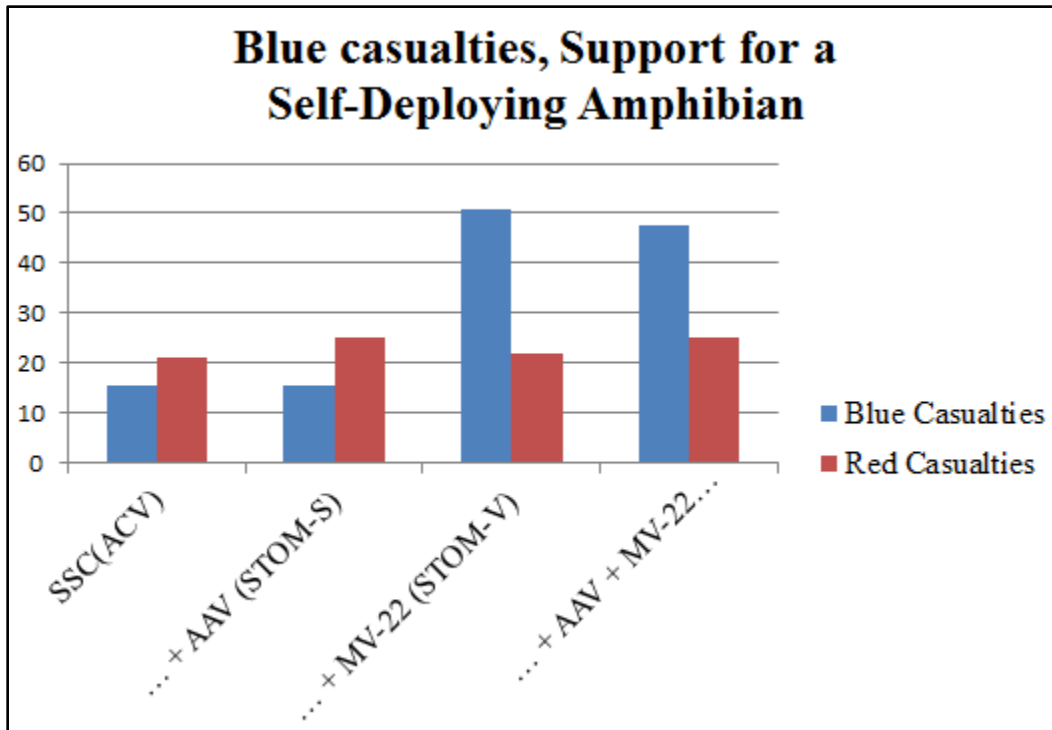
Figure 75.   What is the most important vehicle type in an amphibious assault?
Of the four scenarios, scenario 3 masses Blue force the fastest with
the MV-22; however, dismounted infantry are not afforded the same
protection as those inside vehicles like the ACV and AAV.

To give this research the pedigree of a traceable scenario, the author uses EW 12. Two ACVs will carry a reinforced squad, which means that with ACVs, Marines will have twice the firepower with two RWSs, as opposed to one on the legacy AAV tractor. Nevertheless, the affect from a self-deploying amphibious vehicle is a single wave, which masses firepower ashore without paying the price of being a serial in a wave of SSCs.

1. MOE Insights

Blue casualties are fewer when just connectors and an autonomous AAV wave are used. Blue casualties increase when Marines are dismounted early as with the STOM-V. An MV-22 long-range raid does increase Red casualties and the times that Blue attrites Red to one-third their strength. Red casualties depend on ACV speed, debark distance, LCAC quantity, and LCAC speed. The LCAC is the SSC. Time increases with distance; however, the benefit in going from three to four LCACs is not as great as the benefit in going from two to three. Depending on the size of the force, there are diminishing returns with the arrival of additional LCACs. Here, the fourth LCAC had a negligible impact, save functioning as a reserve for the other three.

D. FUTURE RESEARCH

The Marine Corps and DOD have many highly useful spreadsheet tools and calculators for specific needs. Before creating another, this author suggests asking, "What is not being modeled because it is too complex?" and then making an attempt to model it. Future work includes exploring the metamodels from this simulation in a future decision tool that shows operational energy and operational effectiveness. This analysis was broad and much can be done to refine it, such as:

- Impacts of terrain. Adjusting the RGB terrain file at the water's edge from water, to surf, to shore, and then inland.

- Increased fidelity in the transition through an active surf.

- Increased ranges and lethality of Red forces.

- A reduced signature offload of ACVs.

- Applying methods from Chapter V to: MLP launch of LCAC, LCAC launch of ACV, ACV dismount of infantry.

- Impact of mobile artillery.

- Increased constraints on the well deck of the LHA/LHD.

- Egress from the ACV; exploring how best to employ a reinforced squad of Marines split between two ACV vehicles.

E. SUMMARY

- Complex spreadsheet tools, with thousands of lines of VBA, are less adaptive than object-oriented models.

- This research modeled over 100 agents and 75 factors.

- The LCAC, ACV, AAV, and MV-22 all are distributed systems, but it was a self-deployer that provided the desired affect against an enemy in the defense.

- Speed, though highly influential, need not be at top capability to be effective.

- Two million dollars in fuel savings may seem insignificant; however, when one considers the logistics required to transport additional fuel for "holding," then this result could be magnified many times over.

The force that responds to the next crisis or contingency will be the force that is closest to it—the Marine Expeditionary Units (MEUs) embarked on ships. This research is leaning forward by making a first attempt at modeling an end-to-end amphibious assault. In hundreds of thousands of simulated amphibious assaults, we observe the trade-space formed by the many complex parameters considered when employing concept complementary platforms of surface and vertical ship-to-objective-maneuver. In the end, we realize quantifiable values that maximize mission effectiveness and better inform the top procurement priorities for the United States Naval forces.

THIS PAGE INTENTIONALLY LEFT BLANK

APPENDIX A. COMPLETE TABLE OF BLUE SQUADS

Table 9.   Complete table of the 113 Blue squads in MANA.

Squad Number	Squad	Parent	Number of Agents	Agent Class Number	Run Start Delay
1	LHD	None	1	99	0
2	LPD-19	None	1	99	0
3	LSD-41	None	1	99	0
4	LCAC-1-1	3	1	88	430
5	LCAC-2-1	3	1	88	430
6	LCAC-3-1	3	1	88	430
73	LCAC-4-1	3	1	88	430
7	LCAC-1-2	3	1	88	4720
8	LCAC-2-2	3	1	88	4720
9	LCAC-3-2	3	1	88	4720
74	LCAC-4-2	3	1	88	4720
10	LCAC-1-3	3	1	88	9010
11	LCAC-2-3	3	1	88	9010
12	LCAC-3-3	3	1	88	9010
13	*LCAC-1-4 (NOT ACTIVE)*	3	1	88	
14	*LCAC-2-4 (NOT ACTIVE)*	3	1	88	
15	*LCAC-3-4 (NOT ACTIVE)*	3	1	88	
75	LCAC-4-3	3	1	88	9010
34	M1A1-1	4	1	2	0
35	M1A1-2	5	1	2	0
36	M1A1-3	7	1	2	0
37	M1A1-4	8	1	2	0
76	ACV-P-1	6	1	4	0
77	ACV-P-2	6	1	4	0
78	ACV-P-3	6	1	4	0
79	ACV-P-4	73	1	4	0
80	ACV-P-5	73	1	4	0
81	ACV-P-6	73	1	4	0
82	ACV-P-7	75	1	4	0
83	ACV-P-8	9	1	4	0
84	ACV-P-9	9	1	4	0
85	ACV-P-10	9	1	4	0
86	ACV-P-11	74	1	4	0
87	ACV-P-12	74	1	4	0
88	ACV-P-13	74	1	4	0

Squad Number	Squad	Parent	Number of Agents	Agent Class Number	Run Start Delay
89	ACV-P-14	74	1	4	0
90	ACV-P-15	12	1	4	0
91	ACV-P-16	12	1	4	0
92	ACV-P-17	75	1	4	0
93	ACV-R-1	6	1	4	0
94	ACV-C-1	73	1	4	0
50	Inf-1	76	3	1	0
51	Inf-2	77	3	1	0
52	Inf-3	78	3	1	0
53	Inf-4	79	3	1	0
54	Inf-5	80	3	1	0
55	Inf-6	81	3	1	0
56	Inf-7	82	3	1	0
57	Inf-8	83	3	1	0
58	Inf-9	84	3	1	0
59	Inf-10	85	3	1	0
60	Inf-11	86	3	1	0
61	Inf-12	87	3	1	0
62	Inf-13	88	3	1	0
63	Inf-14	89	3	1	0
64	Inf-15	90	3	1	0
65	Inf-16	91	3	1	0
66	Inf-17	92	3	1	0
67	Inf-18	93	3	1	0
95	Inf-19	94	3	1	0
96	Inf-20	25	3	1	0
97	Inf-21	26	3	1	0
98	Inf-22	27	3	1	0
99	Inf-23	28	3	1	0
100	Inf-24	29	3	1	0
101	Inf-25	30	3	1	0
102	Inf-26	31	3	1	0
103	Inf-27	32	3	1	0
104	Inf-28	33	3	1	0
105	Inf-29	16	3	1	0
106	Inf-30	17	3	1	0
107	Inf-31	18	3	1	0
108	Inf-32	19	3	1	0
109	Inf-33	20	3	1	0
110	Inf-34	21	3	1	0
111	Inf-35	22	3	1	0
112	Inf-36	23	3	1	0
113	Inf-37	24	3	1	0

APPENDIX B. FER BY SCENARIO WITH THE RAW OUTPUT DATA
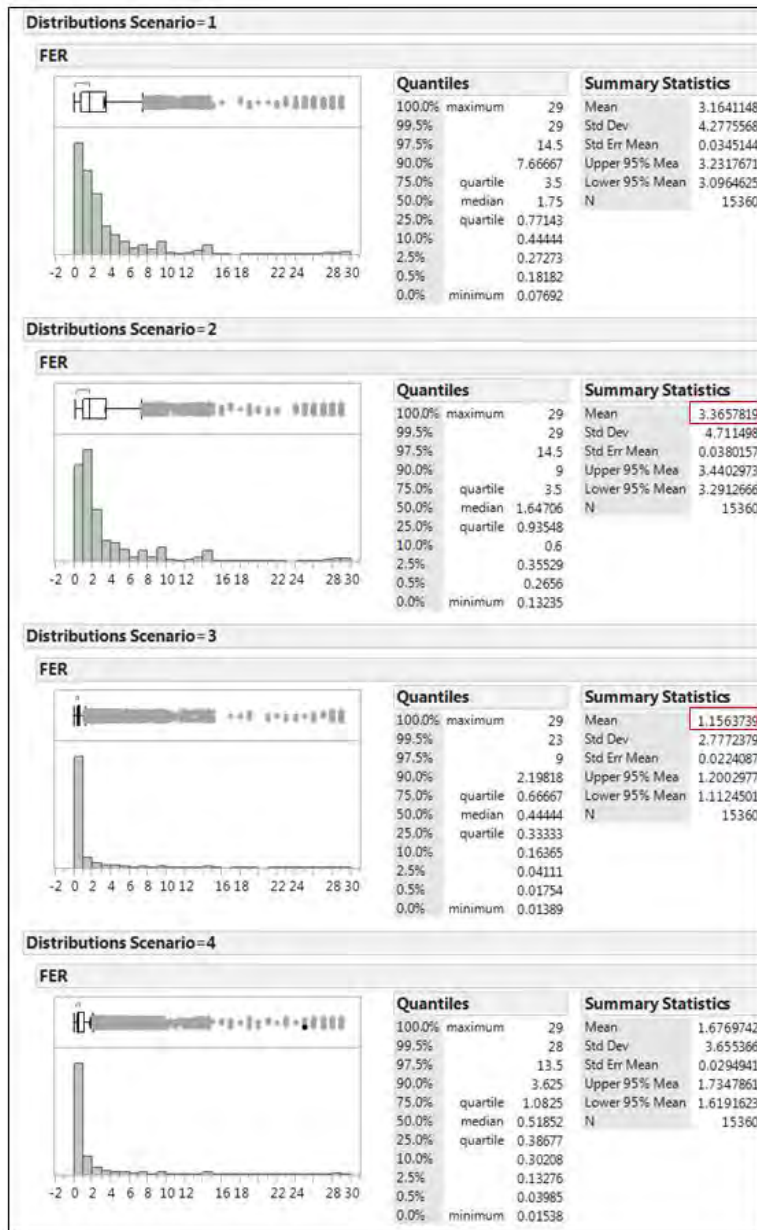
Figure 76.   Shows the FER, by scenario, with the non-collapsed data.

THIS PAGE INTENTIONALLY LEFT BLANK

APPENDIX C. COLLAPSED DATA BY SCENARIO, PAIRED
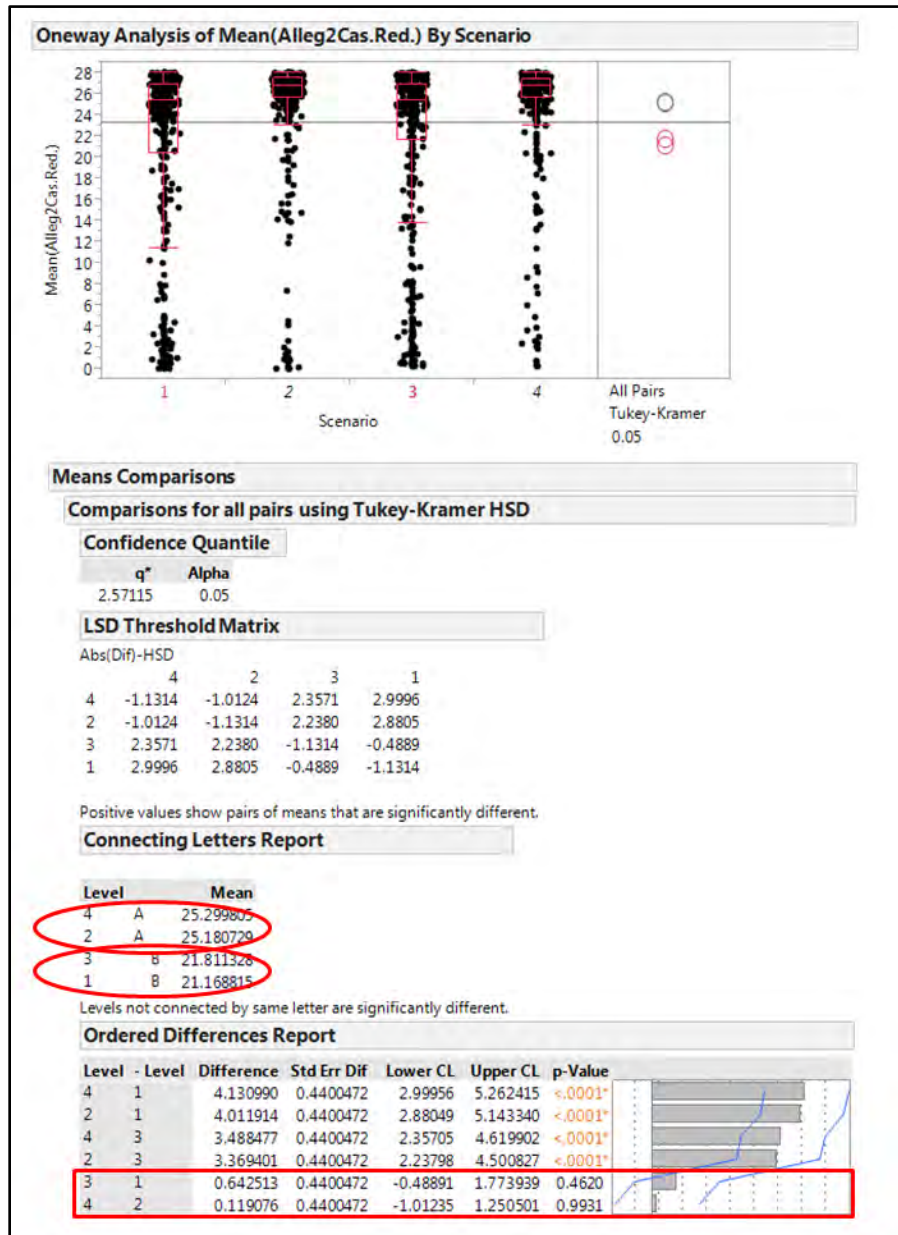
Figure 77.   One-way analysis of mean "Red casualties" MOE by scenario.

THIS PAGE INTENTIONALLY LEFT BLANK

APPENDIX D. RAW OUTPUT DATA, PAIRED
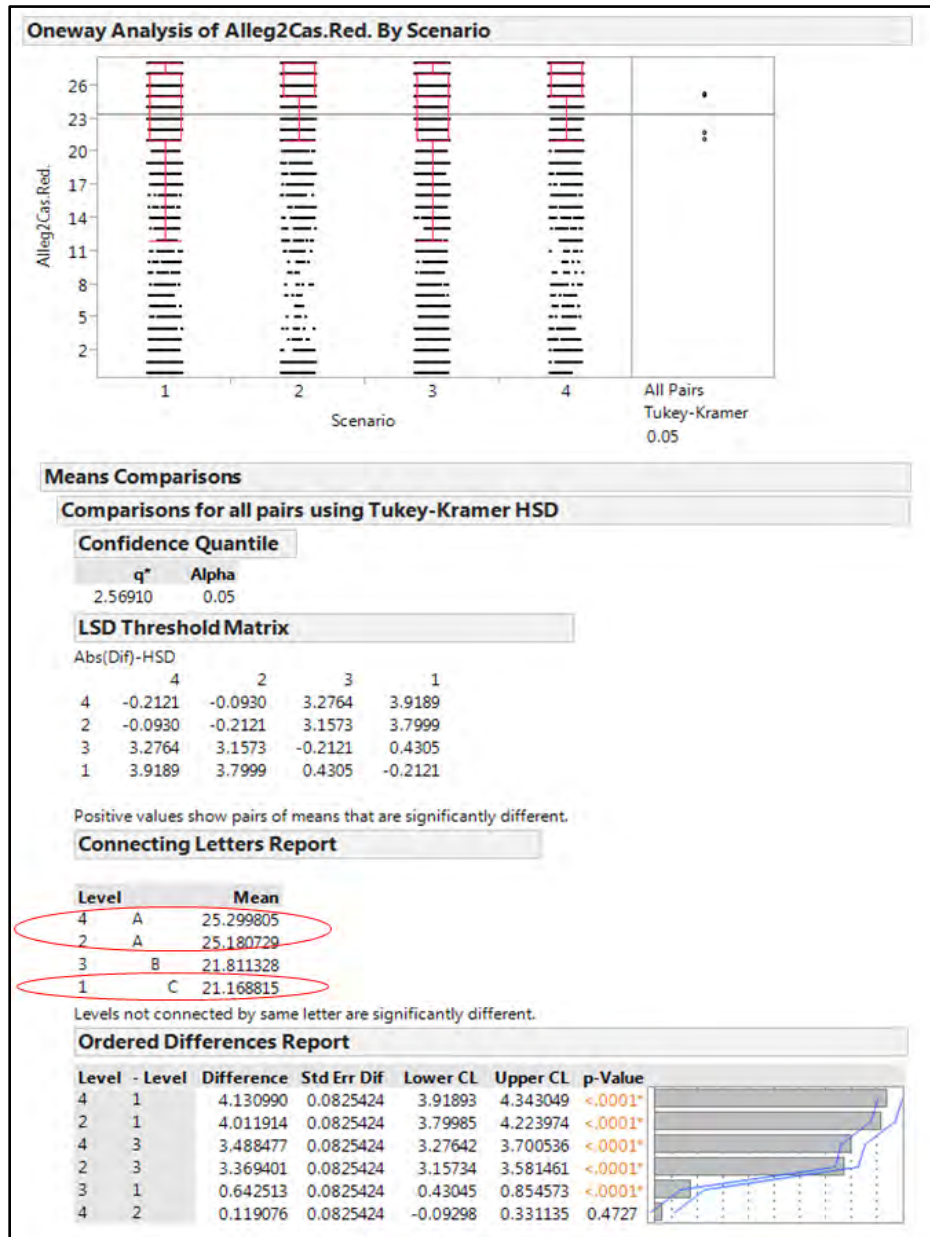
Figure 78.   One-way analysis of the mean "Red casualties" MOE by scenario with the non-collapsed output data.

THIS PAGE INTENTIONALLY LEFT BLANK

APPENDIX E. MULTIPLE LINEAR REGRESSION COMPARISON TABLE

Figure 80. MOE "Blue casualties" actual by predicted, summary of fit, prediction profiler, and Pareto plots.

Response Mean(Alleg2Cas.Red.)

Actual by Predicted Plot

[Plot: Mean(Alleg2Cas.Red.) Actual (y-axis, 0–28) vs Mean(Alleg2Cas.Red.) Predicted P<.0001 (x-axis, 0–30)]
RSq=0.48 RMSE=5.2705

Summary of Fit

RSquare	0.480168
RSquare Adj	0.476588
Root Mean Square Error	5.270466
Mean of Response	23.36517
Observations (or Sum Wgts)	2048

Analysis of Variance

Source	DF	Sum of Squares	Mean Square	F Ratio
Model	14	52163.40	3725.96	134.1343
Error	2033	56472.29	27.78	Prob > F
C. Total	2047	108635.69		<.0001*

Sorted Parameter Estimates

Term	Estimate	Std Error	t Ratio		Prob>|t|
LCDbkDist[25-12]	-10.28631	0.50422	-20.40		<.0001*
ACVMvtSpd	0.1933118	0.010966	17.63		<.0001*
LCDbkDist[25-12]*LCACQty[3-2	8.1278321	0.697515	11.65		<.0001*
Scenario[1]	-2.196354	0.201718	-10.89		<.0001*
Scenario[2]	1.8155599	0.201718	9.00		<.0001*
Scenario[3]	-1.553841	0.201718	-7.70		<.0001*
RedInfClsRng	0.0001235	1.614e-5	7.65		<.0001*
Scenario[1]*(ACVMvtSpd-26.5)	0.1266342	0.01884	6.72		<.0001*
Scenario[2]*(ACVMvtSpd-26.5)	-0.105782	0.01884	-5.61		<.0001*
LCDbkDist[12-5]	-2.314777	0.424185	-5.46		<.0001*
Scenario[3]*(ACVMvtSpd-26.5)	0.0933938	0.01884	4.96		<.0001*
LCDbkDist[12-5]*LCACQty[3-2]	1.6942506	0.486529	3.48		0.0005*
LCDbkDist[12-5]*LCACQty[4-3]	1.0103107	0.471621	2.14		0.0323*
LCDbkDist[25-12]*LCACQty[4-3	1.3062766	0.675271	1.93		0.0532

Prediction Profiler

[Prediction profiler plots]
Mean (Alleg2Cas.Red) 23.22059 [22.64518, 23.79599]

26.5 ACVMvtSpd | 12501 RedInfClsRng | 1 Scenario | 5 LCDbkDist | 2 LCACQty

Effect Screening

Pareto Plot of Transformed Estimates

Term	Orthog Estimate	
LCDbkDist[12-5]*LCACQty[3-2]	2.629192	
ACVMvtSpd	2.102333	
LCDbkDist[25-12]	-1.776987	
LCDbkDist[25-12]*LCACQty[3-2	1.688921	
Scenario[1]	-1.460525	
LCDbkDist[12-5]	-1.338871	
RedInfClsRng	0.927280	
Scenario[1]*(ACVMvtSpd-26.5)	0.911825	
Scenario[3]	-0.897111	
Scenario[2]	0.794622	
LCDbkDist[12-5]*LCACQty[4-3]	0.671572	
Scenario[3]*(ACVMvtSpd-26.5)	0.577314	
Scenario[2]*(ACVMvtSpd-26.5)	-0.489443	
LCDbkDist[25-12]*LCACQty[4-3	0.225290	

Figure 81.   MOE "Red casualties" summary of fit, sorted parameter estimates, prediction profiler, and Pareto plots.

Response Mean(RedKillTime)

Actual by Predicted Plot

Summary of Fit

RSquare	0.590067
RSquare Adj	0.58693
Root Mean Square Error	479.2593
Mean of Response	4317.937
Observations (or Sum Wgts)	1844

Analysis of Variance

Source	DF	Sum of Squares	Mean Square	F Ratio
Model	14	604705567	43193255	188.0506
Error	1829	420102059	229689.48	Prob > F
C. Total	1843	1024807626		<.0001*

Sorted Parameter Estimates

Term	Estimate	Std Error	t Ratio		Prob>|t|
ACVMvtSpd	-31.48698	1.075517	-29.28		<.0001*
LCACMvtSpd	-19.49544	1.111239	-17.54		<.0001*
LCDbkDist[12-5]	437.26368	27.02503	16.18		<.0001*
LCDbkDist[25-12]	411.90172	27.47519	14.99		<.0001*
LCACQty[3-2]	-362.5238	28.88748	-12.55		<.0001*
Scenario[1]	248.62223	19.88459	12.50		<.0001*
RedInfClsRng	-0.01782	0.001582	-11.27		<.0001*
AAVMvtSpd	-11.98871	1.070287	-11.20		<.0001*
Scenario[2]	-175.7256	19.00824	-9.24		<.0001*
Scenario[3]	177.53991	19.69331	9.02		<.0001*
Scenario[2]*(AAVMvtSpd-23.9572)	-15.39381	1.81273	-8.49		<.0001*
Scenario[3]*(AAVMvtSpd-23.9572)	15.465485	1.867478	8.28		<.0001*
Scenario[1]*(AAVMvtSpd-23.9572)	15.001022	1.881813	7.97		<.0001*
LCACQty[4-3]	-12.29966	26.29656	-0.47		0.6400

Prediction Profiler

Figure 82.   MOE "time" summary of fit, sorted parameter estimates, prediction profiler, and Pareto plots.

133

Response Mean(FER)

Actual by Predicted Plot

Mean(FER) Predicted P<.0001 RSq=0.34
RMSE=2.7918

Summary of Fit

RSquare	0.341796
RSquare Adj	0.337915
Root Mean Square Error	2.79177
Mean of Response	2.340811
Observations (or Sum Wgts)	2048

Analysis of Variance

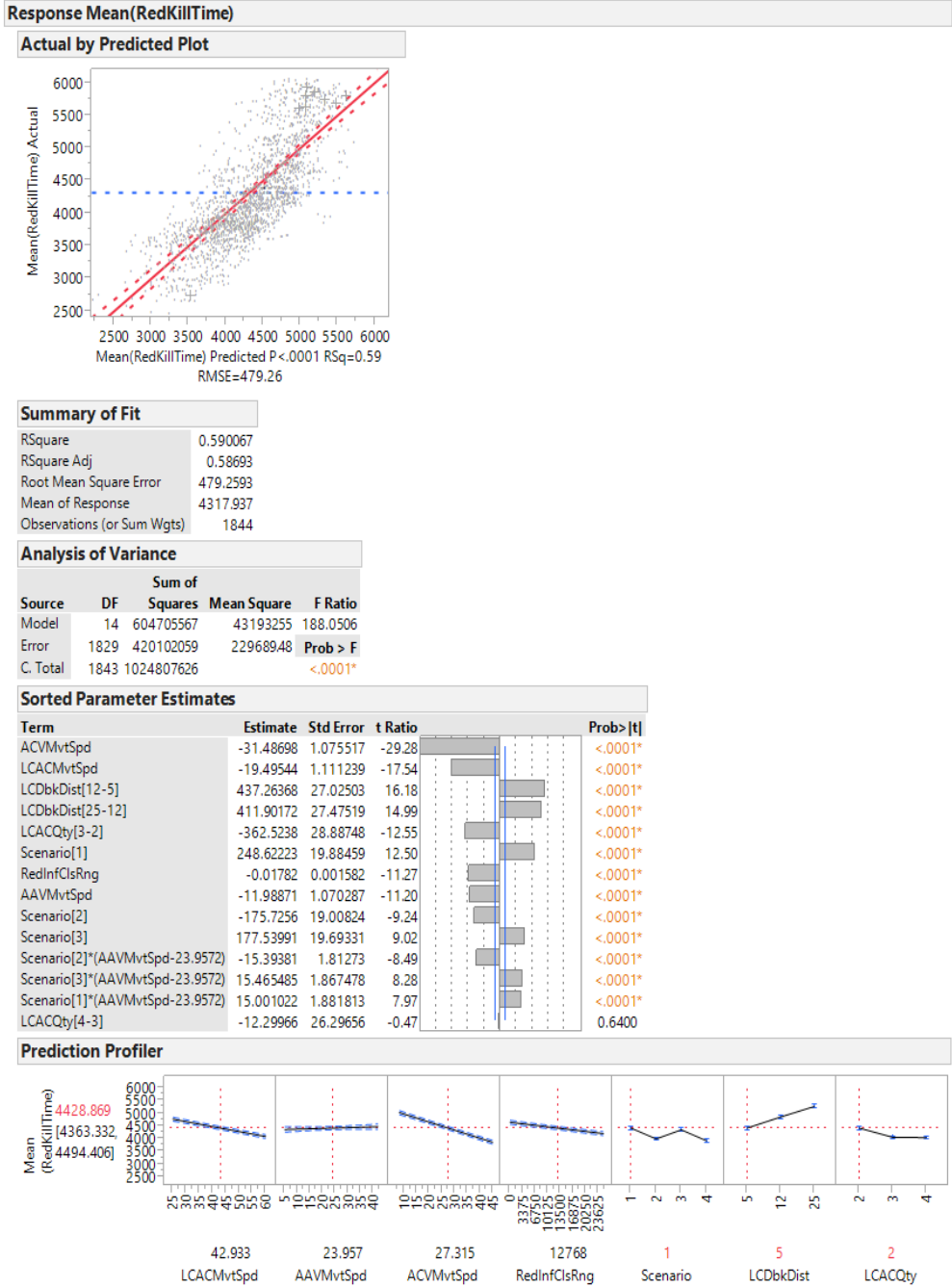| Source	DF	Sum of Squares	Mean Square	F Ratio
Model	12	8236.269	686.356	88.0623
Error	2035	15860.754	7.794	Prob > F
C. Total	2047	24097.023		<.0001*

Parameter Estimates

Term	Estimate	Std Error	t Ratio	Prob>|t|
Intercept	0.7455818	0.285444	2.61	0.0091*
InfHit2k	0.6534908	0.055874	11.70	<.0001*
ACVMvtSpd	0.0420899	0.005796	7.26	<.0001*
RedInfClsRng	-0.000105	8.532e-6	-12.25	<.0001*
RedInfWpnMaxEff	-0.000348	2.752e-5	-12.66	<.0001*
(RedInfClsRng-12500.5)*(RedInfClsRng-12500.5)	2.0182e-8	1.324e-9	15.24	<.0001*
(RedInfWpnMaxEff-4125)*(RedInfWpnMaxEff-4125)	1.1548e-7	1.38e-8	8.37	<.0001*
Scenario[1]	0.8233036	0.10685	7.71	<.0001*
Scenario[2]	1.0249707	0.10685	9.59	<.0001*
Scenario[3]	-1.184437	0.10685	-11.09	<.0001*
Scenario[1]*(RedInfWpnMaxEff-4125)	-7.29e-5	4.767e-5	-1.53	0.1263
Scenario[2]*(RedInfWpnMaxEff-4125)	-0.000253	4.767e-5	-5.31	<.0001*
Scenario[3]*(RedInfWpnMaxEff-4125)	0.0002235	4.767e-5	4.69	<.0001*

Prediction Profiler

Sorted Parameter Estimates

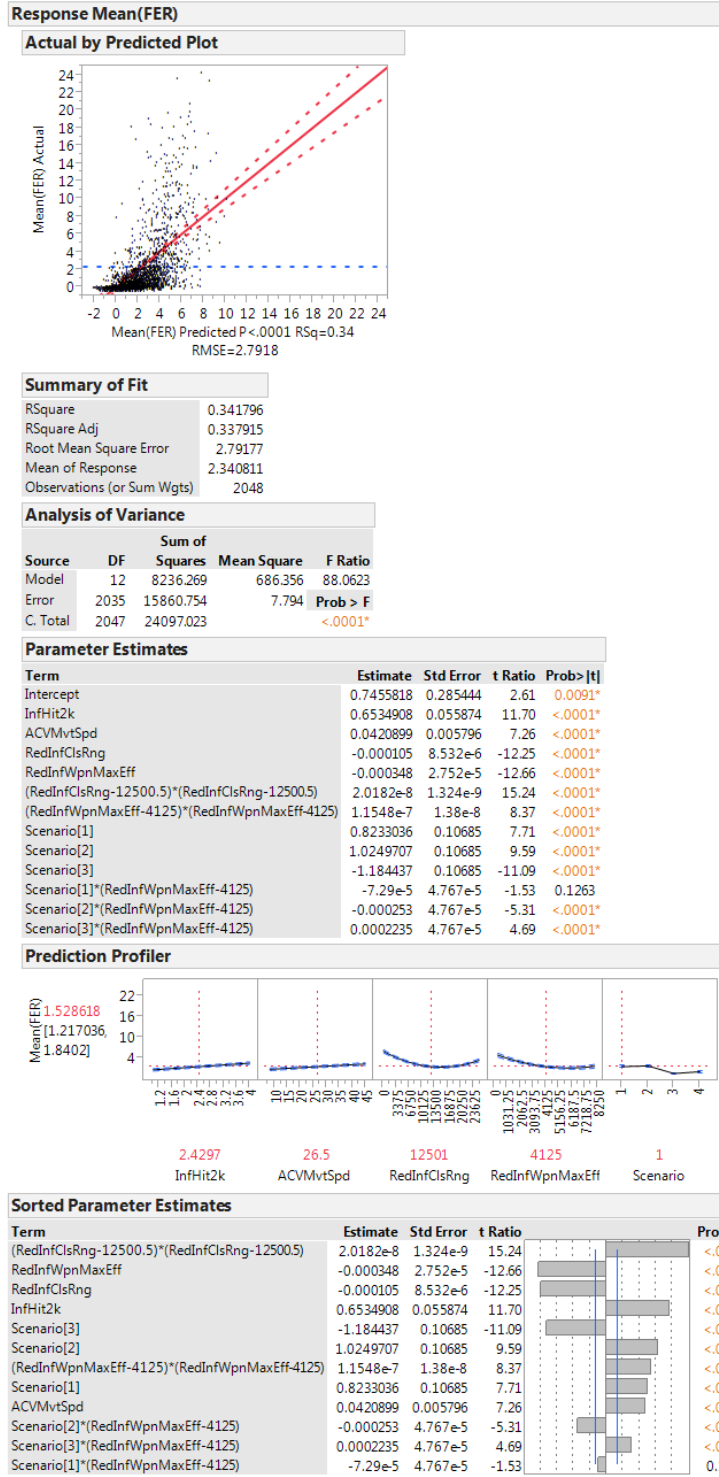| Term	Estimate	Std Error	t Ratio		Prob>|t|
(RedInfClsRng-12500.5)*(RedInfClsRng-12500.5)	2.0182e-8	1.324e-9	15.24		<.0001*
RedInfWpnMaxEff	-0.000348	2.752e-5	-12.66		<.0001*
RedInfClsRng	-0.000105	8.532e-6	-12.25		<.0001*
InfHit2k	0.6534908	0.055874	11.70		<.0001*
Scenario[3]	-1.184437	0.10685	-11.09		<.0001*
Scenario[2]	1.0249707	0.10685	9.59		<.0001*
(RedInfWpnMaxEff-4125)*(RedInfWpnMaxEff-4125)	1.1548e-7	1.38e-8	8.37		<.0001*
Scenario[1]	0.8233036	0.10685	7.71		<.0001*
ACVMvtSpd	0.0420899	0.005796	7.26		<.0001*
Scenario[2]*(RedInfWpnMaxEff-4125)	-0.000253	4.767e-5	-5.31		<.0001*
Scenario[3]*(RedInfWpnMaxEff-4125)	0.0002235	4.767e-5	4.69		<.0001*
Scenario[1]*(RedInfWpnMaxEff-4125)	-7.29e-5	4.767e-5	-1.53		0.1263

Figure 83.   MOE "FER" sorted parameter estimates, prediction profiler, and
Pareto plots.

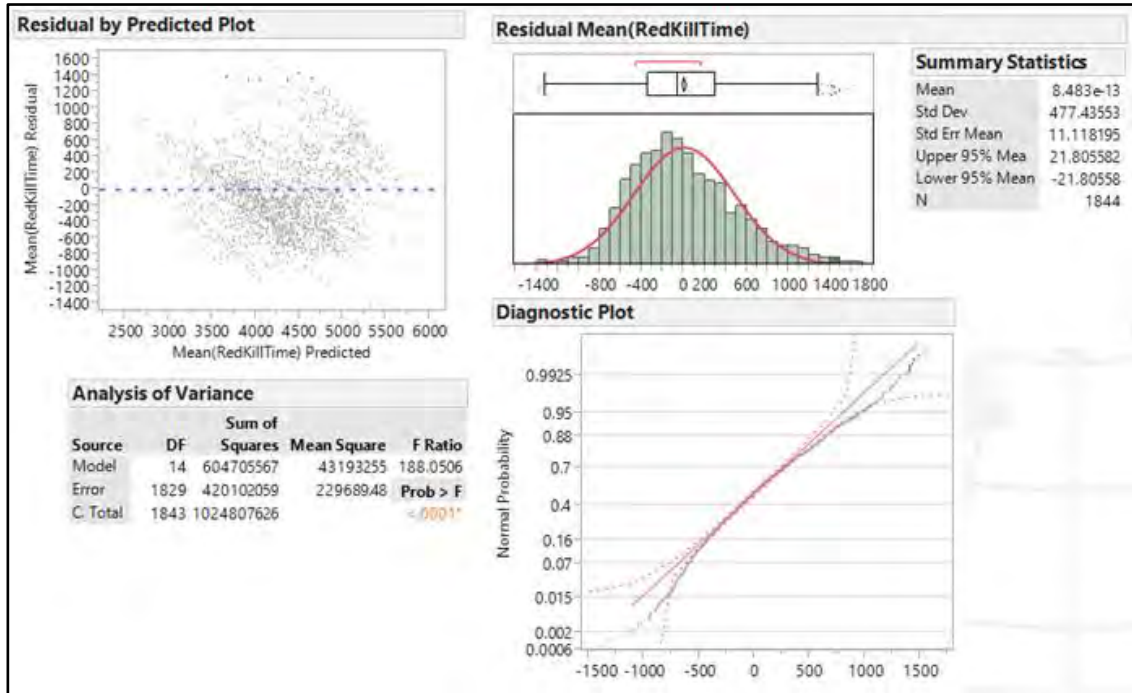# APPENDIX F. "TIME" MOE, MULTIPLE LINEAR REGRESSION, ASSUMPTIONS

Figure 84. MOE "time" advanced regression model, normal Q-Q plot, closely
fits along the line, passes the "fat pencil test."
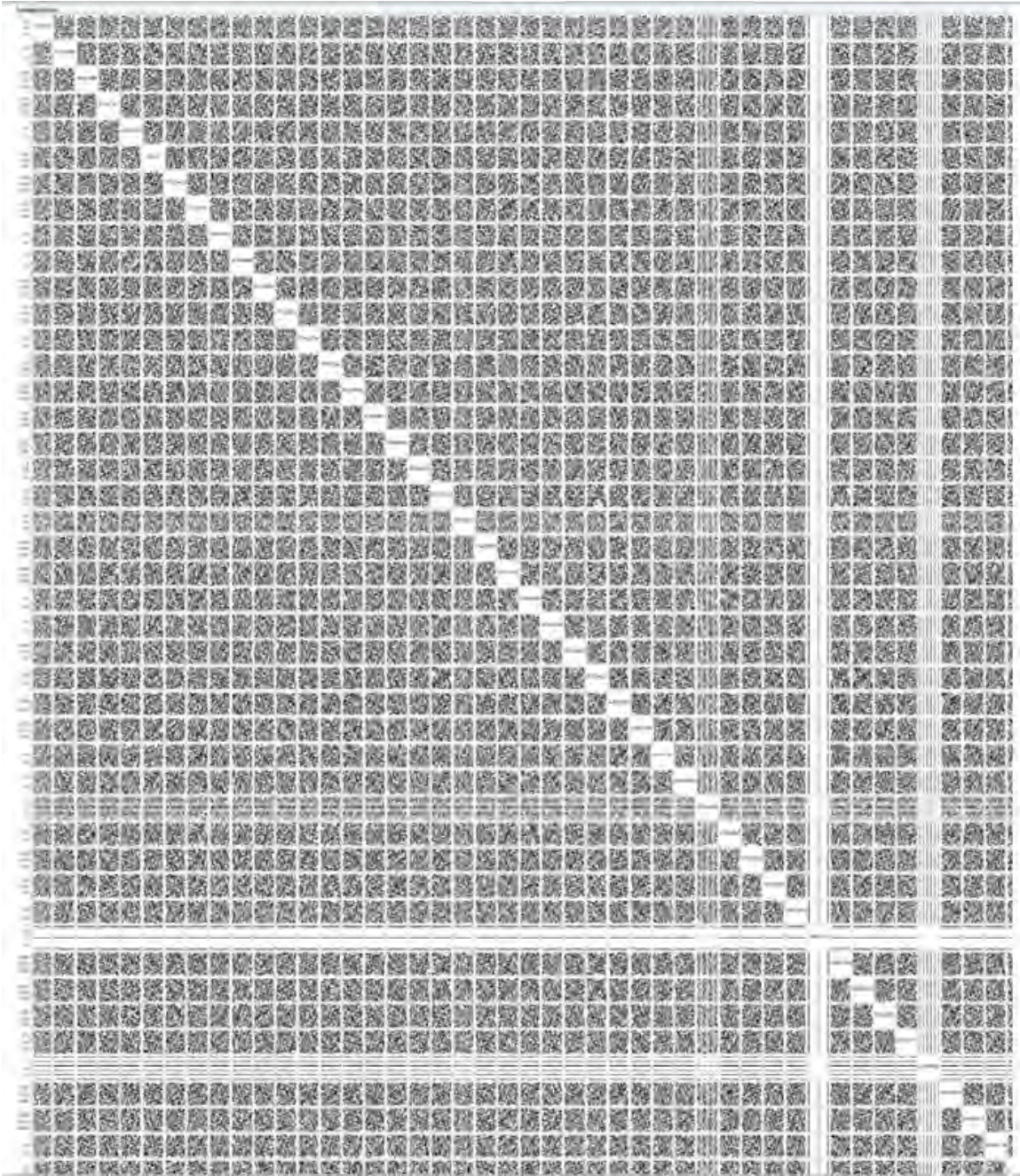
THIS PAGE INTENTIONALLY LEFT BLANK
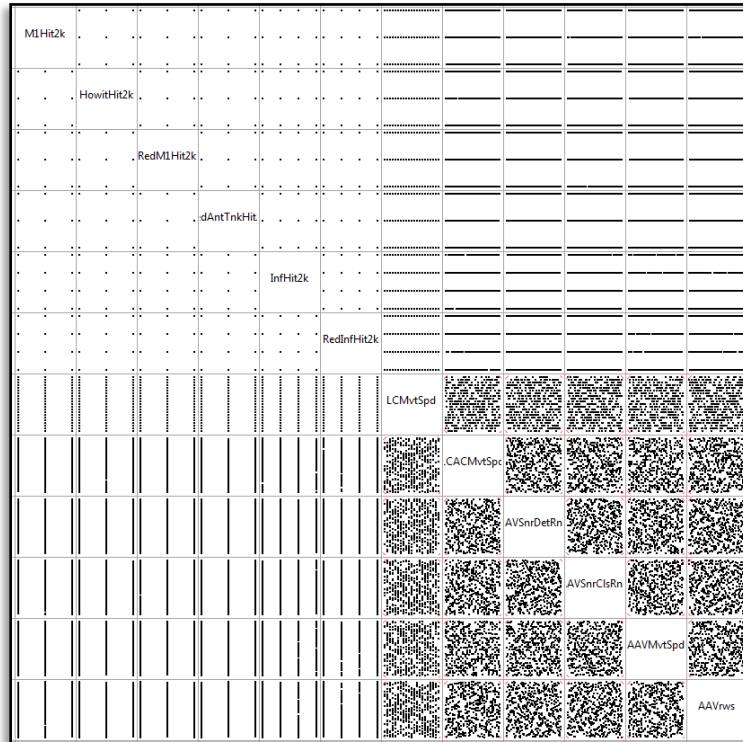
Figure 86.   Complete NOB, 77 factor DOE.

Figure 87. Screen grab of the 12 factors combined using the techniques described from Efficient, nearly orthogonal-and-balanced, mixed designs: an effective way to conduct trade-off analyses via simulation. Retrieved from Vieira, 2013.

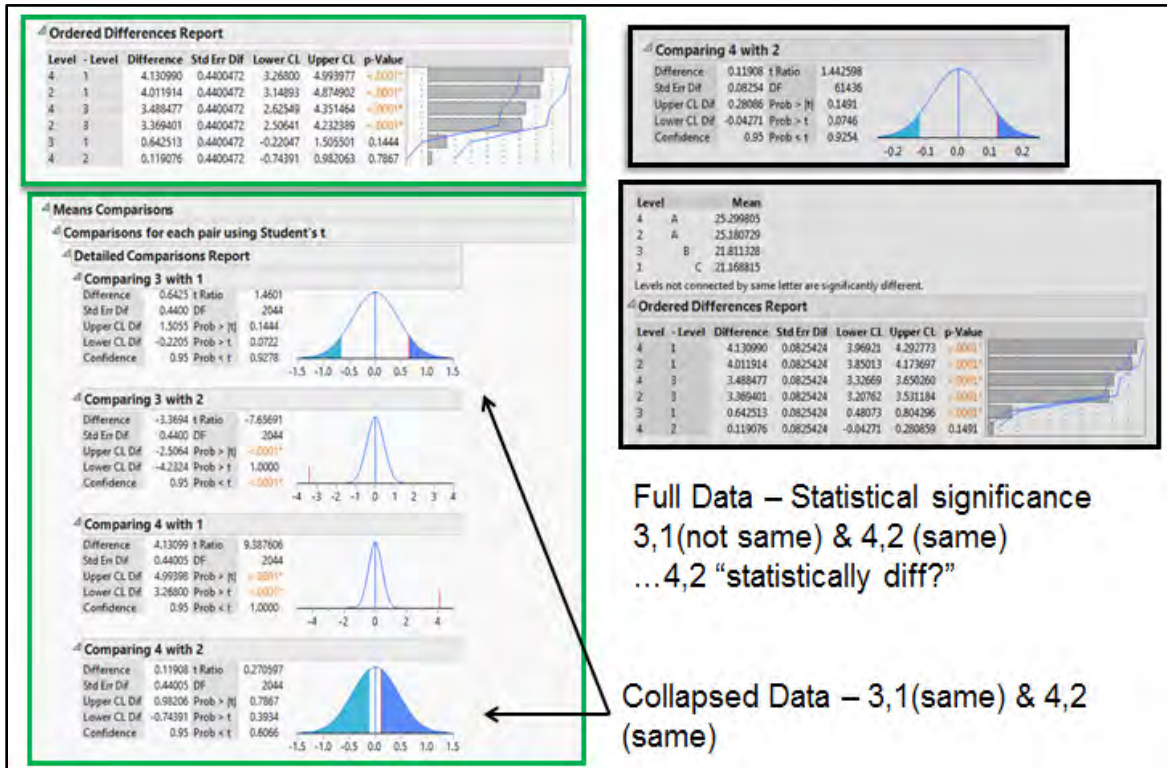# APPENDIX H. MEANS COMPARISON USING STUDENT T-TEST

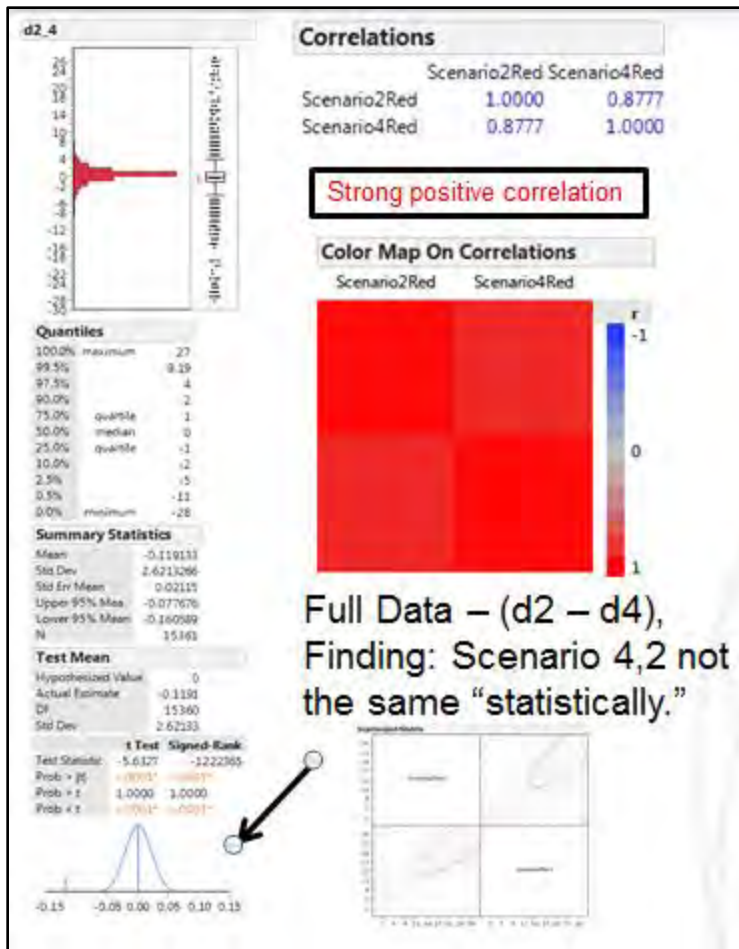Figure 88.   T Means comparison for statistically significant scenarios using student t-Test.

Figure 89.   Paired comparison, scenarios two and four for statistical significance
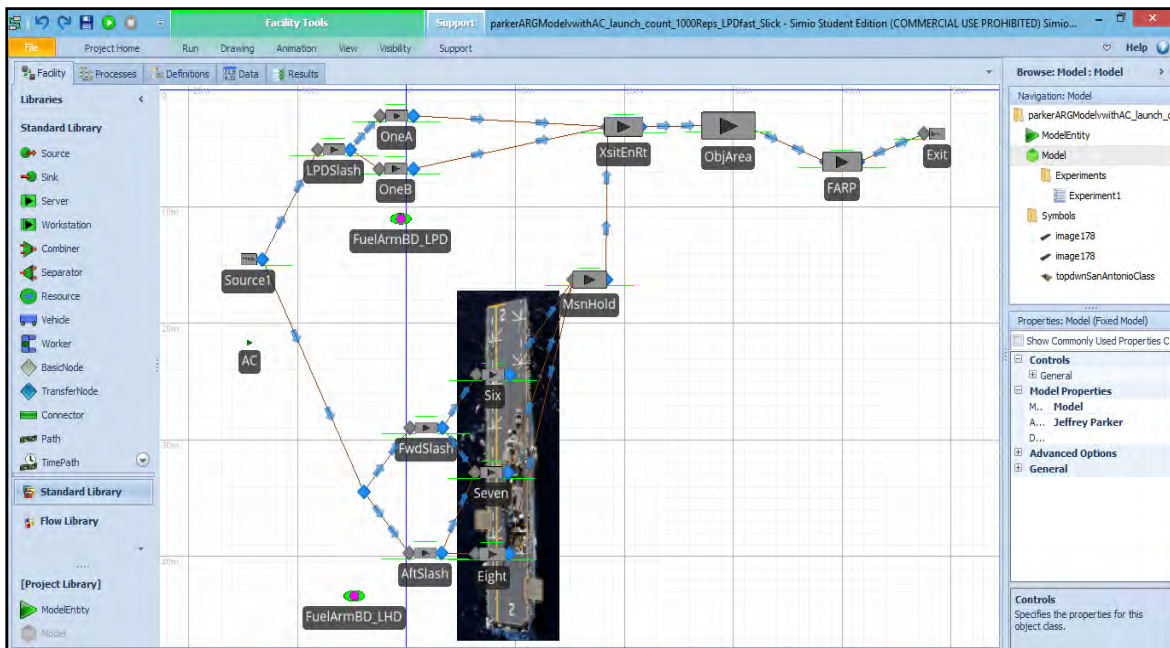
APPENDIX I. SIMIO AND MANA DASHBOARD COMPARISON

Figure 90.   Screen shot of Simio dashboard

Figure 91.   Screen shot of terrain billboard in MANA.
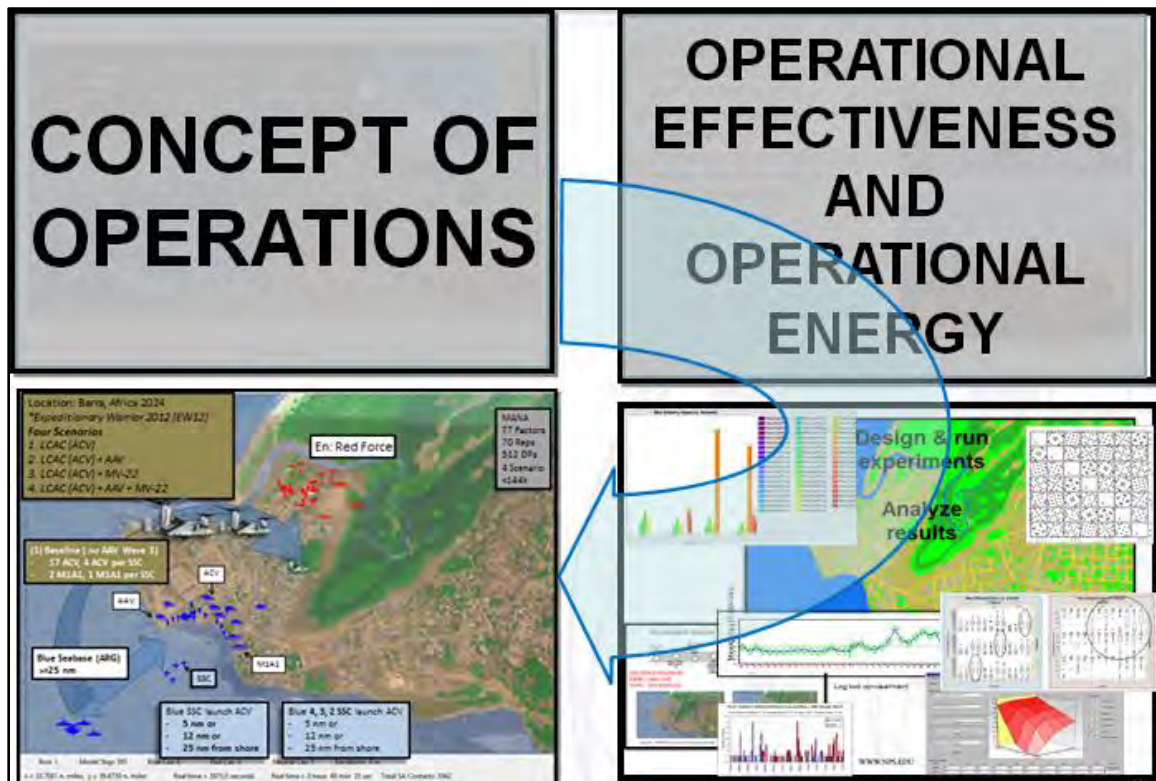
THIS PAGE INTENTIONALLY LEFT BLANK

Figure 92.   An illustration of the model-test-model approach, see chapter III for actual concept of operations and scenario development.

THIS PAGE INTENTIONALLY LEFT BLANK

LIST OF REFERENCES

15th Marine Expeditionary Unit. (2012). 15th Marine Expeditionary Unit History. Retrieved from http://www.15thmeu.marines.mil/About/History.aspx

Achterling, M. (2014). U.S. Navy photo by Mass Communication Specialist, 2nd Class, Michael Achterling. Retrieved from http://www.ctf76.navy.mil/gallery/2014/apr/apr.htm

Axe, D. (2012). Inside the Army's doomed quest for the 'perfect' radio. *Wired*. Retrieved from http://www.publicintegrity.org/2012/01/10/7816/failure-communicate-inside-armys-doomed-quest-perfect-radio

Besser, J., Hobbs, J., Hovis, K., Hunter, D., Leaman, B., McPherson, J., . . . Valliere, E. (2013). *Expeditionary energy efficiency in support of foreign humanitarian aid/disaster relief* (Capstone Report). Monterey, CA: Naval Postgraduate School.

Charette, R. N. (2008). What's wrong with weapons acquisitions? *Spectrum*, IEEE, *45*(11), 33–39.

Cioppa, T. M., Lucas, T. W., & Sanchez, S. M. (2004). Military applications of agent-based simulations. *Proceedings of the 2004 Winter Simulation Conference* (pp. 171–180). Piscataway, NJ: IEEE.

Dempsey, M. E. (2012). Joint operational access concept (JOAC). Washington, D.C.: Department of Defense.

Department of Defense. (1992). 3–02. *Joint doctrine for amphibious operations*. Washington, D.C.: Department of Defense.

Department of the Navy. (1998). MCDP 3: Expeditionary operations. Washington, D.C.: Department of Defense.

Department of the Navy. (2007, October 15). Seabase to shore connector analysis of alternatives final report. Retrieved from https://cle.nps.edu/access/content/group/72686d99-7c35-4290-9670-260641f1f0f0/Lesson%2014%20Case%207%3A%20SSC/SSC_AoA_Report.pdf

Edwards, E. (1868). *The life of Sir Walter Raleigh: Based on contemporary documents... Together with his letters; Now first collected*. I (Vol. 2). Macmillan. London, United Kingdom.

Eckstein, M. (2015, March 11). Marines may merge ACV increments as industry chases higher requirements. Retrieved from http://news.usni.org/2015/03/11/marines-may-merge-acv-increments-as-industry-chases-higher-requirements

Feickert, A. (2013, June). Marine Corps amphibious combat vehicle (ACV) and Marine personnel carrier (MPC): Background and issues for Congress. Retrieved from http://www.fas.org/sgp/crs/weapons/R42723.pdf

Fuentes, G. (2015, March 10). Picture of MV-22 nacels and Ground Combat Element (GCE), pilot program forges bonds between Marines and U.S. Special Operations Forces. *The USNI News*. Volume I, issue I, p. 1-5. Retrieved from http://news.usni.org/2015/03/10/pilot-program-forges-bonds-between-marines-and-u-s-special-operations-forces

Galante, A. (2009). USS 'Wasp' (LD1) com Ospreys. Retrieved from http://www.naval.com.br/blog/2009/07/22/uss-wasp-lhd-1-com-ospreys/

Gatchel, T. (1996). *At the water's edge: Defending against the modern amphibious assault*. Annapolis, MD: Naval Institute Press.

Griffith, S. (1971). *The art of war*. London: Oxford University Press.

Heinl, R. D. (1966). Dictionary of military and naval quotations. Naval Institute Press.

Hoe, K. J. (2001). *An analysis of distributed combat systems* (Master's thesis). Monterey, CA: Naval Postgraduate School.

Howard, M., Paret, P., & West, R. (1984). *Carl Von Clausewitz: On war*. Princeton, NJ: Princeton University Press.

Hughes, W. P. (2015). *The U.S. Naval Institute on naval tactics* (2nd ed.). The U.S. Naval Institute. Annapolis, MD.

Kelton, W. D., Smith, J. S., & Sturrock, D. T. (2011). *Simio & simulation: Modeling, analysis, applications*. Learning Solutions. Boston, MA.

LaGrone, S. (2015, February). WEST: Marines plan to issue amphibious combat vehicle request for proposal in March. *The USNI News*. Retrieved from http://news.usni.org/2015/02/12/west-marines-plan-issue-amphibious-combat-vehicle-request-proposal-march

Langworth, R. (2008). Churchill by himself: The definitive collection of quotations. *Public Affairs*, *New York*. p. 576.

Lucas, T. (2014). Lecture notes in statistics class: Hypothesis testing (OA 3102 Statistics). Naval Postgraduate School, Monterey, CA. Retrieved from https://cle.nps.edu/access/content/group/4235b6f3-d2c1-4c6d-b26c-0b9de11575d3/Lecture%20slides/Hypothesis%20Testing.pdf

Marine Corps Expeditionary Energy Office (E2O). (2012). Retrieved from http://www.hqmc.marines.mil/e2o/E2OHome/AboutUs.aspx

McIntosh, G., Galligan, D., Anderson, M. A., & Lauren, M. K. (2007). *MANA-V (Map Aware Non-uniform Automata-Vector) supplementary manual*. Defense Technology Agency. New Zealand

Obama, B. (2011, October 21). Remarks by the President on ending the war in Iraq. White House, Washington, D.C.

Patton, G. S., & Harkins, P. D. (1995). War as I knew it. Houghton Mifflin Harcourt.

Sanchez, S. M. (1994, December). A robust design tutorial. *Proceedings of the 1994 Winter Simulation Conference* (pp. 106–113). Piscataway, NJ: IEEE.

Sanchez, S. M. (2007). Work smarter, not harder: Guidelines for designing simulation experiments. *Proceedings of the 2007 Winter Simulation Conference* (pp. 84–94). doi:10.1109/WSC.2007.4419591. Piscataway, NJ: IEEE.

Sanchez, S. M., Sánchez, P. J., & Wan, H. (2014, July). Simulation experiments: Better insights by design. *Proceedings of the 2014 Summer Simulation Multiconference* (p. 53). Society for Computer Simulation International.

Simio LLC. (2010). Introduction to Simio. Pittsburgh, PA. Retrieved from http://www.Simio.com/about-Simio

Skahen, S., Benner, S., Boyett, M., Brookhart, M., & Kure, J. (2013). *Exploring the reduction of fuel consumption for ship-to-shore connectors of the Marine Expeditionary Brigade* (Capstone Report). Monterey, CA: Naval Postgraduate School.

Smith, S. M. (2013). U.S. Marine Corps MV-22 Osprey tiltrotor aircraft prepare to take off from the amphibious transport dock ship USS Mesa Verde (LPD 19) in the Atlantic Ocean December 14, 2013. Retrieved from http://commons.wikimedia.org/wiki/File:U.S._Marine_Corps_MV-22_Osprey_tiltrotor_aircraft_prepare_to_take_off_from_the_amphibious_transport_dock_ship_USS_Mesa_Verde_(LPD_19)_in_the_Atlantic_Ocean_Dec._14,_2013_131214-N-BD629-087.jpg

Suite of Analytics Software (SAS). (2014). JMP 11 online documentation. Retrieved from http://www.jmp.com/support/help

Taguchi, G. (1986). *Introduction to quality engineering: Designing quality into products and processes*. Tokyo: The Organization.

Team Expeditionary & Cohort 311-132. (2014). *Operational energy/operational effectiveness investigation for scalable Marine Expeditionary Brigade forces in contingency response scenarios* (Master's thesis). Monterey, CA: Naval Postgraduate School. Retrieved from https://cle.nps.edu/xsl-portal/tool/b0d2a28e-bff7-451b-b663-cfd03543d98f/posts/downloadAttach/73963.page

Trickey, W. R., Benbow, R. C., & Taylor, D. G. (2010). *MEB capabilities study*. Alexandria, VA: Center for Naval Analyses.

Unit of Action Maneuver Battle Lab (UAMBL). (2003) Operational requirements document (ORD) for the future combat systems, Fort Knox, KY: UAMBL. Retrieved from http://www.rand.org/content/dam/rand/pubs/monographs/2012/RAND_MG1206.pdf

U.S. History. (2015). History of the U.S. Marine Corps Chronology. Retrieved from http://www.u-s-history.com/pages/h3795.html

U.S. Marine Corps. (1998). *MCDP 3–Expeditionary operations*. Washington, D.C.: Department of Defense.

U.S. Naval War College. (2015). The U.S. Naval War College at the Naval Postgraduate School Course Syllabus. Naval Postgraduate School, Monterey, CA. Retrieved from https://cle.nps.edu/xsl-portal/site/73952c7b-5692-4df5-970a-8aee9260d22d/page/61a4e4ab-4095-4dcd-a0e7-6da0e6985ca9

Vieira, Jr., H., Sanchez, S. M., Kienitz, K. H., & Belderrain, M. C. M. (2011, December). Improved efficient, nearly orthogonal, nearly balanced mixed designs. *Proceedings of the 2011 Winter Simulation Conference* (pp. 3600–3611). Piscataway, NJ: IEEE.

Vieira, Jr., H., Sanchez, S. M., Kienitz, K. H., & Belderrain, M. C. M. (2013). Efficient, nearly orthogonal-and-balanced, mixed designs: An effective way to conduct trade-off analyses via simulation. *Journal of Simulation* (7: 264-275). (Special Issue on Input/Output Analysis).

Wackerly, D., Mendenhall, W., & Scheaffer, R. (2008). *Mathematical statistics with applications*. Cengage Learning.Belmont, CA.

Wargaming Division. (2012). Expeditionary Warrior 2012 (EW 12) Final Report 23 July 2012, Wargaming Division, Marine Corps Warfighting Laboratory, Retrieved from http://www.defenseinnovationmarketplace.mil/resources/Marine_Corps_War_Game.pdf

INITIAL DISTRIBUTION LIST

1.   Defense Technical Information Center
        Ft. Belvoir, Virginia

2.   Dudley Knox Library
        Naval Postgraduate School
        Monterey, California